The Aeronian/Telychian (Llandovery, Silurian) boundary, with particular reference to sections around the El Pintado reservoir, Seville Province, Spain

4 authors, including:

The Aeronian/Telychian (Llandovery, Silurian) boundary, with particular reference to sections around the El Pintado reservoir, Seville Province, Spain

DAVID K. LOYDELL, JIŘÍ FRÝDA & JUAN CARLOS GUTIÉRREZ-MARCO

The upper Aeronian to lower Telychian (Llandovery Series, lower Silurian) strata at the east end of El Pintado reservoir, Seville Province, Spain are documented in terms of their lithologies, graptolite biostratigraphy and $\delta^{13}C_{org}$ record. This is the first time that a continuously graptolitic section throught the Aeronian/Telychian boundary has been studied in detail. The upper Aeronian part of the section is assigned to the *Stimulograptus halli* Biozone which is divisible into three, the middle part being referred to the *Lituigraptus rastrum* Subzone. The Telychian strata are assigned to the *Spirograptus guerichi* Biozone and lower *Sp. turriculatus* Biozone. Unusually, two specimens of *Sp. turriculatus* were found at a level low in the *guerichi* Biozone. 118 graptolite species are recorded, 18 of which are new and described here together with other species for which the El Pintado material provides new information. Diversity increases considerably in some genera (*Glyptograptus*, *Parapetalolithus*, *Rastrites*, *Streptograptus*) in the upper *halli* Biozone and/or lower to middle *guerichi* Biozone only to decline again (except for *Streptograptus*) in the upper part of the *guerichi* Biozone as part of the "*utilis* Event". This diversity decline coincides with an interval of elevated $\delta^{13}C_{org}$ values. There are no major $\delta^{13}C_{org}$ excursions present in the El Pintado sections. The $\delta^{13}C_{org}$ record through the *guerichi* Biozone is very similar to that in Arctic Canada. • Key words: graptolite, biostratigraphy, palaeobiogeography, Aeronian, Telychian, Llandovery, Spain.

David K. Loydell, School of Earth and Environmental Sciences, University of Portsmouth, Burnaby Road, Portsmouth PO1 3QL, UK; david.loydell@port.ac.uk • Jiří Frýda, Faculty of Environmental Sciences, Czech University of Life Sciences Prague, Kamýcká 129, 165 21, Praha 6 and Czech Geological Survey, Klárov 3, 118 21 Praha 1, Czech Republic; belerophon@seznam.cz • Juan Carlos Gutiérrez-Marco, Instituto de Geociencias (CSIC-UCM), Facultad de Ciencias Geológicas, E-28040 Madrid, Spain; jcgrapto@ucm.es

Our knowledge of the geological column is remarkably patchy. For some stratigraphical intervals numerous papers exist documenting sections, their contained fossils and chemostratigraphical record. Other intervals – unfortunately these are often around chronostratigraphical boundaries – are remarkably bereft of useful published stratigraphical data. This is usually because of the paucity or even absence of sections without major facies changes that are continuously fossiliferous. One such "unknown" interval has been the uppermost Aeronian to lowermost Telychian (middle to upper Llandovery Series). Recognition that the GSSP for the base of the Telychian Stage is unsatisfactory from a number of viewpoints (Temple 1988; Loydell 1993a; Davies *et al.* 2011, 2013) has heightened recent interest in the search for more informative sections. The aim of this paper is to document the upper Aeronian and lower Telychian graptolitic strata through sections on the shores of El Pintado reservoir in Seville Province, Spain and to discuss the bio-, chrono- and chemostratigraphy of this part of the Silurian System.

The paper commences with a review of published sections, to indicate why the El Pintado sections are so important. It continues with documentation of the sections studied, including their graptolite biostratigraphy and discusses the different upper Aeronian to lower Telychian biozonations previously proposed and their advantages and disadvantages. The organic carbon isotope record of the sections is presented and compared with the only other two locations with $\delta^{13}C_{org}$ data (Bohemia and Arctic Canada). Finally, there are descriptions of new graptolite species and of those previously described species for which the El Pintado material provides new information.
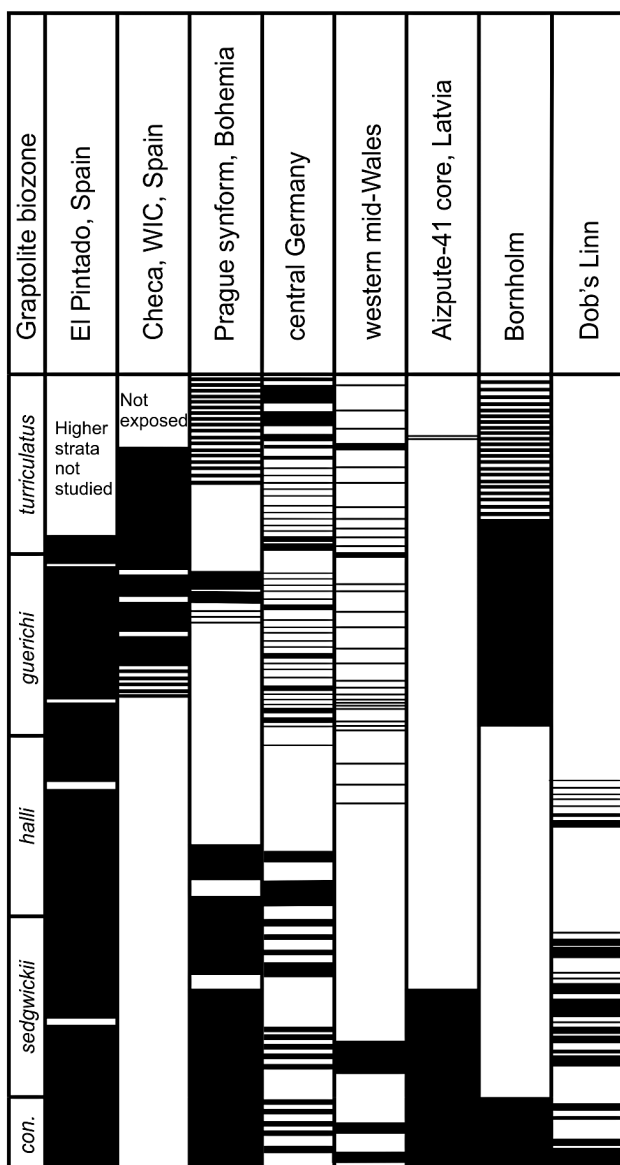
Figure 1. Graptolitic strata through the upper Aeronian–lower Telychian of sections in Europe. Note that although the graptolitic horizons are largely a record of sediments deposited during intervals of bottom water anoxia or dysoxia, the Welsh Telychian records, particularly in the lower *guerichi* Biozone, are from turbiditic sandstones deposited on an oxic seafloor, protected from destructive taphonomic processes by the overlying finer-grained turbiditic sediment (Bouma D and/or E units). Details of sections are derived from the papers listed in the text. See text for further details and information on additional sections. Abbreviations: *con.* = *convolutus*; WIC = Western Iberian Cordillera.

Aeronian/Telychian boundary sections

The importance of the El Pintado sections in providing a continuous graptolite record through the Aeronian/Telychian boundary is shown below where a brief review is provided of sections through this interval on the various Silurian palaeocontinents. Coverage is not exhaustive, but included

are all regions that have been studied monographically or where stratigraphical ranges of taxa are provided together with lithological information. The graptolite assemblages from some sections require documentation or revision, but at the time of writing there is no fully documented continuously graptolitic outcrop section known through the Aeronian/Telychian boundary worldwide. Only in outer shelf/deep basinal environments are such sections likely to be encountered and even here in many cases, as documented below, the highest Aeronian graptolitic strata are separated from the lowest Telychian graptolitic strata by lithologies yielding either no graptolites or too few to be of any great biostratigraphical value. Figure 1 summarizes the stratigraphical occurrence in Europe of graptolitic strata through the upper Aeronian and lower Telychian.

Sections located in peri-Gondwanan Europe. – Štorch & Frýda (2012) provided lithological, graptolite biostratigraphical and carbon isotope data through the upper Aeronian to lowermost Telychian of the Prague synform, Bohemia. The base of the Telychian here lies within a pale non-graptolitic mudstone unit. Although this is only 0.5 m thick in the Radotín tunnel section, it evidently encompasses a significant amount of time, represented in the El Pintado sections by the upper *Stimulograptus halli* Biozone and lower two-thirds of the *Spirograptus guerichi* Biozone. Whereas in Bohemia the highest graptolitic sample beneath the non-graptolitic pale mudstone yields *Lituigraptus rastrum*, in the El Pintado section higher parts of the *Stimulograptus halli* Biozone are represented within which *Rastrites linnaei* appears (and co-occurs with stratigraphically higher specimens of *L. rastrum*; Figs 9, 11) and *L. rastrum* itself disappears more than a metre below the first appearance of *Spirograptus guerichi*. The lowermost Telychian black shale horizon in the Radotín tunnel section yields *Torquigraptus planus*, a species that makes its first appearance in China (Loydell 1993a), Wales (Loydell 1993b) and Sweden (Loydell & Maletz 2004), and also in the El Pintado section (Fig. 10) in the upper part of the *guerichi* Biozone. Barrande's classic locality of Želkovice shows a similar stratigraphical sequence with *Torquigraptus planus* again present in the lowest Telychian black shale. The non-graptolitic nature of the lowermost Telychian at Želkovice may explain why "*Monograptus*" *gemmatus*, first described by Barrande (1850) from Želkovice, is so uncommon there – the very few specimens found are amongst the last before the species became extinct.

Schauer (1967, 1971) provided detailed sedimentary logs and graptolite biostratigraphical data for sections in east-central Germany. Although diverse well-preserved (although tectonically deformed) graptolite assemblages occur in the lower Telychian *Spirograptus guerichi* Biozone, the uppermost Aeronian yielded either no

graptolites (Ronneburg-Raitzhain I section) or rare, poorly preserved monospecific assemblages of *Stimulograptus*.

The Lower Palaeozoic of the Iberian Peninsula is divided into five structural "zones" each with a distinctive stratigraphy reflecting palaeogeographical location (Fig. 2), in particular proximity either to land areas on Gondwana or to the Rheic Ocean. In the Western Iberian Cordillera (Gutiérrez-Marco & Štorch 1998) graptolitic shales with *guerichi* Biozone assemblages immediately overlie sandstones in some cases of uncertain age, but in the case of the Orihuela del Tremedal roadcut section underlain by lower *Lituigraptus convolutus* Biozone graptolitic shales. In the Checa section the shales overlying the sandstone are interpreted by Gutiérrez-Marco & Štorch (1998) to be from the lower part of the *guerichi* Biozone; in other sections they are considered to be from higher levels within the *guerichi* Biozone. The Corral de Calatrava section in the Central Iberian Zone is similar in having upper *guerichi* Biozone graptolites in the lowermost black shale overlying the Rhuddanian–Aeronian Criadero Quartzite (Štorch *et al.* 1998).

Sections located on Avalonia. – The upper Aeronian–lower Telychian graptolite record on the shelf surrounding the Welsh Basin is very sparse. Deeper water deposits in central Wales, however, have been extensively investigated for more than a century, with detailed descriptions of sections and records of graptolitic occurrences in numerous publications (*e.g.* Jones 1909; Jones & Pugh 1916; Cave & Hains 1986; Loydell 1991a, 1992, 1993b; Davies *et al.* 1997). The sedimentary record of the Aeronian and Telychian in the Welsh Basin is one dominated by strata deposited under oxic conditions with graptolites preserved either in hemipelagites during generally brief periods of bottom water anoxia or where they were rapidly buried within turbidites, mostly within Bouma-C units, often when bottom waters were oxic as evidenced by trace fossils on the base of the turbidite arenites.

Within the lower part of the *Stimulograptus sedgwickii* Biozone in central Wales is a distinctive, often several metres thick unit comprising interbedded black graptolitic shales and thin distal turbidites long used as a lithostratigraphical marker during mapping. The presence of *Neolagarograptus tenuis* at the base of this unit suggests, from the ranges presented by Štorch & Frýda (2012) through a continuously graptolitic *convolutus/sedgwickii* Biozone transition, that the base of these "*Monograptus-sedgwicki* shales" (Jones & Pugh 1916, Davies *et al.* 1997) lies above that of the *sedgwickii* Biozone. Above the "*Monograptus-sedgwicki* shales" the succeeding upper Aeronian strata represent deposition under predominantly oxic conditions with thin graptolitic shales comprising a very small percentage of the total thickness of strata. Jones & Pugh (1916) recognised three such bands
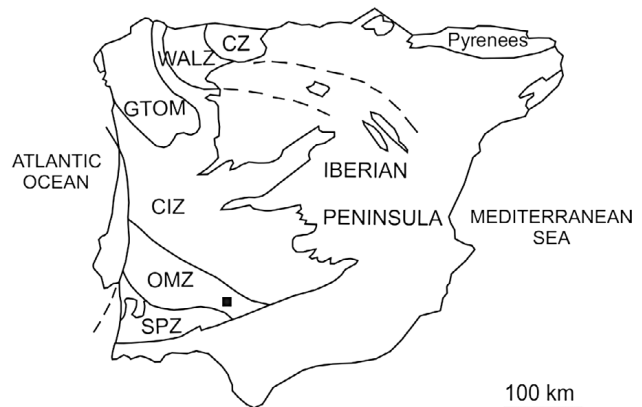
Figure 2. The location of the Valle syncline (black square) on a map of the Iberian Peninsula showing the subdivisions of the Hesperian (= Iberian) Massif. Abbreviations: CIZ – Central Iberian Zone; CZ – Cantabrian Zone; GTOM – Galicia/Trás-os-Montes Zone; OMZ – Ossa Morena Zone; SPZ – South Portuguese Zone; WALZ – West Asturian-Leonese Zone. Map modified from Gutiérrez-Marco *et al.* (1998).

within their newly erected *Monograptus* (now *Stimulograptus*) *halli* Biozone: a lowest with *Stimulograptus halli*, *Metaclimacograptus undulatus* and *Torquigraptus involutus*, a middle band with *St. halli* and *Rastrites* and an upper band dominated by *Metaclimacograptus undulatus* and *Pristiograptus*. Nowhere is there a graptolitic Aeronian/Telychian transition, and the lowest Telychian *Spirograptus guerichi* Biozone graptolites occur within turbidite sandstones and siltstones in the Devil's Bridge Formation *e.g.* at Nant Fuches-wen quarry (Jones 1909, locality F.29; Loydell 1992, locality D13) and in the Glan-fred core (Loydell 1992). Numerous generally very thin (usually sub-mm to a few mm thick) graptolitic shales occur sporadically through the remainder of the *Spirograptus guerichi* and *Spirograptus turriculatus* biozones which are represented overall by many hundreds of metres of turbidites.

In the Spengill section, Howgill Fells, there are more than 3 m of non-graptolitic mudstone between the highest graptolitic Aeronian horizon assigned by Rickards (1970) to the *sedgwickii* Biozone and the lowest graptolitic mudstone yielding *Spirograptus guerichi*. It is possible, however, that Rickards' "94,7.4 band" is in fact of Telychian age (but lacking *Spirograptus guerichi*), as its very limited graptolite assemblage includes "*Monograptus*" *gemmatus*. If this proves to be the case, there are more than 4 m of non-graptolitic strata beneath this band before the preceding graptolitic horizon is reached. In the Lake District, there is a similar gap in the graptolite record, probably of greater biostratigraphical extent than in the Howgill Fells: in Stockdale Beck (Hutt 1974) non-graptolitic mudstones overlie graptolitic mudstones of the *sedgwickii* Biozone. Three graptolitic bands with a total thickness of 50 mm occur 5 m above the *sedgwickii*

Biozone graptolitic mudstones and are undoubtedly of early Telychian *Spirograptus guerichi* or *Spirograptus turriculatus* Zone age.

In the Brabant Massif, Belgium Van Grootel *et al.* (1998) record an interval 30 m thick with few and poorly preserved graptolites between a "well-developed" *convolutus* Biozone and graptolitic early Telychian strata.

Sections located on Baltica. – The Aizpute-41 core Latvia (Loydell *et al.* 2003) contains graptolites from the *Stimulograptus sedgwickii* Biozone at a depth of 969.05 m at the top of the Dobele Formation, a condensed, largely dark grey shale unit comprising the uppermost Rhuddanian and most of the Aeronian. Above this formation, at the base of the Jūrmala Formation, are 1.3 m of claystone overlain by 4.1 m of red beds within the top metre of which thin graptolitic horizons yield *Spirograptus turriculatus* Biozone assemblages, including *Torquigraptus proteus* and *Streptograptus johnsonae*. The former indicates a level significantly above the base of the biozone. Thus the Aizpute-41 core lacks graptolitic horizons from the entirety of the *Stimulograptus halli* and *Spirograptus guerichi* biozones, from the lower part of the *Spirograptus turriculatus* Biozone and possibly from part of the *Stimulograptus sedgwickii* Biozone.

The Ohesaare core, Saaremaa, Estonia exhibits a substantial unconformity comprising most of the Aeronian and the lowermost Telychian (Loydell *et al.* 1998), with the lowest Telychian strata yielding *Spirograptus turriculatus* Biozone graptolites, again including *Torquigraptus proteus*. An unconformity, encompassing fewer graptolite biozones than in Ohesaare, but including the uppermost Aeronian and lowermost Telychian has also been interpreted from the Kolka-54 core, Latvia record (Loydell *et al.* 2010).

Graptolitic sections through the Aeronian/Telychian boundary appear to be present in the subsurface of western Lithuania: range charts and descriptions of the graptolites are provided by Paškevičius (1979). Sections appear to be condensed with the thickness from base *sedgwickii* Biozone to base *crispus* Biozone ranging between 4.5 m and 7.5 m. High resolution sampling through the interval will be needed should the cores be restudied.

The graptolite biostratigraphy and sedimentary record of the Øleå section, Bornholm were described by Bjerreskov (1971, 1975). Here dark graptolitic shales of the upper *Lituigraptus convolutus* Biozone are overlain by 0.65 m of light grey silty mudstone containing pyritic burrows, then 1.45 m of unfossiliferous light grey shale, before the graptolitic record recommences in the lower part of the *Spirograptus guerichi* Biozone.

Sections in Sweden lack detailed recent studies through the Aeronian–Telychian transition. Whilst graptolites from limestone nodules within the lower Telychian *Spiro-*

graptus guerichi and *Spirograptus turriculatus* biozones of Osmundsberget have been the subject of several studies (*e.g.* Loydell *et al.* 1993; Loydell & Maletz 2002, 2004) and the *Stimulograptus sedgwickii* Biozone is shown on figures describing this section and others in the Siljan region of Dalarna (*e.g.* Bergström *et al.* 2008, 2012; Inanli *et al.* 2009), the precise level of the Aeronian/Telychian boundary is yet to be established as is whether these sections are stratigraphically complete through this interval. Similarly, Maletz *et al.* (2014) provide a preliminary account of the graptolite biozonation of the Röstånga-1 core from Scania, but until a thorough study is completed, the nature of the Aeronian/Telychian boundary here will remain uncertain.

In the Oslo region of Norway, the Aeronian–Telychian transition lies within the Rytteråker Formation, a unit of shelfal carbonates lacking graptolites (Worsley *et al.* 1983).

Sections located in Siberia. – In none of the numerous sections documented by Sennikov *et al.* (2008) is the Aeronian–Telychian transition shown to be graptolitic. In the Chernaya Mountain section more than 65 m of unfossiliferous strata occur between a mudstone yielding *Stimulograptus sedgwickii* and the lowermost horizon identified as Telychian (based upon a monospecific assemblage of "*Streptograptus* sp.").

Sections located on Gondwana. – Zalasiewicz *et al.* (2007) provided logs and graptolite records through the Llandovery of central Saudi Arabia. Although both the *Lituigraptus convolutus* and *Spirograptus guerichi* biozones were recognised (the latter for the first time on the Arabian Peninsula) intervening strata were barren of graptolites.

In Australia it is possible that the localities around Cottons Hill in the Forbes district of New South Wales include the Aeronian/Telychian boundary. Sherwin (1974) described the graptolites, but the most diverse collection was from loose blocks in the quarry west of the trigonometrical station. Detailed logging and collecting would be needed to establish the continuity of the graptolite record.

Sections located on Laurentia. – The Southern Uplands of Scotland host important sections of Llandovery age, Dob's Linn being the best known resulting from the classic work of Lapworth (1878). Toghill (1968) restudied the section and identified 14 graptolitic horizons within the *sedgwickii* Biozone and seven in the overlying strata which he assigned to the *Rastrites maximus* Biozone, traditionally a lower Telychian biozone or subzone in the British Isles. Loydell (1991b) re-examined Toghill's (1968) collection and, in the absence of *Rastrites maximus* and any other indicative Telychian taxa, assigned his top seven horizons to the upper Aeronian *halli* Biozone. More than 3 m of barren mud-

stones overlie the highest graptolitic *halli* Biozone horizon and these are in turn overlain by the turbidites of the "Gala Greywackes" (now the Gala Group) occupying a very similar stratigraphical level to the lowest thick turbidite unit in central Wales, the Devil's Bridge Formation. At Dob's Linn the Gala Group has not yielded graptolites.

The base of the Gala Group is highly diachronous and at other localities lies demonstrably within the Telychian (Floyd 2001). However, where biostratigraphical studies have been undertaken, *e.g.* at Pot Burn (Williams *et al.* 2003), the Aeronian/Telychian boundary has been shown to lie within oxic grey mudstones. At Pot Burn, graptolites from the *guerichi* Biozone occur within a single 10 mm thick hemipelagite layer, the only graptolitic horizon in 9 m of otherwise barren grey mudstones.

Of the sections collected by Lenz (1982) in the Northern Canadian Cordillera, the Blackstone River section would seem to have the greatest potential for exposing a continuous section through the Aeronian/Telychian boundary, with the upper Aeronian *Cephalograptus extrema* present at 77.2 m and a lower Telychian assemblage at 80.2 m. Whether the section is graptolitic through these 3 m is not known. In Arctic Canada Melchin (1989) recorded (at *e.g.* Huff Ridge, Ellesmere Island) a massive non-graptolitic unit bounded below by *Lituigraptus convolutus* or earlier Aeronian graptolitic strata and above by strata bearing lower Telychian (*Spirograptus guerichi* Biozone) graptolites. A biostratigraphically more complete section, Cape Manning on Cornwallis Island, was described by Melchin & Holmden (2006). The *halli* Biozone (referred to as the upper *sedgwickii* Biozone) was recognised together with an overlying *Spirograptus guerichi* Biozone. Details of assemblages and stratigraphical ranges from this section remain to be published.

Sections located in South China. – No graptolites were recorded from between the *convolutus* and *guerichi* biozones in the sections in south Shaanxi (Zhongliangsi and Dazhuba-Wangjiawan) described by Chen (1984). In the Qiaotin section, Nanjiang, Sichuan, also described by Chen (1984), graptolitic *guerichi* Biozone strata unconformably overlie the Hirnantian. The Bajiaokou section described by Fu & Song (1986) has 47.2 m of non-graptolitic strata below the first appearance of *Spirograptus guerichi*. Study is ongoing on the Bajiaomiao section, in the Shennongjia Forest District of northwest Hubei where initial investigations have suggested the presence of a graptolitic Aeronian–Telychian transition (Fan Junxuan, pers. comm.).

Sections located in Sibumasu. – Ni *et al.* (1982) recorded an apparently continuously graptolitic section through the Llandovery at Laojianshan, Yunnan. Unfortunately the upper Aeronian and lower Telychian strata here are currently obscured by a landslide (Zhang *et al.* 2014).
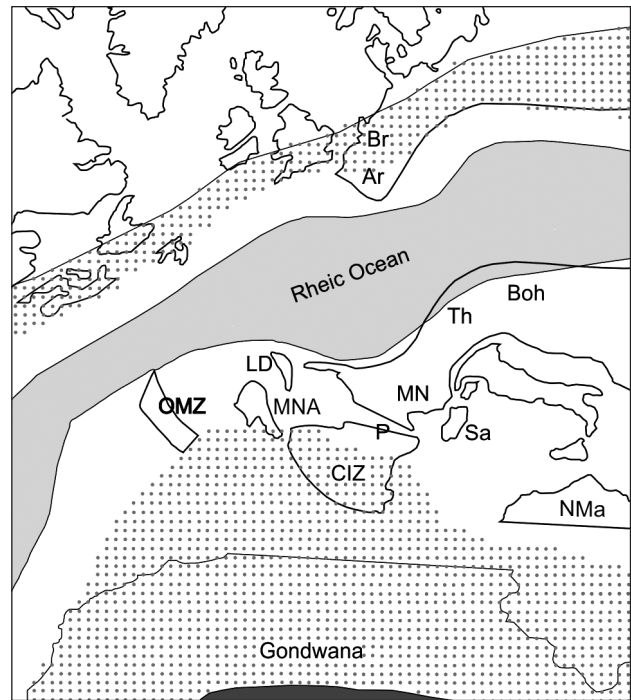
Figure 3. Tentative palaeogeographical reconstruction of the North Gondwanan regions during the Silurian Period (after Robardet & Gutiérrez-Marco 2002). Key: dark grey – land; coarse stipple – inner shelf; white – outer shelf; pale grey – ocean. Abbreviations: Ar – Ardenne; Boh – Bohemia; Br – Brabant; CIZ – Central Iberian Zone; LD – Ligerian Domain; MN – Montagne Noire; MNA – Middle-North Armorican Domain; NMa – northern Maghreb; OMZ – Ossa Morena Zone; P – Pyrenees; Sa – Sardinia; Th – Thuringia.

The El Pintado locality, geological background and previous work

The El Pintado reservoir lies in the northern part of Seville Province, approximately 13 km WNW of the town of Cazalla de la Sierra. There are numerous exposures of Lower Palaeozoic strata around the eastern end of the reservoir, within the Valle syncline. The most important Silurian sections are on the northern shore of the reservoir and along gulleys leading into it.

The Valle syncline lies within the Zafra-Córdoba-Alanís Unit of the Ossa Morena Zone, one of the five tectono-stratigraphic "zones" comprising the Iberian Massif (Fig. 2). Robardet & Gutiérrez-Marco (2004) provide an overview of the geology of the Ordovician–Devonian of the Ossa Morena Zone. By contrast with the Central Iberian Zone and Western Iberian Cordillera (the subject of recent graptolite biostratigraphical studies, *e.g.* Gutiérrez-Marco & Štorch 1998, Štorch 1998, Loydell *et al.* 2009), the environment was outer shelf rather than proximal to mid shelf and this presumably explains the stratigraphically earlier appearance of graptolitic facies here. Robardet & Gutiérrez-Marco (2002) show the Ossa Morena Zone stretching across a
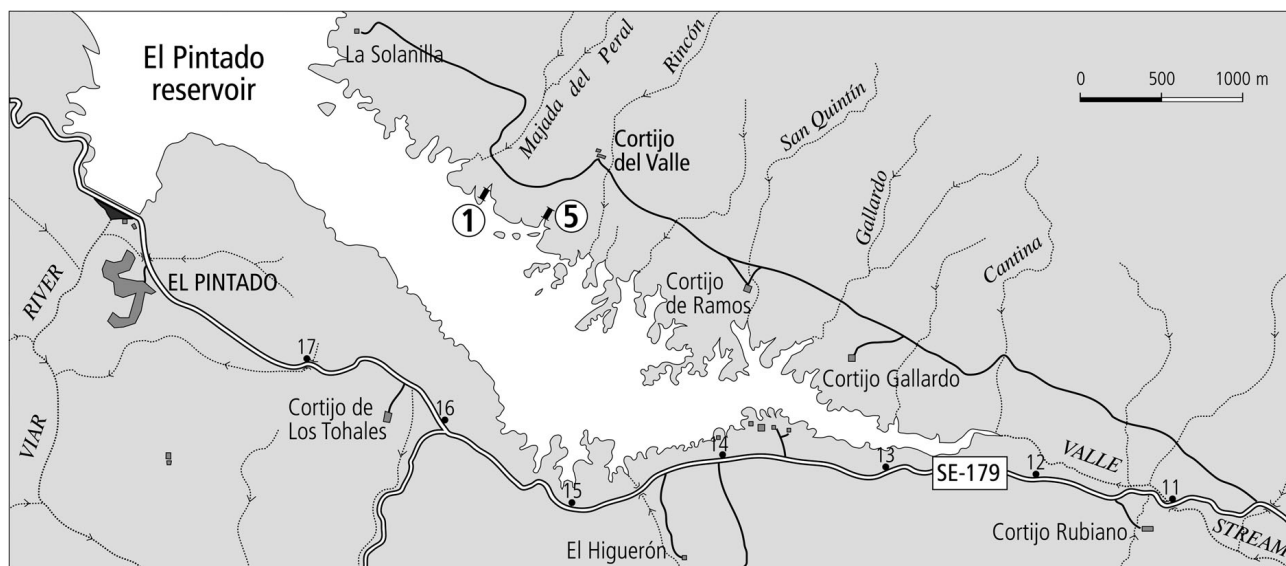
Figure 4. Map of the eastern end of El Pintado reservoir showing the locations of sections 1 and 5.

broad outer shelf region on the passive southern margin of the Rheic Ocean (Fig. 3) and separated by several hundred kilometres from the Central Iberian Zone, which today adjoins it to the north-east (Fig. 2).

The potential stratigraphical importance of the El Pintado area was demonstrated by Jaeger & Robardet (1979). In particular, their section 1, named "SW. de la ferme du Valle", was shown as continuous from the Ordovician through to the upper Silurian and for much of its thickness to be lithologically monotonous "black shales". Graptolites were recorded from numerous horizons, ranging from the Rhuddanian to close to the Ludlow/Přídolí boundary. The Silurian in this section has a stratigraphical thickness exceeding 100 m. Additional records from the section were provided by Robardet *et al.* (1998) in which the locality was referred to as "Stop 1". Faunal lists were provided for more than 20 numbered beds within the Llandovery Series, numbers having been painted on the exposures in readiness for the visit of the Silurian 1998 Field Meeting participants. These faunal lists indicated the high graptolite diversity and potential for high resolution biostratigraphy.

The Silurian strata around El Pintado have been divided lithostratigraphically into "Lower Graptolitic Shales" and "Upper Graptolitic Shales" separated by the "Scyphocrinites Limestone" which is of Přídolí age (Piçarra *et al.* 1998, Robardet & Gutiérrez-Marco 2004). Brief mention of preliminary results of work on the Aeronian of the El Pintado sections was included in Štorch & Frýda (2012). Other works on graptolites from El Pintado are those of Hernández Sampelayo (1932), Carvajal Acuña (1944), Simon (1951), Gutiérrez-Marco *et al.* (1996), Lenz *et al.* (1996) and Piçarra *et al.* (1998).

Methods

Two sections were studied: Jaeger & Robardet's (1979) section 1 ("SW. de la ferme du Valle" = "Stop 1" of Robardet *et al.* 1998), and a new section. In order to retain Jaeger & Robardet's section numbering system, we refer to this new section herein as section 5. The locations of the sections are shown in Fig. 4. Photographs of the two sections are provided in Fig. 5.

The graptolites and other samples that form the basis of this paper were collected during two field visits each of several days' duration, in June 1999 and in September 2009. The sections were divided up into sampling horizons, by hammering small numbered flags into the exposure at intervals of 20 cm stratigraphical thickness (Fig. 5D, E). Notes were made on lithologies in each 20 cm interval and graptolites collected. Collecting ceased in section 1 where exposure became poor (marked by the arrow on Fig. 5A), with quartz veins prominent, immediately above a level with slightly tectonically deformed graptolites. The lowest stratigraphical level in section 5

Figure 5. Field photographs. • A – overview of section 1; arrow marks the top of the measured section; from arrow to green rucksack is *ca* 6 m. • B – collected part of section 5. • C – nodule near top of *guerichi* Biozone in section 5. • D – sandstone beds in lower *guerichi* Biozone in section 1. • E – dark grey graptolitic shales and mudstones in middle *guerichi* Biozone in section 1; "flags" are 0.2 m apart.
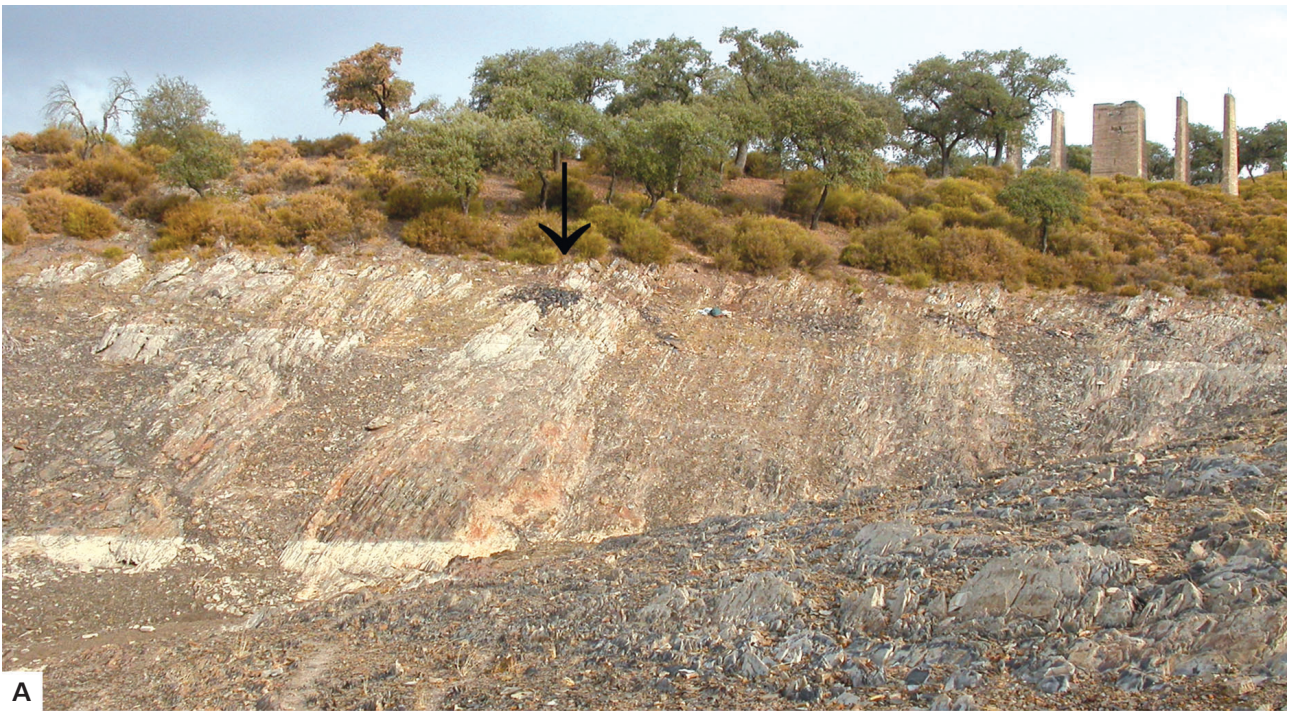
was chosen to ensure stratigraphical overlap between the two sections. Sample numbers (in the systematic palaeontology section and figure captions) indicate the section number first followed by the horizon, with S used as an abbreviation for sample number. So, for example, S1.13 would be from 2.4–2.6 m above the base of the studied part of section 1. All horizons were numbered, including the very few lacking fossils. Where a horizon was collected twice (in 1999 and 2009) the samples are differentiated using the suffix a or b respectively; this applies only to 0.8 m of strata in the upper *halli* Biozone. 12.4 m of strata were studied in section 1 and 7.6 m in section 5. The stratigraphical overlap between the two sections is 1.2 m in the middle part of the *guerichi* Biozone.

The number of graptolites collected from each horizon reflects their abundance and ease of collection: some mudstones split almost conchoidally across bedding planes whilst others more usefully split parallel to bedding. In order to reduce sample weight for shipping, slabs bearing examples of common taxa were often discarded, so that the relative abundances indicated in the range charts (Figs 9, 10) are in many cases underestimating the percentages of the most common taxa. Graptolites were identified under the binocular microscope and photographed using a Leica EZ4 HD USB microscope.

It is estimated that a total of approximately 60,000 graptolites was examined under the microscope, of which more than 7,000 were identified to species level. The large number of specimens that could be identified to genus level only reflects the difficulty of distinguishing small fragments or early growth stages to species level.

Test samples were processed using standard HCl-HF-HCl techniques to see if any chitinozoans, visible on several bedding surfaces (Fig. 8C, D), and other palynomorphs could be extracted, but nothing identifiable was present in the residues.

Samples for organic carbon isotope and TOC analysis were collected from each 20 cm interval. Hand specimens were cut and rock powder was prepared from a few grams of fresh sample. About 50 milligrams of rock powder were taken for total organic carbon (TOC) and total organic carbon isotope analyses. Before analyses, rock powders were decarbonatized with 10% HCl at 40 °C for several hours, then washed and dried. About 20 mg of rock powder were used for TOC and about 10 mg for isotope analyses. Samples were combusted in a Fisons 1108 elemental analyzer coupled on-line to a Finnigan Mat 251 mass spectrometer via a ConFlo interface. As reference material, NBS 22 (Gulf oil, with $\delta^{13}C$ value –29.75‰) and acetanilid (Analytical Microanalysis, UK) were measured. Accuracy and precision were controlled by replicate measurements of laboratory standards and were better than ±0.1‰ (1σ) for total carbon isotope analyses and better than ±0.02% (1σ) for total organic carbon content.
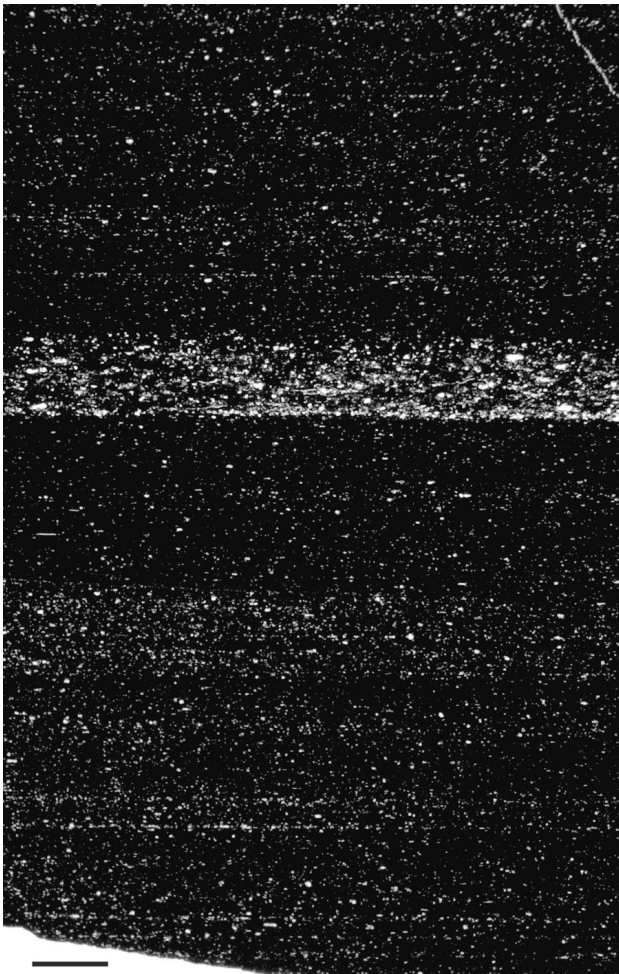
Sedimentology and palaeontology

The strata studied lie within a lithostratigraphical unit referred to in the literature as the "Lower graptolitic shales" (*e.g.* Robardet & Gutiérrez-Marco 2004). A wider range of lithologies is represented within the sections, however: although dark-grey to black mudstones and shales are common (Fig. 5E), they are interbedded with innumerable thin micaceous siltstones and occasional fine sandstones (Figs 5D, 6). These have sharp bases, variable thickness and are in many cases laterally discontinuous: they are interpreted as distal tempestites. The lithologies are typical of an outer shelf setting, with intervals of fine-grained deposition punctuated by storms introducing coarser grained sediment. The absence of shelly benthos within the tempestites suggests that the sediments may have been derived from locations in which bottom water anoxia prevailed. The only trace fossils recorded from the El Pintado sections were some possible *Chondrites* mottling (several examples in sample 1.38, one in sample 5.25; middle and upper *guerichi* Biozone respectively). This, combined with the absence of demonstrably benthic fossils, indicates that the El Pintado depositional environment was anoxic (or very nearly so) throughout the late Aeronian and early Telychian.

Sandstones occurred predominantly within the lower *guerichi* Biozone of section 1. The micaceous siltstones were too numerous to log individually – the spacing shown on Figs 9 and 10 is intended to shown their relative abundance at any particular level – they were least common in the *halli* Biozone and middle *guerichi* Biozone of section 1.

Nodules or nodular layers were recorded at a number of stratigraphical levels and suggest brief periods of non-deposition to enable their growth (Raiswell 1987). They proved to be useful marker beds, the 0.2 m thick nodular layer 3.2 m above the base of the studied part of section 1 enabling confident correlation of collections made in 1999 and 2009, and a nodule 12 cm thick by 18 cm wide near the top of the *guerichi* Biozone in section 5 (Fig. 5C) was used as the datum from which measurements were made stratigraphically up or down the section.

Graptolites were present in all lithologies with the exception of the nodules. They were generally not evenly distributed through the beds, but were more abundant on certain shale laminae and especially within some of the siltstone/sandstone tempestites presumably as a result of hydrodynamic sorting.

Jaeger & Robardet (1979) placed bars on their illustrations of El Pintado graptolites "to denote the direction of stretching (lineation)" with crosses placed on photographs where there was a "more or less pronounced all-round enlargement of the graptolites due to a second factor of deformation that runs parallel to the bedding". Tectonic deformation of graptolites was recorded in our samples only adjacent to a zone of quartz veining in the highest sample

Figure 7. Small-scale chocolate-tablet (tablette de chocolat) boudins, MGM6717-O, S5.21. Scale bar represents 10 mm.

Figure 6. Thin section (MGM6716-O) from the upper part of the part of the *Stimulograptus halli* Biozone (S1.18a) showing the interlaminated micaceous siltstones (paler layers) and dark grey to black mudstones that characterize much of the El Pintado section. Scale bar represents 10 mm.

from section 1. A few specimens show minor displacement (measured in mm) along micro-faults, but overall, features such as rhabdosome width and thecal spacing are identical to those in undeformed material from other localities. It appears that tectonic deformation in the section is concentrated at certain levels, in some cases manifested in small-scale chocolate-tablet (tablette de chocolat) boudins (Fig. 7) present within sub-millimetre thick layers.

All of the graptolites (and chitinozoans) are surrounded by clay minerals, the organic material of the graptolite periderm presumably having acted as a template for clay mineral growth (Underwood 1992, Page *et al.* 2008). This clay mineral coat is generally thickest in the coarser lithologies and around graptolites preserved in relief regardless of lithology (although these are most common in the siltstones and sandstones); it grew preferentially parallel to bedding (Fig. 20F). It commonly obscures fine de-

tails, for example in many cases preventing identification of the position of the sicular apex. Measurements of graptolites preserved in relief quoted in the systematic descriptions below exclude the clay mineral coating. Very occasionally, the clay minerals enhanced the detail visible on the graptolites, *e.g.* in the case of the *Glyptograptus fastigatus* illustrated in Fig. 20K, but this was the case in only a very few specimens.

Diagenetically flattened graptolites characterize the shales and mudstones, with partial to full relief specimens occurring predominantly in the siltstones and sandstones within which flattened specimens are also often present. It is very likely that the three dimensionally preserved specimens were originally pyrite internal moulds.

The only identifiable macrofossils other than graptolites encountered in either of the El Pintado sections were lingulate brachiopods (Fig. 8A) of which six were found in the upper *guerichi* Biozone and lower *turriculatus* Biozone of section 5. Only one conodont was encountered, a specimen of *Distomodus staurognathoides* (Fig. 8B) in the lowest sample from section 5 (middle *guerichi* Biozone). This extremely low conodont abundance contrasts with the moderate number of specimens seen on graptolitic bedding surfaces from Corral de Calatrava in the Central Iberian Zone (Loydell *et al.* 2009). This may be a reflection of the location of the Ossa Morena Zone farther from the shoreline of Gondwana (Fig. 3). Chitinozoans were noticed on several slabs and were particularly conspicuous where concentrated within laminae (Fig. 8C). As noted in the methods section above, it did not prove possible to extract any using standard palynological techniques. Sample 5.13 contained numerous fragments of non-mineralized arthropod cuticle.
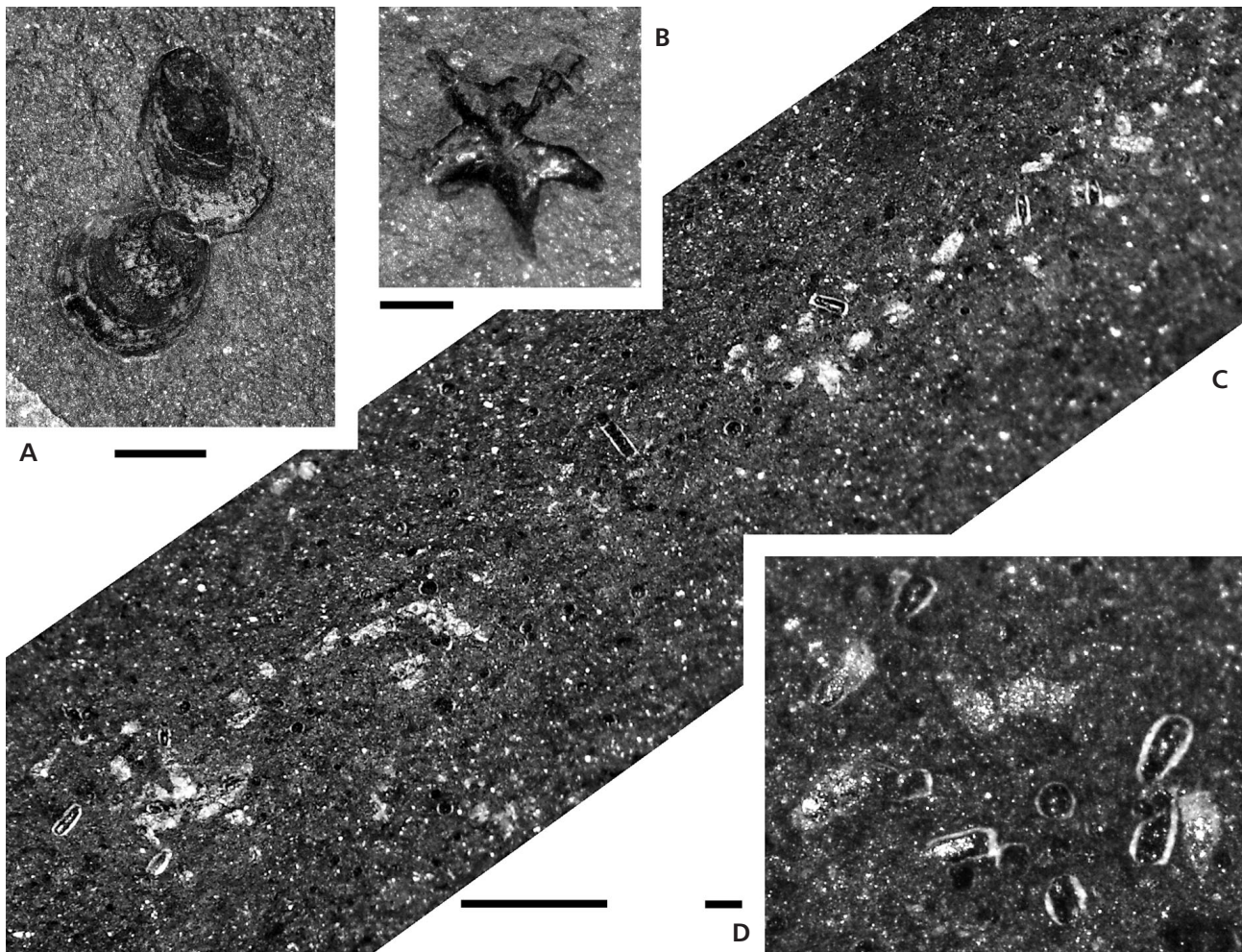
Figure 8. A – partially pyritized lingulate brachiopods, MGM6718-O, S5.25. • B – *Distomodus staurognathoides* Pa element, MGM6719-O, S5.22. • C – lamina with concentration of chitinozoans, oblique view, MGM6720-O, S1.14. • D – chitinozoans surrounded by clay mineral(s), MGM6720-O, S1.14. Scale bars represent 2 mm (A), 0.4 mm (B), 1 mm (C) and 0.1 mm (D).

Graptolite biostratigraphy

Background

The late Aeronian–early Telychian interval witnessed the demise of *Cephalograptus* and *Comograptus* followed by the last major diversification of non-retiolitid biserial graptolites, with several new species appearing, particularly of *Parapetalolithus*. Following the *utilis* Event (Loydell 1994, Štorch 1995), which commenced in the late *guerichi* Zone, the remaining non-retiolitid biserial genera (*Glyptograptus*, *Metaclimacograptus*, *Parapetalolithus*) are represented by few species in the succeeding lower–middle Telychian biozones and in the *spiralis* Biozone none of these genera has any remaining representatives. Retiolitid graptolites also showed a major phase of diversification during the early Telychian and they were also seriously affected by the *utilis* Event (Loydell 1994), but they remained an important element of graptolite faunas through

to their eventual demise in the Ludlow Epoch. It is important to note that Cooper *et al.* (2014) mistakenly placed the *utilis* Event in the late *turriculatus* and *crispus* zones. They refer also to "high levels of species richness through the *turriculatus* zone". The *turriculatus* Biozone worldwide is characterized by significantly lower species diversity than the underlying *guerichi* Biozone, so this statement by Cooper *et al.* (2014) is also incorrect.

Melchin (1989) demonstrated that provincialism within Llandovery graptolites was greater than generally previously appreciated except perhaps by those working in North Africa where endemism had necessitated the erection of new biozones and created major challenges in correlation with the "standard" scheme (see *e.g.* Legrand 2003). Melchin (1989) showed that certain graptolite taxa were restricted to the Silurian tropics. The degree of provincialism of Silurian graptolites appears to have varied through the period; for the late Aeronian and early Telychian it does not appear to have been pronounced. Although Loydell

(1990a) noted that records of the multicladiate early Telychian genus *Sinodiversograptus* are restricted to localities at tropical palaeolatitudes, few other taxa appear to show a significant geographical restriction. Within the El Pintado collections are several examples of species previously recorded only from South China, *e.g. Glyptograptus nanjiangensis*, *Parapetalolithus curvithecatus*, *Pa. fusiformis* and *Pristiograptus xiushanensis* and/or other Silurian tropical locations, *e.g. Torquigraptus minutus* and *Streptograptus richardsonensis*. Overall, therefore, this interval appears to be one characterized by largely cosmopolitan taxa.

Loydell (1994) emphasized the difference between graptolite assemblages from different Llandovery environments, with *Parapetalolithus* and retiolitid genera being less common in deeper water settings. It may be that the outer shelf location of the El Pintado sections is responsible for the relatively low abundance of *Parapetalolithus* here (by comparison for example with Bohemian sections, the Western Iberian Cordillera, Spain and the Yangtze Platform) and very low abundance and diversity of retiolitids.

Graptolite biostratigraphy of the El Pintado sections

Charts showing the stratigraphical ranges and relative abundance of all taxa collected are presented in Figs 9 and 10.

Three biozones are recognised in the measured part of the El Pintado sections: *Stimulograptus halli*, *Spirograptus guerichi* and the lowermost part of the *Sp. turriculatus* Biozone. Collecting commenced in the lower part of the *Stimulograptus halli* Biozone which overall is represented by 4 m of strata. The biozone can readily be split into three parts: a lower subzone containing several species known also from the *Stimulograptus sedgwickii* Biozone in addition to *St. halli*; a middle part characterized by *Lituigraptus rastrum* (referred to here as the *rastrum* Subzone) within which several species of *Rastrites* appear; and an upper subzone, between the LAD of *L. rastrum* and the FAD of *Spirograptus guerichi*, containing in its basal 0.4 m common *Oktavites zanclus* sp. nov. (Figs 19E, 21C, I, J).

The *Spirograptus guerichi* Biozone is represented by approximately 13.8 m of strata. Numerous species appear within the biozone, notably of *Streptograptus* (which shows very low diversity in the Aeronian) and *Parapetalolithus*. "*Monograptus*" *gemmatus* occurs in the lower two-thirds of the biozone. Within the upper third of the biozone several species have their LADs; biostratigraphically important taxa appearing within the upper *guerichi* Biozone include *Monograptus marri*, *Streptograptus barrandei*, *Torquigraptus planus* and *Pristiograptus bjerringus*.

Only the lowermost part of the *Spirograptus turriculatus* Biozone was sampled. *Streptograptus johnsonae* appears at the base of the biozone together with

Torquigraptus dextrorsus and other taxa, including *Monograptus priodon*, appear in the succeeding samples.

The total number of species (including those left in open nomenclature) present in the two sections is 118, of which 18 are new. This high number of species overall is undoubtedly in part a reflection of the very large sample size, but also is a manifestation of the major diversifications taken place within some genera globally at this time. The large number of new species is most probably a result also of the lack of studies on (and of sections yielding) uppermost Aeronian and lowermost Telychian graptolites.

The biostratigraphy of the various genera present at El Pintado is discussed briefly below.

Biserial graptolites. – *Cephalograptus extrema*, the last surviving species in the genus, makes its final appearance in the same sample in which *Lituigraptus rastrum* makes its first, within the lower half of the *halli* Biozone. *Comograptus* is represented at El Pintado by a single specimen of *C. barbatus* in the lower *halli* Biozone.

Glyptograptus is represented by 13 species at El Pintado, including four new species and one left in open nomenclature. Specimens that are preserved obliquely to bedding can be difficult to identify and far more specimens of this genus are specifically indeterminate than are, for example, those of *Parapetalolithus* which are generally preserved in the optimal (from an identification perspective) bi-profile orientation. Of the previously described species, some are stratigraphically long-ranging, *e.g. G. elegans* (Fig. 18K), *G. latus* (Figs 16H, 18R) previously recorded only from the lower Aeronian *Demirastrites triangulatus* Biozone; Packham 1962) and *G. tamariscus* (Figs 16N, W, 18P) the El Pintado specimens of which are characterized by shallow apertural excavations and long supragenicular walls and are thus similar to those recorded from the upper Aeronian and lower Telychian of Wales (Loydell 1992). Some other *Glyptograptus* species are restricted to the uppermost Aeronian and lowermost Telychian, *e.g. G. auritus* (some mature specimens of which show the oval carbon film at the proximal end; Fig. 19H), *G. nanjiangensis* (described below, previously recorded only from China, *e.g.* Chen 1984) and *G. supernus* (Figs 16C, 18E, S). Probably the most useful species biostratigraphically is the distinctive *G. fastigatus* (Figs 16V, AA, 18B–D, 20K), which occurs at El Pintado only in the lower Telychian *Spirograptus guerichi* Biozone as it does also in Wales (Loydell 1992).

Three species of *Metaclimacograptus* are present in the upper Aeronian to lower Telychian of the El Pintado sections. Both *Me. hughesi* (Fig. 16X, AC) and *Me. undulatus* (Fig. 16Q) are stratigraphically long-ranging species, first appearing in the Rhuddanian (*e.g.* in the *vesiculosus* Biozone in Jordan; Loydell 2007b) and making their last appearances in the middle *halli* Biozone and lower *guerichi* Biozone respectively. Although *Me. undulatus* is
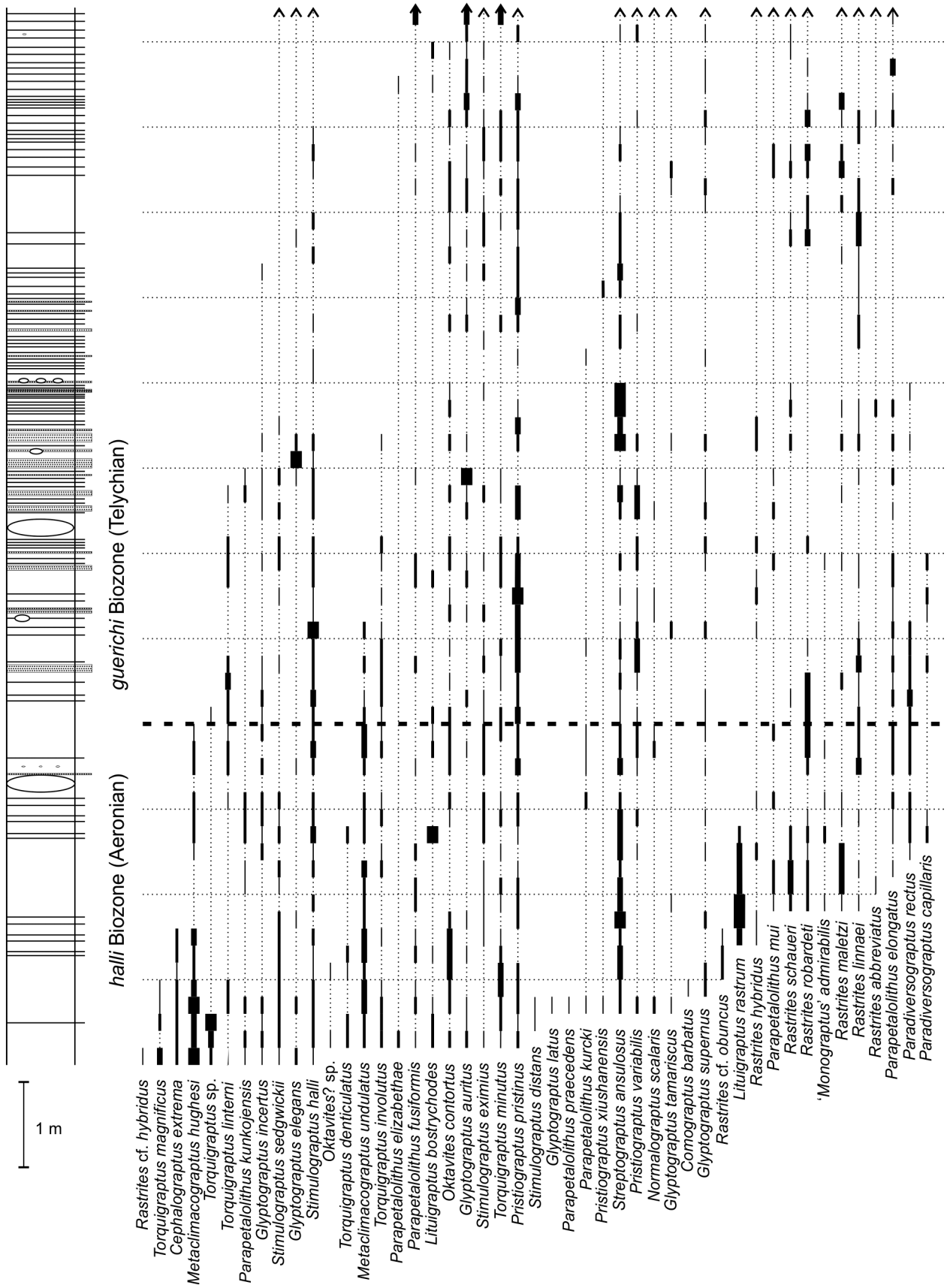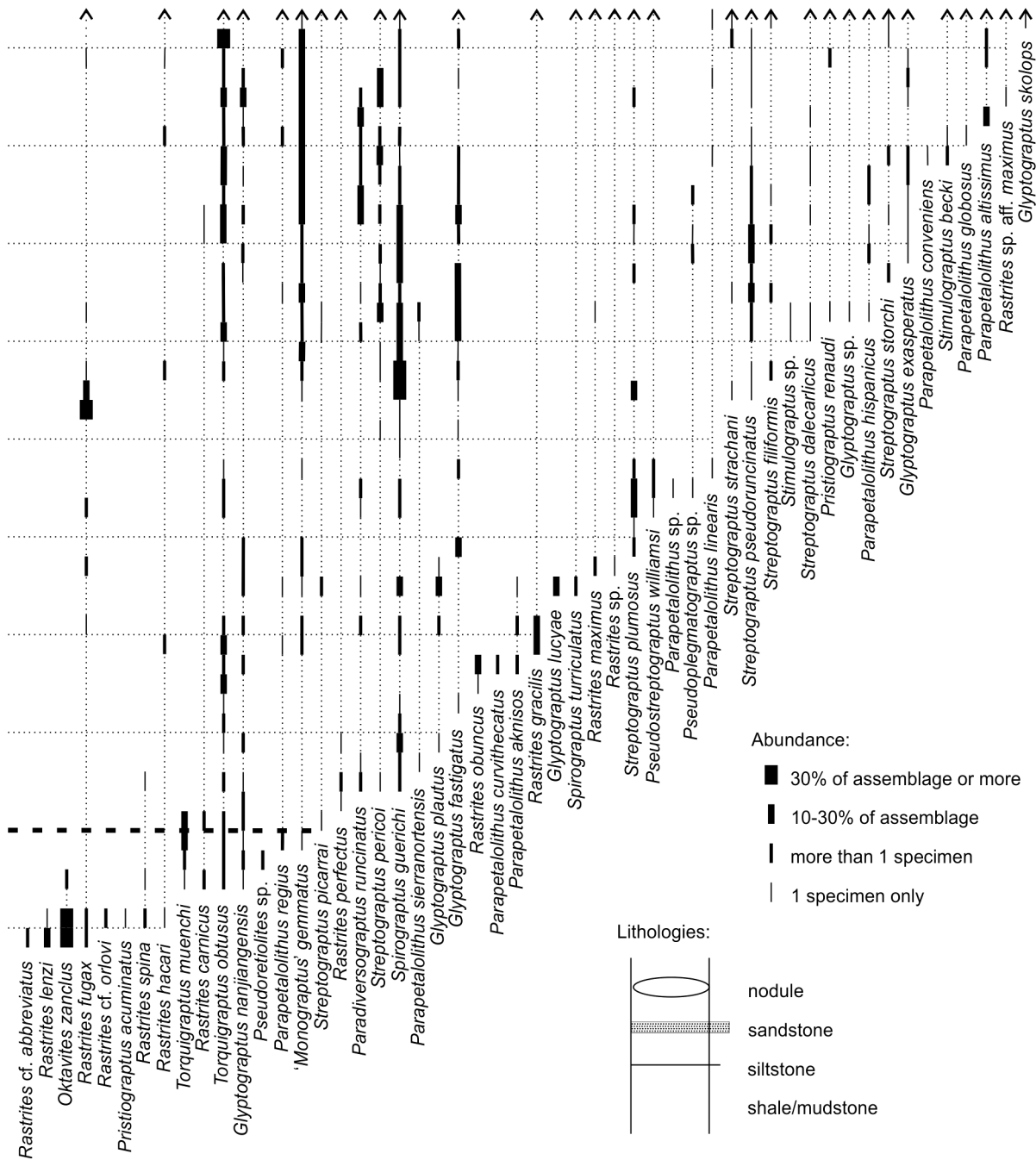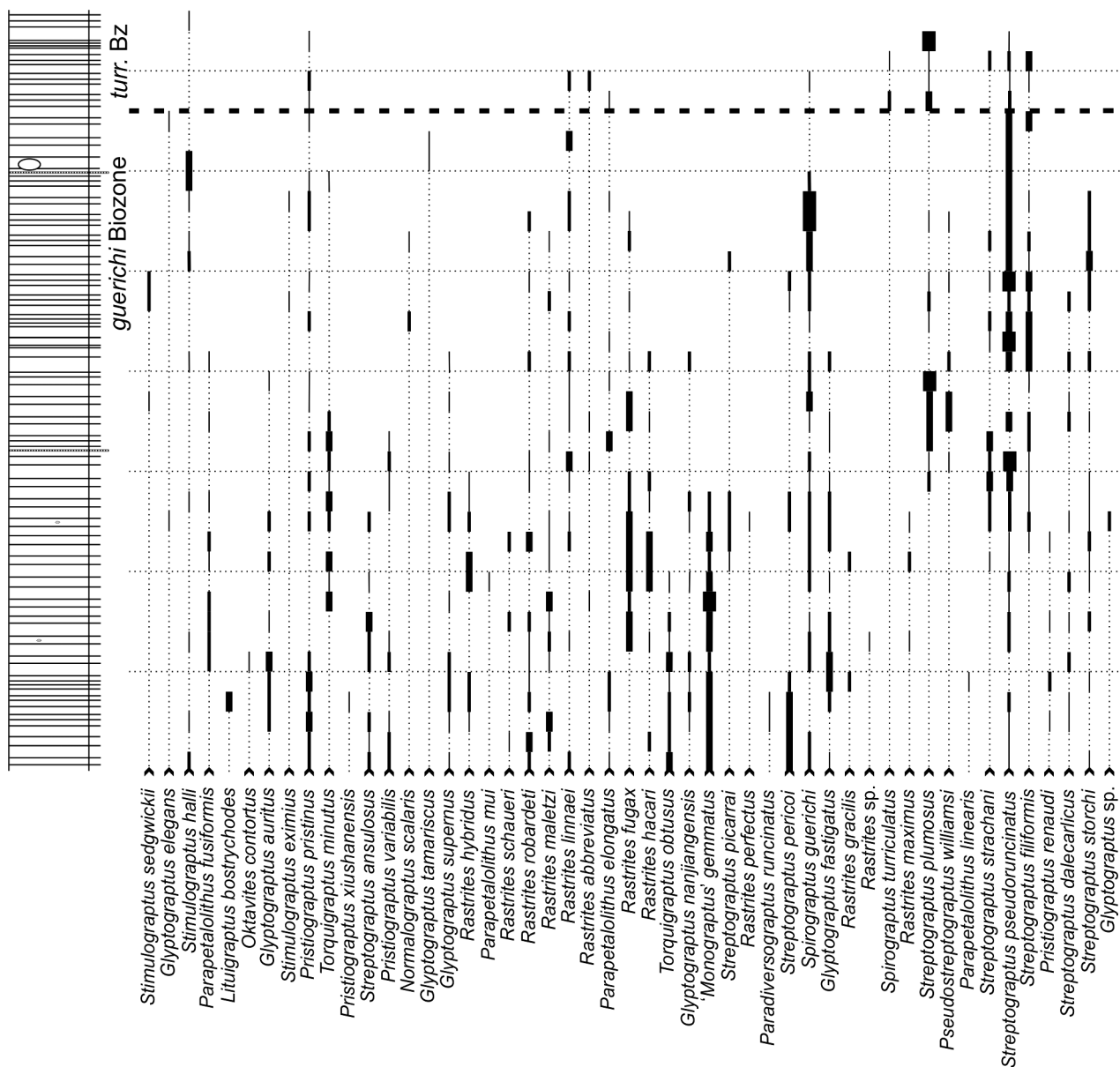
Figure 9. Range chart of graptolites in El Pintado section 1. Arrows indicated that stratigraphical ranges extend into higher strata in section 5.

common at El Pintado, it does not attain the very high abundances that characterize some levels in the upper Aeronian in the Czech Republic (Štorch & Frýda 2012) and in mid Wales (Loydell 1991a, 1992). Instead and unusually, *Me. hughesi* is very abundant in the lower part of the *halli* Biozone. *Me. undulatus* disappears at El Pintado at a similar level to that in Wales, low in the *guerichi* Biozone. *Me. asejradi* (Fig. 16AB) appears at a similar stratigraphical level in El Pintado section 5 to that at which it

appears in the Central Iberian Zone and Western Iberian Cordillera of Spain (Štorch 1998a), but is much less common at El Pintado. Robardet & Gutiérrez-Marco (2002) observed that *Me. asejradi* has "never been found in the Ossa Morena Zone" so the rare specimens documented herein are the first to be recorded.

Parapetalolithus experienced a major diversification through the late Aeronian and early Telychian, with 20 species recorded from El Pintado. Many species are rare. Several
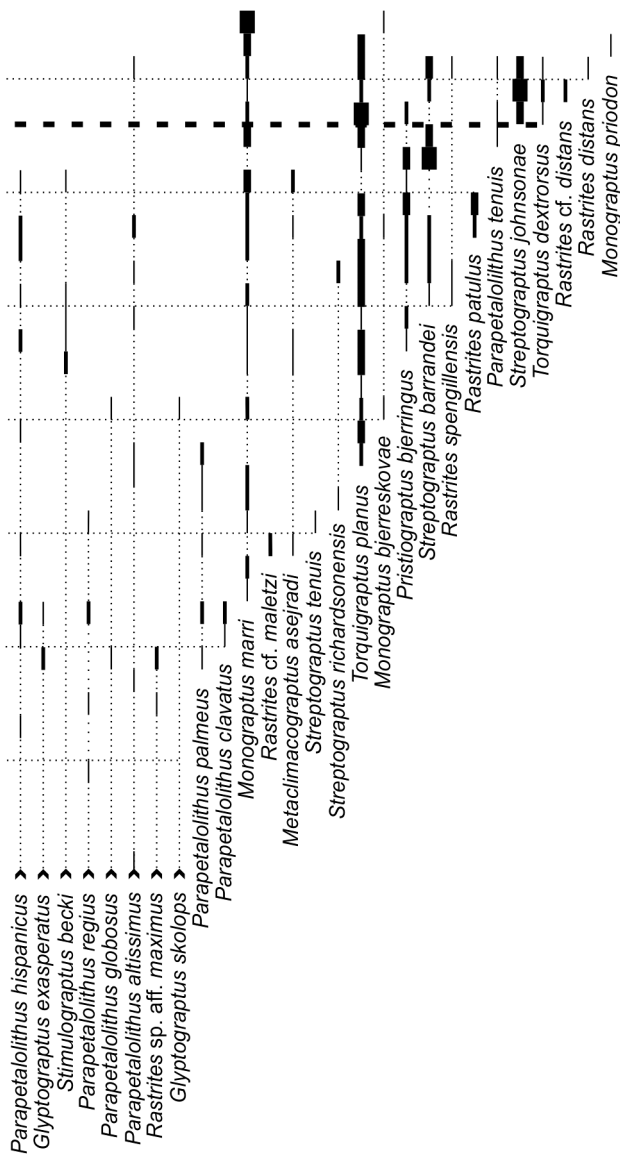
Figure 10. Range chart of graptolites in El Pintado section 5. Arrows indicate that taxa occur at lower stratigraphical levels in section 1. See Fig. 9 for explanation of bar widths and lithological symbols used. *turr.* Bz – *turriculatus* Biozone.

are known only from the *guerichi* Biozone. *Pa. tenuis* (Fig. 18AJ) appears at the base of the *turriculatus* Biozone. The stratigraphical range of *Pa. altissimus* (Figs 16AE, 18AE) is extended downwards to the middle *guerichi* Biozone; previous records were from the *turriculatus* Biozone and higher stratigraphical levels. Retiolitid graptolites are also rare in the collected El Pintado material. Whilst it is possible that they were overlooked in the field, the large area of bedding surfaces examined under the microscope would suggest that they were not at all common. The material collected is fragmentary and identifiable only to genus level (*Pseudoretiolites* and *Pseudoplegmatograptus*). It is not illustrated herein.

Uniserial graptolites. – *Lituigraptus* is represented by the relatively long-ranging *L. bostrychodes* sp. nov. (identified previously by several authors as "*Monograptus*" *pulcherrimus*) and the very useful subzonal index *L. rastrum*. *Oktavites* exhibits a similar low diversity: *O. contortus* (Figs 19D, 20E, 21W) ranges through the upper Aeronian through to the middle *guerichi* Biozone; *O. zanclus* sp. nov. is common in the upper *halli* Biozone, but is known only from El Pintado.

Monograptus sensu stricto is represented by three species at El Pintado. *Monograptus bjerreskovae* (Fig. 21AI) is rare by comparison with Wales (Loydell 1993b), perhaps suggesting that it is predominantly a deeper water taxon.

Parapetalolithus hispanicus
Glyptograptus exasperatus
Stimulograptus becki
Parapetalolithus regius
Parapetalolithus globosus
Parapetalolithus altissimus
Rastrites sp. aff. maximus
Glyptograptus skolops
Parapetalolithus palmeus
Parapetalolithus clavatus
Monograptus marri
Rastrites cf. maletzi
Metaclimacograptus asejradi
Streptograptus tenuis
Streptograptus richardsonensis
Torquigraptus planus
Monograptus bjerreskovae
Pristiograptus bjerringus
Streptograptus barrandei
Rastrites spengillensis
Rastrites patulus
Parapetalolithus tenuis
Streptograptus johnsonae
Torquigraptus dextrorsus
Rastrites cf. distans
Rastrites distans
Monograptus priodon

Pseudostreptograptus is represented by one species, *Ps. williamsi* (Fig. 21Q), which ranges through much of the *guerichi* Biozone.

Many *Rastrites* specimens are fragmentary (Fig. 20B), in some cases occurring as single thecae, particularly in the coarser laminae. With the exception of the extraordinarily long thecae of *Rastrites maximus* (Fig. 23AB) these fragments are not identifiable to species level. More complete material is fortunately also abundant and has enabled identification of 26 species overall (including those in open nomenclature). Stratigraphical ranges are in accord with previous studies (*e.g.* Schauer 1967, Štorch & Loydell 1992, Loydell 1993b).

The two *Stimulograptus* species after which upper Aeronian biozones are named, *St. sedgwickii* and *St. halli*, both range significantly above the top of their biozones into the upper *guerichi* and lower *turriculatus* biozones respectively both at El Pintado and in Wales (Loydell 1993b). The other *Stimulograptus* species are rare at El Pintado, with the exception of *St. eximius* sp. nov. (Figs 19C, 20D, I, 21AT), which is currently known only from this locality.

Major diversification occurred in *Streptograptus* in the early to mid *guerichi* Zone. Of the 12 species recorded from the *guerichi* Biozone at El Pintado, only one makes its first appearance in the Aeronian, eight in the lower half of the *guerichi* Biozone and three [*S. richardsonensis* (Fig. 17C), *S. tenuis* (Fig. 21U) and *S. barrandei* (Figs 21AN, AO)] in its upper part. *S. ansulosus* (Figs 19N, 21AG) is conspicuously more common at El Pintado than at other localities. *S. tenuis* is a rare species, both at El Pintado and elsewhere, and has not previously been recorded from the *guerichi* Biozone, so its range has been extended stratigraphically downwards. *S. storchi* (Fig. 17B, I) is most characteristic of the *turriculatus* Biozone (being common in Bohemia in the uppermost part of the biozone), but has been recorded previously from the upper *guerichi* Biozone in Wales (Loydell 1993b). In the El Pintado sections it first appears in the middle of the *guerichi* Biozone. *S. johnsonae* (Fig. 19M) is a very useful marker for the base of the *turriculatus* Biozone. It is far more common at this level at El Pintado than it is in Wales (Loydell 1993b).

Short proximal fragments of many *Torquigraptus* species are impossible to identify and rhabdosome torsion can produce inconvenient views of mesial and distal fragments, with thecal details obscured. The *halli* Biozone contains several species, including two [*T. denticulatus* (Fig. 21F, N, S), *T. magnificus* (Fig. 22A, J)] at the end of their stratigraphical range and others, *e.g. T. minutus* and *T. obtusus* (both described below) that first appear in the *halli* Biozone and range into the *guerichi* Biozone. A narrow species, referred to here as *T.* sp. (Fig. 22H), is abundant in the lower *halli* Biozone. The range of *T. obtusus* does not extend into the upper part of the *guerichi* Biozone within which *T. minutus* is represented by a single

M. marri (Fig. 21AJ) first appears in the upper part of the *guerichi* Biozone as it does also in Wales (Loydell 1993b) and Sweden (Loydell & Maletz 2004). *M. priodon* (Fig. 21AK) makes its only appearance at El Pintado low in the *turriculatus* Biozone, similar to its first occurrence on Bornholm (Bjerreskov 1975; see Loydell 1993b for further discussion). It has never been recorded from the *guerichi* Biozone.

Pristiograptus species can be divided into those that have straight rhabdosomes and those that are dorsally curved. Within the former group, *P. bjerringus* (Figs 18P, W, 22E) is the most useful, first appearing in the upper *guerichi* Biozone at El Pintado, on Bornholm (Bjerreskov 1975), in Wales (Loydell 1993b) and in Bohemia. The two dorsally curved species, *P. renaudi* (Fig. 19R) and *P. xiushanensis* (Fig. 22G), are rare at El Pintado. They are discussed further below.

specimen. At this stratigraphical level *T. planus* (Fig. 20C) appears at El Pintado and at other localities (*e.g.* in Wales and China; Loydell 1993a, b).

The abundance of individual species varies significantly from horizon to horizon (Figs 9, 10), highlighting the value of sampling from all horizons to get as complete a picture as possible of species' ranges and abundance.

Upper Aeronian–lower Telychian graptolite biozonations and the base of the Telychian Stage

Upper Aeronian graptolite biozonations. – Loydell (1991a) resurrected the *Stimulograptus halli* Biozone, erected by Jones & Pugh (1916) in mid Wales, for uppermost Aeronian strata between the *sedgwickii* Biozone and the *guerichi* Biozone. The biozone has not received universal acceptance. In some places of course there are no graptolitic strata of latest Aeronian age, but in Arctic Canada Melchin & Holmden (2006) placed uppermost Aeronian strata yielding *Stimulograptus halli* in their upper *sedgwickii* Biozone. Štorch & Frýda (2012) erected a new biozone for the distinctive, abundant, short-ranging *Lituigraptus rastrum*. The latter is undoubtedly an extremely useful species, as can be seen from its stratigraphical range in El Pintado section 1 and for this reason the middle part of the *halli* Biozone at El Pintado is referred to the *rastrum* Subzone. Reasons for not according this interval full biozonal status (but retaining it as a subzone) are discussed below. Melchin *et al.* (2015) suggested that the lower part of the *L. rastrum* Biozone of Štorch & Frýda (2012) correlates closely with the base of the *halli* Biozone. The El Pintado ranges indicate that this is not the case, with *St. halli* appearing significantly lower in the section.

It is very straightforward to distinguish *Stimulograptus halli* from *Stimulograptus sedgwickii* if one has a proximal end where the difference in rate of increase in dorso-ventral width is easily seen (compare Fig. 21AR and Fig. 21AS). Problems can arise when only fragmentary or obliquely preserved material is available – these will not be identifiable to species level and the accompanying assemblage, should there be one, will be required to determine the biozone. It is likely that Jones & Pugh (1916) and Loydell (1991a, 1992) found the *halli* Biozone to be so readily recognizable because of the nature of the mid Welsh stratigraphical record: the black graptolitic mudstones of the *sedgwickii* Biozone are separated from thin graptolitic bands within the upper half of the *halli* Biozone by several metres of non-graptolitic strata (Fig. 1). During the time taken to deposit these, the composition of graptolite faunas changed and the differences within collected assemblages is obvious. In the Prague Synform, however, the transition from *sedgwickii* to *halli* Biozone is within graptolitic strata

and thus changes within assemblages of graptolites collected bed-by-bed are more gradual. Recognition of the base of the *halli* Biozone would most probably depend upon identification of the eponymous species. It is very likely that the upper part of Štorch & Frýda's (2012) upper *sedgwickii* Biozone is equivalent to the lower *halli* Biozone of El Pintado.

A comparable situation to that affecting the base of the *halli* Biozone in Wales, but this time resulting from non-graptolitic strata in the Prague Synform, affects the *Lituigraptus rastrum* Biozone which is separated from the succeeding Telychian strata in Bohemia by non-graptolitic mudstones. The lowermost Telychian biozone recognised here is the *Rastrites linnaei* Biozone and the assemblage from the lowermost graptolitic bed in this biozone indicates that this horizon lies at a level equivalent to the upper part of the *guerichi* Biozone. The last appearance of *L. rastrum* is immediately beneath the non-graptolitic mudstones. Looking at the El Pintado section 1 record it seems very likely that the graptolitic part of the *L. rastrum* Biozone of Štorch & Frýda (2012) in Bohemia comprises perhaps only the lower one-third of the total stratigraphical range of the species, which at El Pintado comprises a total thickness of 1.4 m. This is supported also by the $\delta^{13}C_{org}$ records (see below). Of the several *Rastrites* (and two *Parapetalolithus*) species appearing within the range of *L. rastrum* at El Pintado, only *R. schaueri* is known from the *L. rastrum* Biozone in Bohemia, suggesting that the other *Rastrites* species first appeared during the time when non-graptolitic muds were being deposited in the Prague area. There is more than 1 m of strata between the last appearance of *L. rastrum* at El Pintado and the base of the Telychian (if based on the first appearance of *Sp. guerichi*).

Loydell (1991a, 1992) recorded *Rastrites linnaei* from the *halli* Biozone of Wales and it occurs also within the same biozone at Dob's Linn (Loydell 1991b). It makes its first appearance at El Pintado 0.4 m above the first appearance of *L. rastrum* (Fig. 9). Figure 11 shows the two species on the same bedding surface.

As is frequently the case, a continuously fossiliferous section with extensive collections blurs the simpler picture available from less continuously fossiliferous locations. The Bohemian biozonation proposed by Štorch & Frýda (2012) for the upper Aeronian and lower Telychian (*Stimulograptus sedgwickii*, *Lituigraptus rastrum* and *Rastrites linnaei* biozones) if used at El Pintado would result in a *rastrum* Biozone only 0.4 m thick overlain by a *Rastrites linnaei* Biozone approximately 15 m thick which would include the "traditional" base of the Telychian based upon the first appearance of *Spirograptus guerichi*. Use of the biozonation that originated from study of Welsh sequences (*Stimulograptus sedgwickii*, *St. halli* and *Spirograptus guerichi* biozones) retains the problem of recognising the base of the *St. halli* Biozone when proximal

ends of the eponymous species are not available. There is no perfect solution. For the El Pintado sections we are using the *halli* and *guerichi* biozones and recognise that there is a very distinctive stratigraphical interval (the *rastrum* Subzone) in the middle of the *halli* Biozone comprising the total stratigraphical range of *L. rastrum*.

The base of the Telychian Stage. – The base of the Telychian Stage has long been recognised to be poorly defined biostratigraphically at its GSSP in the type Llandovery area (Temple 1988, Loydell 1993a). As a result, for practical purposes most authors have simply assumed that the base of the Telychian and that of the *Spirograptus guerichi* graptolite Biozone are effectively coincident, following the original contention that the boundary correlated with the base of the *Spirograptus turriculatus* Biozone (Bassett 1985), a biozone subsequently divided into a lower *Spirograptus guerichi* Biozone and an upper *Spirograptus turriculatus* Biozone (see Loydell *et al.* 1993 for differences between the two taxa based upon chemically isolated material). *Sp. guerichi* and *Sp. turriculatus* have a very similar helically coiled rhabdosome morphology and it is not uncommon to see incomplete or poorly preserved specimens referred to as *Sp. turriculatus sensu lato* (meaning either *Sp. guerichi* or *Sp. turriculatus*). In addition to the biostratigraphical inadequacies of the GSSP, recent mapping of the type Llandovery area has revealed that the area around the Telychian GSSP was subject to intra-Wenlock synsedimentary sliding which has generated a complex mélange here of Llandovery and Wenlock strata (Davies *et al.* 2011, 2013). It is clear that this GSSP can no longer serve its original purpose.

Defining the base of the Telychian Stage using the FAD of *Spirograptus guerichi* seems sensible and, given that the upper Aeronian and lower Telychian are encompassed by a single conodont biozone (*Distomodus staurognathoides*) and a single chitinozoan biozone (*Eisenackitina dolioliformis*) (Melchin *et al.* 2012) it appears that for this stage boundary graptolites are the only fossil group available to aid in its definition. Other graptolite species appear at about the same stratigraphical level as *Sp. guerichi*, *e.g.* "*M.*" *gemmatus* (Fig. 21AF) and several species of *Streptograptus*, providing a good number of biostratigraphical indicators for the lowermost Telychian.

The limited amount of chemostratigraphical data available through this interval (Melchin & Holmden 2006, Štorch & Frýda 2012; Fig. 13) suggests that there are no major carbon isotope excursions close to the stage boundary, although detailed comparison of δ^{13}C shows remarkable similarities between Arctic Canada and El Pintado (see below).

Although the first appearance of *Spirograptus guerichi* is in the sample from 4.4–4.6 m above the base of the studied part of El Pintado section 1, a *Spirograptus* proximal
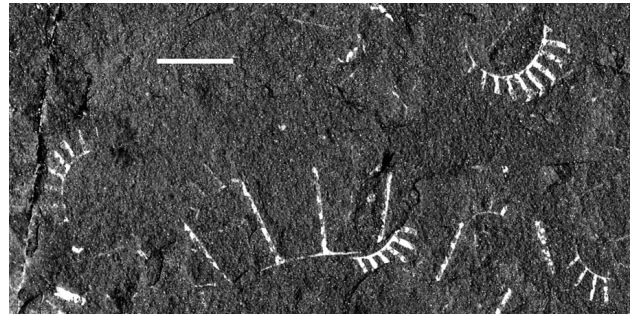
Figure 11. Slab from just below half way through the total stratigraphical range (sample 1.10) of *Lituigraptus rastrum* (Richter) bearing both *L. rastrum* and the stratigraphically lowest specimen of *Rastrites linnaei* (Barrande), MGM7800-O. Scale bar represents 5 mm.

end was found in the collection from 4.0–4.2 m. It is very possible therefore that more intensive collecting would reveal additional specimens confidently identifiable as *Spirograptus guerichi* from a slightly lower stratigraphical level than its first appearance as shown on Fig. 9. Field notes record that graptolites were generally "very sparse" in the interval from 4.0 to 4.4 m: the collections of 98 and 48 specimens identifiable to species level from 4.0–4.2 m and 4.2–4.4 m respectively required several hours to amass. In the 3.8–4.0 m level, however, the strata contained "moderately abundant" graptolites and a collection of 215 specimens identifiable to species level was more easily obtained, but without any *Spirograptus*. On this basis it would seem likely that the base of the Telychian, as based upon the FAD of *Spirograptus guerichi*, lies at about the 4.0 m level and this is where it is shown on Figs 9, 13 and 14.

Inevitably, given that this is the first graptolitic section through the Aeronian–Telychian transition to be documented, some species previously recorded only from either the Aeronian or the Telychian are shown herein to occur also in the over- or underlying stage. *Torquigraptus linterni*, recorded previously only from the upper Aeronian (Williams *et al.* 2003) occurs at El Pintado also in the lower fifth (in terms of stratal thickness) of the *guerichi* Biozone. Of those species previously recorded as restricted to the lower Telychian, *Glyptograptus auritus*, *G. nanjiangensis*, *Parapetalolithus elongatus*, *Pa. fusiformis*, *Pa. kunkojensis*, *Rastrites fugax* and *Torquigraptus minutus* all occur in the Aeronian at El Pintado with first appearances 1 m or more below the first appearance of *Sp. guerichi*. It is appropriate to note here that *Paradiversograptus runcinatus* does appear to be restricted to the lower Telychian. Loydell (1991a) recorded *Par. runcinatus* from the *halli* Biozone. This record was based upon a single occurrence at Nant Fuches-wen quarry (Loydell 1992, Loc. C3), an identification subsequently corrected to *Par. rectus* in Loydell (1993b). Melchin *et al.* (2012) refer to an Aeronian occurrence of *Par. runcinatus* in Wales, but this was based upon Loydell's (1991a) misidentification.
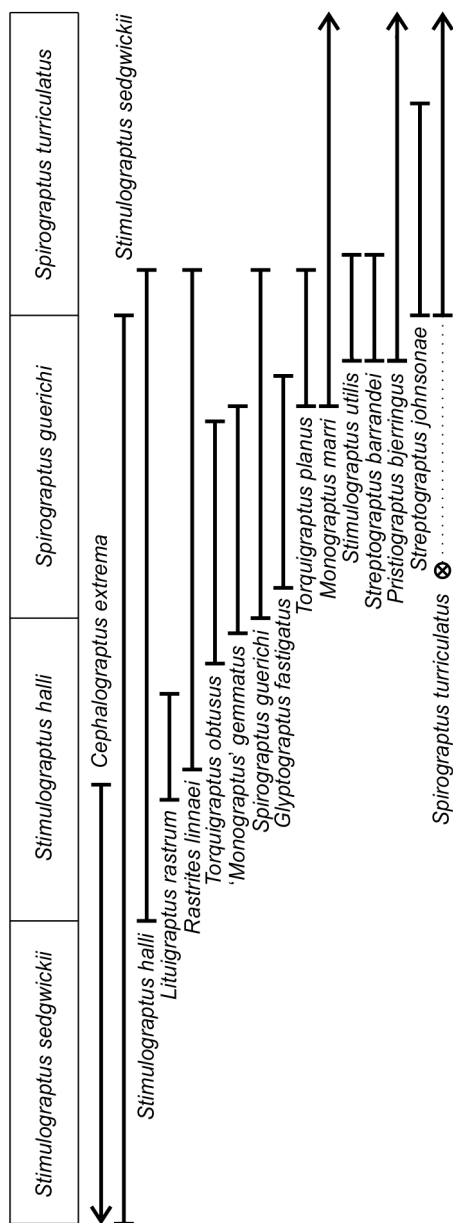
Figure 12. Stratigraphical ranges of key graptolite species through the upper Aeronian and lower Telychian, based on records from published sections worldwide. The circle with the cross marks the level of the stratigraphically very early specimens of *Spirograptus turriculatus* from El Pintado section 1. Arrows indicate that stratigraphical range extends downwards or upwards.

Lower Telychian biozones and subzones. – There have been various local subzonations applied to what is now the *Spirograptus guerichi* Biozone. Bouček (1953) divided what is now recognised to be the middle to upper part of the biozone into a lower *Parapetalolithus palmeus* Subzone and an upper *Pa. hispanicus* Subzone. Loydell (1993b) divided the *guerichi* Biozone of western mid Wales into four subzones: *Paradiversograptus runcinatus*, "*Monograptus*" *gemmatus*, *Pristiograptus renaudi* and lower *Stimulo-graptus utilis*. These subzones were subsequently recognised individually or in combination elsewhere in Wales (Davies *et al.* 1997) and in the Western Iberian Cordillera of Spain (Gutiérrez-Marco & Štorch 1998).

Loydell (1992) observed that the *Pa. palmeus* and *Pa. hispanicus* subzones could not be recognised in western mid-Wales and indeed the taxa first appeared there in the reverse of the order seen in Bohemia. Gutiérrez-Marco & Štorch (1998) were able to recognise these subzones in the Western Iberian Cordillera, but in the El Pintado sections, as in Wales, *Pa. hispanicus* appears before *Pa. palmeus* and the two subzones cannot be used.

Loydell (1992) warned that the abundance of *Paradiversograptus runcinatus* in the lower *guerichi* Biozone of western mid-Wales might reflect current sorting by turbidity currents – the graptolites are preserved primarily within turbidite sandstones – rather than original abundance. Loydell (1993b) noted also that although assemblages with abundant *Par. runcinatus* occurred in western mid-Wales only in the lower *guerichi* Biozone, the species' overall stratigraphical range there was significantly greater, encompassing the entirety of the *guerichi* Biozone, and that, although on Bornholm the species was restricted to the lower part of the biozone (Bjerreskov 1975), in the Cross Fell inlier of northern England it is not uncommon in the upper part of the *guerichi* Biozone. In the El Pintado sections, *Par. runcinatus* (Fig. 22O) occurs throughout the lower half of the *guerichi* Biozone, with the greatest relative abundance recorded towards the top of its stratigraphical range here (Fig. 9). At some levels, indifferent preservation prevents separation of the species from others with similar rhabdosome morophology and width, but rather more complex thecae, *e.g. Streptograptus pericoi* (Figs 17G, 21AB, AL, AM).

"*Monograptus*" *gemmatus* first appears in western mid-Wales, as it does also in El Pintado section 1 at a very similar level to *Spirograptus guerichi*. It becomes abundant in the middle–upper part of its range and seems a very useful indicator of the lower two-thirds of the *guerichi* Biozone.

Pristiograptus renaudi was common within the middle to upper *guerichi* Biozone in western mid-Wales, but has not proved to be so abundant elsewhere, with the exception of Saudi Arabia (Zalasiewicz *et al.* 2007) where it was part of a very low diversity assemblage enabling for the first time recognition of a Teychian graptolite assemblage on the Arabian plate. Care must be taken in distinguishing *P. renaudi* from the similarly dorsally curved *P. xiushanensis*.

Stimulograptus utilis was, as its name implies, extremely useful biostratigraphically in Wales. It is yet to be identified from elsewhere, however.

A common result of the examination of very large collections of fossils is the discovery of taxa (usually as rare or
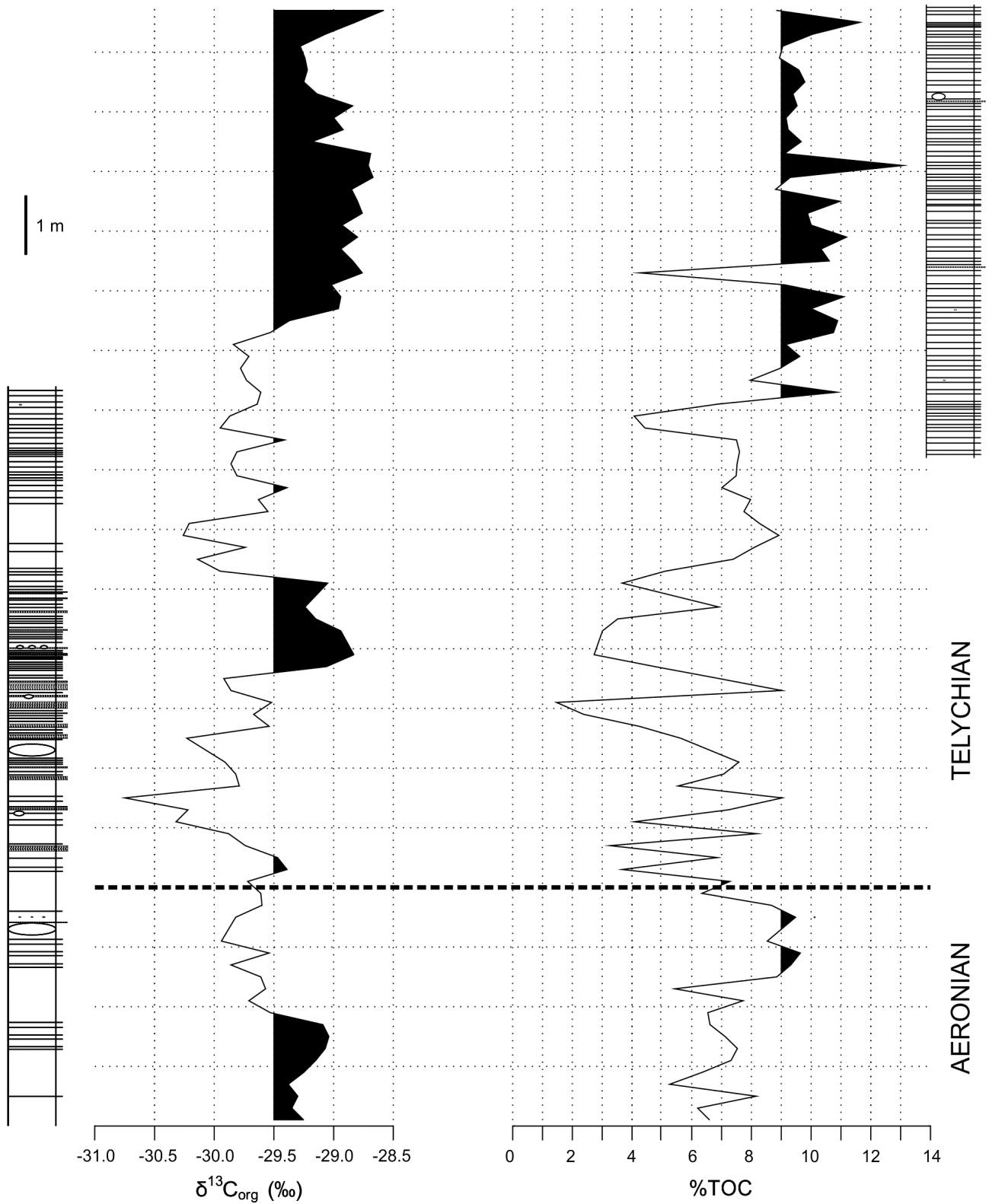
Figure 13. The $\delta^{13}C_{org}$ and TOC records through El Pintado sections 1 and 5. Shading is used to highlight higher (*i.e.* less negative) $\delta^{13}C_{org}$ (above −29.5‰) and TOC (above 9%) values. See Fig. 9 for explanation of lithological symbols used.

unique specimens) outside of their previously recorded stratigraphical ranges. In some cases this can provide insights into the pattern and severity of extinction events. A good example is Štorch *et al.*'s (2011) study of the Upper Ordovician of Nevada in which several "typical" Katian taxa (including, for example, *Appendispinograptus* and *Dicellograptus*) were found to be present in the Hirnantian. For biostratigraphical work such rare anomalous occurrences are very significant. Now when visiting a new locality a collection made comprising a single specimen of *Dicellograptus* no longer can be taken to demonstrate with absolute certainty a pre-Hirnantian age for the strata present, although of course, given the extreme rarity of the genus in Hirnantian strata worldwide, this is the most likely age. The El Pintado section provides a similar anomalous occurrence, in this case of a taxon appearing significantly lower than previously recorded: two well-preserved specimens of *Spirograptus turriculatus* (Fig. 17T) occur low in the *Spirograptus guerichi* Biozone. Elsewhere in Spain (Gutiérrez-Marco & Štorch 1998) and in peri-Gondwanan Europe in general (*e.g.* Bohemia: Bouček 1953, Štorch 1994; Germany: Schauer 1971) *Sp. turriculatus* appears at a higher stratigraphical level in the lower Telychian and its appearance marks the base of the *Sp. turriculatus* Biozone. Loydell *et al.* (1993) reviewed the occurrence of *Spirograptus* species worldwide and demonstrated the ubiquity of a lowest Telychian *Sp. guerichi* Biozone succeeded by a *Sp. turriculatus* Biozone, their bases being defined by the first appearances of the eponymous species.

The question arises as to how to deal with the early occurrence of a biozonal index species. The fact that a *turriculatus* Biozone has been used successfully worldwide suggests that there would be little practical value in redefining the base of the *turriculatus* Biozone at El Pintado or elsewhere. In large part this is because there is such a wide range of taxa that occur in the preceding *guerichi* Biozone but not in the *turriculatus* Biozone. The transition from the *guerichi* to the *turriculatus* biozones is marked by the "*utilis*" Event, an interval of extinction and/or rapid species turnover in many graptolite genera (Loydell 1994, Štorch 1995). Combining the biozones to produce a *guerichi-turriculatus* Biozone is a possible approach, but this would mask the general usefulness of the two separate biozones in lower Telychian stratigraphy and is a dramatic step to take based upon the occurrence of just two specimens of *Sp. turriculatus* out of the thousands of

Spirograptus identified worldwide from the *guerichi* Biozone. The proposal here therefore is to retain the existing biozones, but to highlight the possibility (albeit highly unlikely) of encountering *Sp. turriculatus* within the *guerichi* Biozone. The *turriculatus* Biozone at El Pintado is best described as an assemblage zone.

At El Pintado, the base of the *turriculatus* Biozone is placed at the species' first appearance in section 5, near the top of the studied part of section, which is coincident with the first appearance of *Streptograptus johnsonae* (Fig. 10). *S. johnsonae* appears at the base of the *turriculatus* Biozone in both Wales (Loydell 1991a) and Sweden (Loydell & Maletz 2004) and appears to be a very useful marker for this stratigraphical level.

Loydell (1992) placed the base of the *Spirograptus turriculatus* Biozone at the first appearance of the biozonal index. Other taxa (*Parapetalolithus tenuis* and *Streptograptus johnsonae*) appeared at the same level, the latter becoming very abundant a little higher in the *turriculatus* Biozone (the *johnsonae* Subzone erected by Loydell 1991a). *Streptograptus* species are extremely variable in their abundance (see *e.g.* abundance data tabulated by Loydell 1993b and Figs 9 and 10 herein), and it appears that bursts of abundance can occur at any level within each species' stratigraphical range. In El Pintado section 5, two samples containing very abundant *S. johnsonae* can be shown by their accompanying species to be from lower in the *turriculatus* Biozone (at a level equivalent to the upper *utilis* Subzone) than the stratigraphical levels of high abundance characterizing the *johnsonae* Subzone in Wales. The species is, however, exceedingly useful as in indicator of the lower half of the *turriculatus* Biozone.
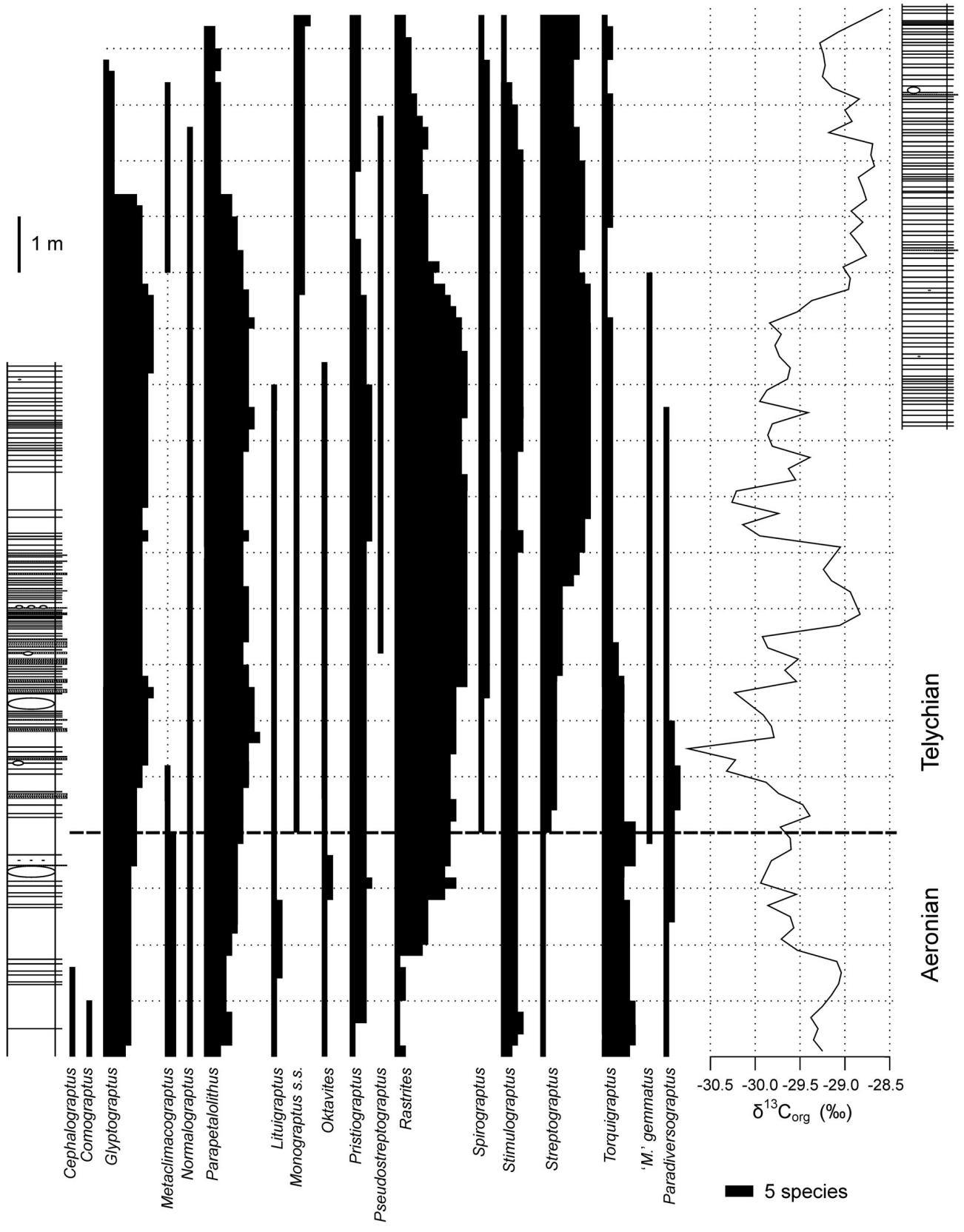
Figure 12 shows the ranges of some of the most stratigraphically important upper Aeronian and lower Telychian graptolite taxa.

The $\delta^{13}C_{org}$ and TOC records

The results of $\delta^{13}C_{org}$ and total organic carbon (TOC) analyses are presented in Fig. 13. No major $\delta^{13}C_{org}$ excursions are evident. Values range from –30.7‰, recorded from the lower *guerichi* Biozone, to –28.6‰, in the lower *turriculatus* Biozone. Intervals of consistently elevated values (above –29.5‰ for more than 1 m of strata) characterize the lower half of the *halli* Biozone (with the peak value in

Figure 14. Graptolite species diversity by genus through the upper Aeronian and lower Telychian of El Pintado sections 1 and 5. A species is counted as present between its FAD and LAD. For the construction of the figure the ranges of some species recorded from the lowermost or uppermost parts of the section have been extended downwards or upwards respectively to reflect absence through collection failure where the species is known to occur at higher stratigraphical levels either at El Pintado or elsewhere. *Monograptus sensu stricto* is shown appearing at the base of the Telychian (reflecting its appearance very low in the *guerichi* Biozone in Wales): *M. bjerreskovae*, the first species of this genus to appear, is very uncommon at El Pintado and its FAD here is much higher than in other sections. See Fig. 9 for explanation of lithological symbols used.

1 m

Cephalograptus
Comograptus
Glyptograptus
Metaclimacograptus
Normalograptus
Parapetalolithus
Lituigraptus
Monograptus s.s.
Oktavites
Pristiograptus
Pseudostreptograptus
Rastrites
Spirograptus
Stimulograptus
Streptograptus
Torquigraptus
'M'. gemmatus
Paradiversograptus

$\delta^{13}C_{org}$ (‰)

-30.5 -30.0 -29.5 -29.0 -28.5

Telychian

Aeronian

5 species

El Pintado   Cape Manning

-31.0   -30.5   -30.0   -29.5   -29.0   -28.5

$\delta^{13}C_{org}$ (‰)

-31.0   -30.5   -30.0

Figure 15. Comparison of the $\delta^{13}C_{org}$ curves for the *Spirograptus guerichi* Biozone of El Pintado and Cape Manning, Cornwallis Island (Melchin & Holmden 2006).

the lowermost *rastrum* Subzone), part of the lower to middle *guerichi* Biozone, and the entirety (more than 5 m of strata) of the upper *guerichi* Biozone and lower *turriculatus* Biozone. Lower values are present within the middle and upper part of the *rastrum* Subzone, upper *halli* and lower *guerichi* biozones (perhaps coinciding with the negative $\delta^{13}C_{carb}$ excursion close to the base of the Telchian shown by Cramer *et al.* 2011) and much of the middle *guerichi* Biozone.

TOC values fluctuate markedly, but are generally highest in the upper *guerichi* Biozone and lower *turriculatus* Biozone. There is no consistent relationship between $\delta^{13}C_{org}$ and TOC values: in the lower part of the section (*halli* to middle *guerichi* biozones) there appears overall to be an inverse relationship; by contrast, both $\delta^{13}C_{org}$ and TOC values are high in the upper *guerichi* Biozone and lower *turriculatus* Biozone, although the TOC values reach their elevated (9–11%) level about 1 m below the level at which $\delta^{13}C_{org}$ values rise to consistently high values (Fig. 13). A similar broad positive correlation between prolonged intervals of high $\delta^{13}C_{org}$ and high TOC was also recorded by Loydell & Frýda (2007) in the upper Telychian–lower Sheinwoodian of the Banwy River section, Wales, and by Loydell *et al.* (2013) in the Rhuddanian of the Murzuq Basin, Libya. No such relationship is apparent in the data of Štorch & Frýda (2012) from Bohemia, however. It appears that the relationship is best developed when TOC values remain high through a significant thickness of strata.

Loydell (2007a) highlighted the relationship between positive carbon isotope excursions and graptolite extinction events. It is noteworthy that graptolite diversity declines markedly through the late *guerichi* Zone (Fig. 14), again at a time of rising/high $\delta^{13}C_{org}$ values. This graptolite event was first examined in detail by Loydell (1994) and named the *utilis* Event by Štorch (1995). The results shown in the El Pintado sections are almost identical to those recorded by Loydell (1994) in his global review of the event (Cooper *et al.* 2014 mistakenly referred to this as a "regional" study), with dramatic diversity declines recorded in *Glyptograptus*, *Parapetalolithus* and *Rastrites* and a significant species turnover in *Streptograptus* within which diversity overall was not seriously affected.

$\delta^{13}C_{org}$ data are available from only three other upper Aeronian to lower Telychian sections. In Bohemia Štorch & Frýda (2012) show a very minor positive excursion low within their *rastrum* Biozone (equivalent to the middle part of the *halli* Biozone of El Pintado) followed by declining values thereafter. The El Pintado record shows a comparable $\delta^{13}C_{org}$ peak in the lowest samples yielding *L. rastrum* with a sharp decline in the middle part of the range of the species. Melchin *et al.* (2015) tentatively correlated the highest of four positive $\delta^{13}C_{org}$ excursions in the Arisaig Group, Nova Scotia, Canada, close to the LAD of *Eocoelia hemispherica*, with this minor positive excursion.

Only three analyses were made of Telychian samples by Štorch & Frýda (2012), from the graptolitic shales in the upper *guerichi* Biozone overlying the barren mudstones straddling the Aeronian/Telychian boundary. This limited dataset and lack of stratigraphically intervening measurements preclude meaningful comparison with the El Pintado lower Telychian record.

Melchin & Holmden (2006) provided a detailed $\delta^{13}C_{org}$

record through the Rhuddanian to lower Telychian of the Cape Manning section, Cornwallis Island, Arctic Canada. There are many similarities with the El Pintado record, particularly in the lower Telychian *guerichi* Biozone (Fig. 15).

It is interesting and perhaps surprising that the last appearances of two genera, *Cephalograptus* and *Comograptus*, are not associated with the major positive $\delta^{13}C_{org}$ excursion coinciding with the *sedgwickii* Event (see Štorch & Frýda 2012 for detailed analysis), but with the minor positive excursion low in the *rastrum* Subzone. *Cephalograptus extrema* makes its last appearance in the lowermost *rastrum* Subzone sample at El Pintado and *Co. barbatus* in the lower part of the *rastrum* Subzone in Bohemia (Štorch & Frýda 2012).

Systematic palaeontology

Many late Aeronian–early Telychian species have been described fully previously (*e.g.* in the monograph by Loydell 1992, 1993b) and are therefore illustrated herein (in Figs 16–24) but not described. Descriptions are provided below for new species, for most species left in open nomenclature and for those species previously not described in detail or for which the El Pintado material provides new morphological information. Papers with detailed descriptions of the species not described here or by Loydell (1992, 1993b) are listed within the *Remarks* section for the genera concerned.

Thecal spacing is quoted in the descriptions below as two thecae repeat distance (2TRD: Howe 1983). The term rhabdosome is used in preference to the recently proposed term tubarium (Mitchell *et al.* 2013, Maletz *et al.* 2014) which should be reserved for rhabdopleurids. All figured specimens are housed in the Museo Geominero of the Spanish Geological Survey (IGME), Madrid (numbers prefixed MGM).

It is appropriate here to list the names now used for those specimens illustrated by Jaeger & Robardet (1979) for graptolites from the lower Telychian of El Pintado section 1. This information is taken largely from the synonymy lists in Loydell (1992, 1993b). Below the identification of Jaeger & Robardet (1979) is followed by their plate and figure number in parentheses and then the new identification. *Monograptus exiguus primulus* (pl. 1, fig. 7): *Streptograptus plumosus*; *Diplograptus* (*Orthograptus*) *ultimus* (pl. 2, fig. 1): *Glyptograptus fastigatus*; *Petalograptus* cf. *conicus* (pl. 2, fig. 8): *Parapetalolithus hispanicus*; *Monograptus pseudoruncinatus* (pl. 2, fig. 11): *Streptograptus pseudoruncinatus*; *Diplograptus* (*Orthograptus*) *ultimus* (pl. 2, fig. 20): *Glyptograptus exasperatus* sp. nov.; *Monograptus turriculatus* (pl. 2, fig. 21); *Spirograptus guerichi*; *Monograptus planus* (pl. 2, fig. 22); *Torquigraptus obtusus*.

Genus *Glyptograptus* Lapworth, 1873, emend. Melchin *et al.* 2011

***Glyptograptus exasperatus* sp. nov.**
Figures 16A, L, 18L–N

partim 1979 *Diplograptus* (*Orthograptus*) *ultimus* Manck. – Jaeger & Robardet, pl. 2, fig. 20 (*non* pl. 2, fig. 1).

Holotype. – MGM6567-O (Fig. 18L), from S5.12, middle *Spirograptus guerichi* Biozone.

Derivation of name. – From the Latin, roughened, referring to the serrated appearance of the rhabdosome outline.

Material. – 17 diagenetically flattened specimens, from the middle part of the *Spirograptus guerichi* Biozone.

Diagnosis. – *Glyptograptus* with a thorn-like rhabdosome with an outline of serrated appearance, increasing rapidly in width proximally from 0.7–0.85 mm at th1^1 to a distal maximum of 2.35 mm. Thecae are conspicuously geniculate.

Description. – Rhabdosomes are up to 24 mm long and have a thorn-like shape, showing a rapid increase in width over the first few thecal pairs. Details of the sicula are not visible. Rhabdosome width is 0.7–0.85 mm at th1^1, 0.8–1.2 mm at th2^1, 1.0–1.5 mm at th3^1, 1.5–2.0 mm at th5^1 and 2.25–2.55 mm at th10^1. 2TRD is 1.6–2.25 mm at th2^1 and 1.7–2.35 mm at th5^1. It is variable distally even within a single rhabdosome, ranging from 1.8 mm to 2.35 mm. Thecae are conspicuously geniculate, especially proximally, with moderately deep excavations. Supragenicular walls are inclined at 15–20° to the rhabdosome axis. There is no median septum visible.

Remarks. – The combination of rhabdosome shape and width and thecal morphology are unique to this species. Other taxa with strongly geniculate thecae proximally, *e.g.* *G. fastigatus* (Figs 16V, AA, 18B–D, 20K) and *G. supernus* (Figs 16C, 18E, S), have narrower rhabdosomes and thecae with shallower excavations.

***Glyptograptus lucyae* sp. nov.**
Figures 16B, 18O

Holotype. – MGM7802-O (Figs 16B, 18O), from S1.33, lower *Spirograptus guerichi* Biozone.

Derivation of name. – After the first author's elder daughter.

Material. – 21 flattened specimens all from one 0.2 m thick sample low in the *Spirograptus guerichi* Biozone.

Diagnosis. – *Glyptograptus* with a bluntly rounded proximal end, supragenicular walls inclined at a very low angle to the rhabdosome axis and a maximum width of 1.8 mm.

Description. – Aseptate rhabdosomes are up to 15 mm long. The proximal end appears bluntly rounded, in part at least because of the low angle of inclination of the ventral thecal walls sub-aperturally. Sicular details are not visible; the virgella is short, extending for up to 0.25 mm from the sicular aperture. Rhabdosome width is 0.75–0.8 mm at th1^1, 1.0–1.1 mm at th3^1, and 1.4–1.8 mm at th10^1. Thecae are closely spaced proximally with a 2TRD of 1.15–1.45 mm at th2^1. 2TRD increases distally to 1.6–2.1 mm at th5^1 and 1.8–2.25 mm at th10^1. Thecal excavations are shallow. Supragenicular walls are very gently curved and inclined at a very low angle (especially distally) to the rhabdosome axis.

Remarks. – The blunt proximal end, close thecal spacing proximally and relatively narrow rhabdosome serve to distinguish *G. lucyae* from other species.

Glyptograptus nanjiangensis Chen, 1984
Figures 16G, 18J, Q, U

> 1984 *Glyptograptus tamariscus* Form C Packham. – Chen, pp. 33, 34, pl. 1, fig. 13.
> 1984 *Glyptograptus serratus nanjiangensis*; Chen, pp. 37, 38, pl. 2, figs 2, 11 (*non* 4).

Holotype. – NIGP59606, figured Chen (1984, pl. 2, fig. 2), from the *Spirograptus guerichi* Biozone of the Qiaotin section, Nanjiang, Sichuan, China.

Material. – 69 specimens from the uppermost *Stimulograptus halli* Biozone through to the upper part of the *Spirograptus guerichi* Biozone. Most specimens are from the lower to middle *Sp. guerichi* Biozone.

Description. – A robust *Glyptograptus*: rhabdosome width is 0.75–0.95 mm at th1^1, 1.0–1.1 mm at th2^1, 1.2–1.4 mm at th3^1, 1.65–1.8 mm at th5^1, then increases to a maximum of 2.55 mm by th15^1. The sicula (visible in very few specimens) is 1.5–1.6 mm long with an apertural width of 0.25 mm. The virgella is up to 0.4 mm long. 2TRD is variable, *e.g.* 1.35–2.05 mm at th2^1, 1.65–2.25 mm at th5^1. Thecae have horizontal to subhorizontal apertures and very gently curved supragenicular walls, which are inclined at 10–20° to the rhabdosome axis. There is no median septum visible.

Remarks. – As noted by Loydell (1992, p. 27), one of Chen's original specimens is *Glyptograptus auritus* Bjerreskov, 1975 which is narrower proximally and develops a rounded structure enveloping the proximal end in fully developed specimens (Fig. 19H).

Glyptograptus plautus sp. nov.
Figures 16U, 18G–I, 20N

Holotype. – MGM6563-O (Fig. 18G), from S1.33, lower *Spirograptus guerichi* Biozone.

*Derivation of name.* – From the Latin, broad, referring to the appearance of the proximal end.

Material. – 27 diagenetically flattened specimens from the lower part of the *Spirograptus guerichi* Biozone; 23 of these come from one sample representing a stratigraphical thickness of 0.2 m.

Diagnosis. – *Glyptograptus* with a bluntly rounded proximal end, closely spaced thecae proximally (2TRD at th2^1 is 1.25–1.35 mm) and a maximum width in excess of 2.0 mm.

Description. – Rhabdosomes are up to 25 mm long. The proximal end appears bluntly rounded in part at least

Figure 16. A, L – *Glyptograptus exasperatus* sp. nov.: A – MGM7801-O, S1.52; L – MGM7812-O, S1.53. • B – *Glyptograptus lucyae* sp. nov.: holotype, MGM7802-O, S1.33. • C – *Glyptograptus supernus* Fu: MGM7803-O, 1.51. • D – *Normalograptus scalaris* (Hisinger): MGM7804-O, S5.27. • E – *Parapetalolithus elizabethae* sp. nov.: holotype, MGM7805-O, S1.2. • F, I, P – *Parapetalolithus mui* sp. nov.: F – holotype, MGM7806-O, S1.16; I – MGM7809-O, S1.54; P – MGM7816-O, S1.53. • G – *Glyptograptus nanjiangensis* Chen: MGM7807-O, S1.58. • H – *Glyptograptus latus* Packham: MGM7808-O, S1.4. • J – *Parapetalolithus palmeus* (Barrande): MGM7810-O, S5.12. • K – *Parapetalolithus fusiformis* (Chen): MGM7811-O, S1.29. • M – *Glyptograptus auritus* Bjerreskov: MGM7813-O, S5.11. • N, W – *Glyptograptus tamariscus* (Nicholson): N – MGM7814-O, S1.52; W – MGM6527-O, S1.37. • O – *Cephalograptus extrema* Bouček & Přibyl: MGM7815-O, S1.4. • Q – *Metaclimacograptus undulatus* (Kurck): MGM7817-O, S1.18a. • R, AF – *Parapetalolithus kunkojensis* (Paškevičius): R – MGM7818-O, S1.16; AF – MGM6536-O, S1.16. • S – *Parapetalolithus linearis* (Bouček & Přibyl): MGM7819-O, S5.5. • T – *Parapetalolithus globosus* (Chen): MGM7820-O, S5.10. • U – *Glyptograptus plautus* sp. nov.: MGM6525-O, S1.33. • V, AA – *Glyptograptus fastigatus* Haberfelner: V – MGM6526-O, S1.49; AA – MGM6531-O, S1.48. • X, AC – *Metaclimacograptus hughesi* (Nicholson): X – MGM6528-O, S1.13; AC – MGM6533-O, S1.14. • Y – *Glyptograptus skolops* sp. nov.: holotype, MGM6529-O, S5.21. • Z – *Glyptograptus incertus* Elles & Wood: MGM6530-O, S1.4. • AB – *Metaclimacograptus asejradi* Legrand: MGM6532-O, S5.29. • AD – *Parapetalolithus elongatus* (Bouček & Přibyl): MGM6534-O, S1.59. • AE – *Parapetalolithus altissimus* (Elles & Wood): MGM6535-O, S5.9. • AG – *Parapetalolithus hispanicus* (Haberfelner): MGM6537-O, S5.28. Scale bar represents 1 mm.
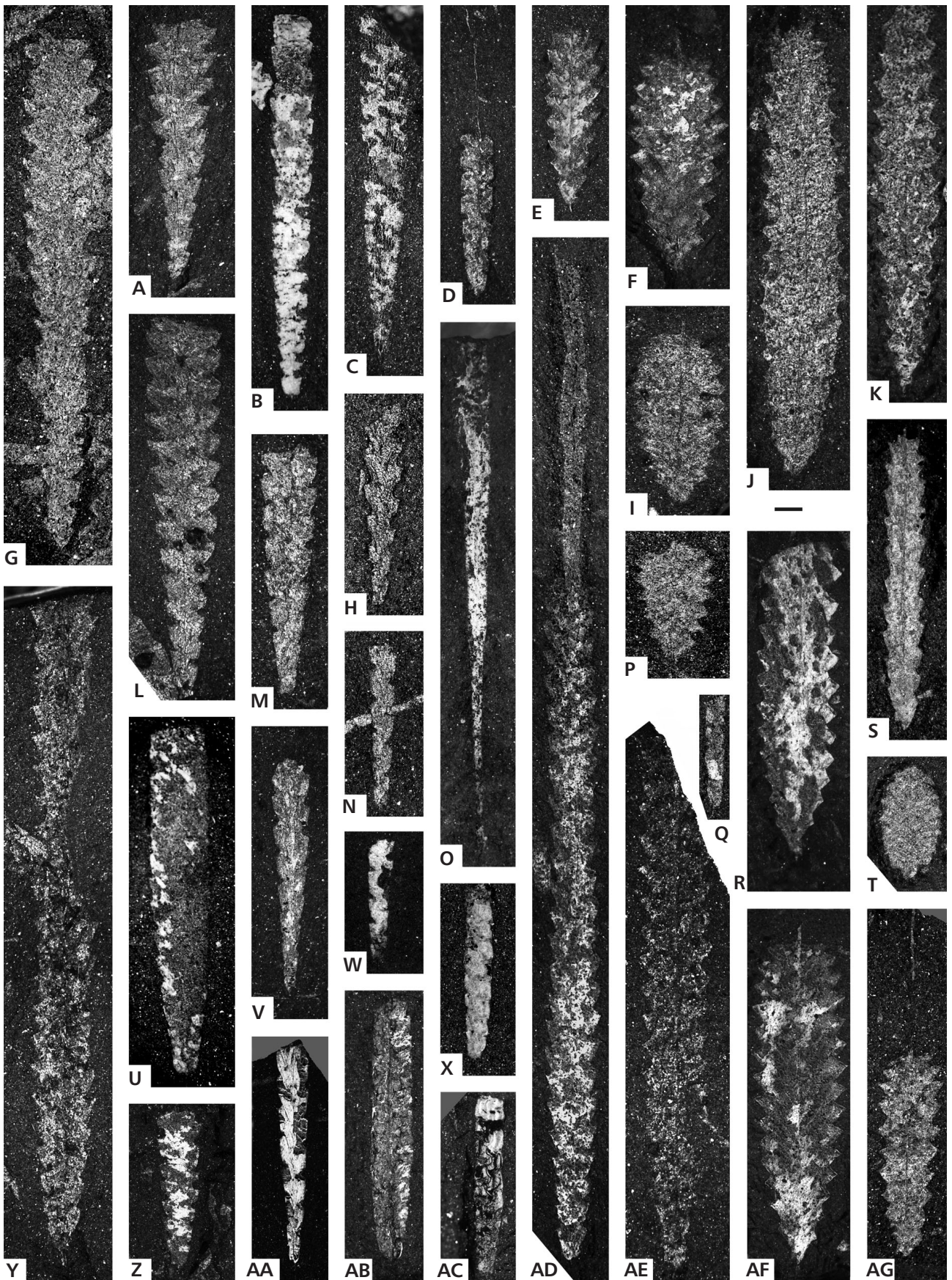
because of the low angle of inclination of the ventral thecal walls of the first thecal pair sub-aperturally. The sicular aperture is visible but other sicular details are not. The virgella is short, extending for 0.25–0.35 mm from the sicular aperture. Rhabdosome width is 0.8–1.0 mm at th1^1, 1.0–1.15 mm at th2^1, 1.2–1.4 mm at th3^1, 1.5–1.85 mm at th5^1 and 2.1–2.25 mm at th10^1. Thecae are closely spaced proximally with a 2TRD of 1.25–1.35 mm at th2^1. 2TRD increases distally to 1.75 mm at th5^1 and 2.0 mm at th10^1. Thecal excavations are shallow. Supragenicular walls are very gently curved and inclined at 10–15° to the rhabdosome axis.

Remarks. – *G. plautus* is characterized by its blunt proximal end and closely spaced thecae proximally and rhabdosome width in excess of 2 mm distally. *Glyptograptus incertus* (Figs 16Z, 18T) exhibits similar 2TRDs to *G. plautus* but is narrower throughout its length. *G. lucyae* sp. nov. (Figs 16B, 18O) has a similar blunt proximal end and closely spaced thecae, but is narrower, with a maximum width of 1.8 mm.

Glyptograptus skolops sp. nov.
Figures 16Y, 18F

Holotype. – MGM6529-O (Figs 16Y, 18F), from S5.21, upper *Spirograptus guerichi* Biozone.

Derivation of name. – From the Greek, pointed, referring to the proximal end.

Material. – Two diagenetically flattened specimens from the upper half of the *Spirograptus guerichi* Biozone.

Diagnosis. – *Glyptograptus* with a pointed, triangular proximal end and attaining a maximum rhabdosome width in excess of 2.3 mm.

Description. – The longer of the two specimens (the holotype) has a (incomplete) rhabdosome length of 23 mm. The proximal end is pointed resulting from the inclination of the ventral thecal walls. Sicular details are not visible; a broad virgella (maximum 0.2 mm wide) is present, but is broken 0.6 mm from its origin. Thecae are of typical glyptograptid form with genicula more pronounced in proximal thecae. Supragenicular walls are very gently curved and inclined at 20–25° to the rhabdosome axis. No median septum is visible. Rhabdosome width is 1.1 mm at th1^1, 1.4 mm at th2^1, 1.55 mm at th3^1, 1.75 mm at th5^1 and 2.1 mm at th11^1. The second thecal series is damaged distal of th11^2 up until the last two thecal pairs preserved. At th21^1 rhabdosome width is 2.35 mm.

2TRD measurements are 1.75 mm at th2^1, 1.85 mm at th5^1, 2.0 mm at th10^1 and 2.15 mm at th20^1.

Remarks. – The combination of pointed proximal end and broad rhabdosome serves to distinguish *G. skolops* from other species. *G. nanjiangensis* Chen, 1984 (Figs 16G, 18J, Q, U) attains a comparable width, but is narrower proximally (0.75–0.95 mm at th1^1, 1.0–1.1 mm at th2^1) and increases in width more rapidly. In overall rhabdosome appearance and proximal dimensions *G. skolops* resembles some specimens of the lower Rhuddanian species *Neodiplograptus parajanus* (Štorch, 1983), particularly when preserved obliquely to bedding (see *e.g.* Loydell 2007b, text-fig. 12C).

Glyptograptus sp.
Figure 18V

Material. – Three flattened proximal ends bearing up to five thecal pairs; from the middle part of the *Spirograptus guerichi* Biozone.

Description. – The best-preserved and most developed specimen bears five thecal pairs, although th5^2 is incomplete. The sicula is 1.6 mm long with an apertural width of 0.2 mm. It is furnished with a short virgella, extending 0.25 mm from the sicular aperture. The proximal end is broadly triangular. Rhabdosome width increases rapidly, from 0.85–0.9 mm at th1^1 to 1.75–1.85 mm at th4^1. 2TRD in the most complete specimen is 1.25 mm at th2^1 and 1.35 mm at 3^1. Genicula are pronounced. Supragenicular walls are inclined at 20–25° to the rhabdosome axis.

Remarks. – The specimens are similar to *G. nanjiangensis*, but the rhabdosome increases in width more rapidly (compare Fig. 18V, with Fig. 18U).

Genus *Parapetalolithus* Koren' & Rickards, 1996

Parapetalolithus aknisos sp. nov.
Figures 17A, 18X

Holotype. – MGM6538-O (Figs 17A, 18X), from S1.29, lower *Spirograptus guerichi* Biozone.

Derivation of name. – From the Greek, meagre, referring to the tenuity of the rhabdosome.

Material. – Eight diagenetically flattened specimens from the lower part of the *Spirograptus guerichi* Biozone.

Diagnosis. – Narrow fusiform *Parapetalolithus* reaching a maximum width of just over 1 mm, with widely spaced thecae overlapping for only *ca* one-sixth their length; thecal apertures are at an angle of less than 90° to the ventral thecal wall.

Description. – The thecate portion of the rhabdosome is up to 8.5 mm long, bearing up to seven thecal pairs; it diminishes in width distally. Sicular details are not visible; a very short narrow virgella is visible on one specimen. Rhabdosome width is 0.85 mm at th1^1, 1.0–1.05 mm at th2^1, 1.0–1.05 mm at th3^1 and 0.8–1.0 mm at th5^1. 2TRDs are 2.2–2.3 mm at th2^1, 2.15–2.2 mm at th3^1 and 1.75–1.95 mm at th5^1. The ventral walls of the first thecal pair are conspicuously concavo-convex. The thecal apertures are at an angle of less than 90° to the ventral thecal wall throughout the rhabdosome and in th1^1 and/or th1^2 are horizontal. Thecae overlap for *ca* one-sixth their length. The nema is simple, extending up to 8 mm from the distal end of the rhabdosome.

Remarks. – This is a highly distinctive species; poorly preserved proximal fragments might be confused with *Pa. conveniens* (Fig. 18W), but this increases in both rhabdosome width and thecal spacing distally.

Parapetalolithus curvithecatus (Ge, 1990)
Figures 17K, 18AB

   1990 *Petalolithus curvithecatus* (sp. nov.); Ge, p. 68, pl. 6, figs 23, 24, 27.

Holotype. – NIGP21146, figured Ge (1990, pl. 6, fig. 23), from the upper part of the Shuanghechang Formation, lower Telychian of Chengkou, Sichuan, China.

Material. – One diagenetically flattened specimen from the lower part of the *Spirograptus guerichi* Biozone.

Description. – The thecate portion of the rhadosome is 6.5 mm long. The sicula is 1.5 mm long, with an apertural width of 0.2 mm; a simple virgella extends 1.1 mm from the sicular aperture. Th1^1 commences its upward growth 0.15 mm below the sicular aperture. Rhabdosome width is 1.55 mm at th1^1, 2.05 mm at th2^1, 2.6 mm at th3^1 and 3.1 mm at th5^1. 2TRDs are 1.3 mm at th2^1, 1.35 mm at th3^1 and 1.65 mm at th5^1. Proximal thecae are conspicuously curved such that the concave thecal apertures are almost parallel to the rhabdosome axis. Distally this curvature diminishes. The nema is simple and narrow, extending 2 mm from the distal end of the thecate portion of the rhabdosome.

Remarks. – The specimen is almost identical to that illustrated by Ge (1990, pl. 6, fig. 27). The apparent lack of curvature of the distal thecae in both this specimen and that from El Pintado is a result of them being earlier growth stages than the holotype in which the distal thecae had not completed their growth. *Pa. curvithecatus* is clearly a rare but geographically widespread species. It has a distinctive appearance with a more protracted proximal end than other

Parapetalolithus species with similarly curved thecae, *e.g.* *Pa. globosus* (Fig. 16T), *Pa. regius* (Fig. 17F) and *Pa. ovatus* (see Loydell 1992, text-fig. 13, fig. 10). *Pa. curvithecatus* probably evolved from *Pa. praecedens* (Bouček & Přibyl, 1941; Fig. 18AA), recorded from the upper Aeronian, which has curved proximal thecae, but a more protracted proximal end and a lesser maximum rhabdosome width (2 mm).

Parapetalolithus elizabethae sp. nov.
Figures 16E, 18AD

Holotype. – MGM7805-O (Figs 16E, 18AD), from S1.2, lower *Stimulograptus halli* Biozone.

Derivation of name. – After the first author's younger daughter.

Material. – Three diagenetically flattened specimens: two are from the *Stimulograptus halli* Biozone, one from the middle part of the *Spirograptus guerichi* Biozone.

Diagnosis. – *Parapetalolithus* 1.1–1.25 mm wide at th1^1 and attaining a maximum rhabdosome width of 2.2 mm. Thecae are inclined at 35° to the rhabdosome axis proximally, 25° distally.

Description. – The thecate portion of the rhabdosome is up to 13 mm long. The sicula is visible on two specimens: it is 1.5–1.7 mm long with an apertural width of 0.25–0.3 mm. The virgella is broken. The ventral thecal walls of the first thecal pair are straight, or nearly so. The proximal end has a distinctly asymmetrical appearance. Rhabdosome width is 1.1–1.25 mm at th1^1, 1.65–1.75 mm at th2^1, 1.85–1.95 mm at th3^1, 2.0 mm at th5^1 and 2.2 mm at th10^1. 2TRD is 1.65–1.75 mm at th2^1, 1.6–1.75 mm at th3^1, 1.7–1.9 mm at th5^1 and 2.0 mm at th10^1. Thecae are inclined at 35° to the rhabdosome axis proximally, 25° distally. Thecal apertures are normal to the thecal axis or slightly everted proximally, approaching subhorizontal distally.

Remarks. – *Parapetalolithus elizabethae* can be distinguished from *Pa. hispanicus* (Figs 16AG, 17Q, S, 18Y; see Štorch 1998a for description of Spanish material) by its less rounded proximal end, the lower angle of inclination of its thecae and its lesser rhabdosome width distally.

Parapetalolithus fusiformis (Chen, 1984)
Figures 16K, 18AH

partim 1982 *Petalograptus elongatus* (Bouček & Přibyl, 1941). – Lenz, pp. 12, 13, fig. 13g (*non* figs 13b, d).

1984 *Petalolithus tenuis* (Barrande). – Chen, p. 43, pl. 4, fig. 7 (*non* figs 3, 5, 6, 15, 18).

1984 *Petalolithus fusiformis* sp. nov.; Chen, p. 44, pl. 4, figs 10, 17, 22 (?figs 11, 12, *non* fig. 13), pl. 5, fig. 2.

1984 *Petalolithus hispanicus* (Haberfelner). – Chen, p. 44, pl. 4, fig. 9 (*non* fig. 8).

1984 *Petalolithus* cf. *antithecaoides* (Hundt). – Chen, pp. 46, 47, pl. 5, fig. 4.

1984 *Petalolithus* cf. *tenuis* (Barrande). – Chen, pl. 4, fig. 19.

1990 *Petalolithus altissimus* Elles & Wood. – Ge, p. 66, pl. 6, figs 5, 6 (?figs 4, 7, 8).

2002 *Petalograptus fusiformis*; Rickards & Chen, fig. 60b.

Holotype. – NIGP59668, figured Chen (1984, pl. 4, fig. 22), from the *Spirograptus guerichi* Biozone of central China.

Material. – 48 diagenetically flattened specimens, from the *Stimulograptus halli* Biozone through to the middle of the *Sp. guerichi* Biozone.

Description. – The thecate portion of the rhabdosome is up to 17 mm long. Rhabdosomes are characteristically fusiform in outline, attaining their maximum width between the seventh to tenth thecal pair. The sicula is 1.45–1.9 mm long with an apertural width of 0.25 mm; it is furnished with a simple virgella up to 1.2 mm long. The ventral thecal walls of the first thecal pair are straight, or nearly so. Rhabdosome width is 0.8–1.0 mm at th1^1, 1.1–1.35 mm at th2^1, 1.35–1.65 mm at th3^1, 1.5–2.15 mm at th5^1 and 1.8–2.25 mm at th10^1. 2TRD is 1.45–1.65 mm at th2^1, 1.45–1.7 mm at th3^1, 1.7–1.85 mm at th5^1 and 1.85–1.95 mm at th10^1. Thecal apertures are concave and slightly everted. Thecae are inclined at 35° to the rhabdosome axis proximally, reducing to 30° distally. The nema is up to 0.15 mm wide, extending up to 13 mm distally from the thecate portion of the rhabdosome.

Remarks. – *Pa. fusiformis* differs from *Pa. elongatus* (Bouček & Přibyl, 1941; Figs 16AD, 18AP) in its more rapidly

increasing rhabdosome width proximally and conspicuously fusiform rhabdosome outline.

Parapetalolithus kunkojensis (Paškevičius, 1979)
Figures 16R, AF, 17E, 18AL–AN, 20A

1979 *Petalograptus palmeus* (Barrande) *kunkojensis* Paškevičius subsp. nov.; Paškevičius, pp. 130, 131, pl. 4, fig. 9, pl. 21, fig. 2.

partim 1982 *Petalograptus altissimus* Elles & Wood. – Lenz, pp. 10, 12, figs 2a, 12h (*non* figs 2b, 12a–c).

Holotype. – The specimen figured Paškevičius (1979, pl. 4, fig. 9), from the *Rastrites linnaei* Biozone of the Kunkojai core, Lithuania.

Material. – 32 specimens (30 diagenetically flattened, two preserved in low relief in weathered pyrite) from the *Stimulograptus halli* Biozone and lower part of the *Spirograptus guerichi* Biozone.

Description. – Rhabdosomes are up to 13 mm long. Details of the sicula are visible in six specimens. It is 1.3–1.5 mm long with an apertural width of 0.25–0.3 mm; the virgella extends up to 0.5 mm from the sicular aperture. Rhabdosome width shows considerable variability (Figs 18AL–AN show narrow, intermediate and broad examples): it is 1.1–1.35 mm at th1^1, 1.6–1.9 mm at th2^1, 1.7–2.45 mm at th3^1, 1.9–2.85 mm at th5^1 and 2.45–2.8 mm at th10^1. 2TRD is 1.45–1.9 mm at th2^1, 1.55–1.85 mm at th3^1, 1.55–1.85 mm at th5^1 and 1.75–2.0 mm at th10^1. The ventral walls of the first thecal pair are concave, most noticeably approaching the thecal aperture. Thecal apertures are everted proximally, but become normal to the thecal axis to subhorizontal distally. Thecae are inclined at 50° to the rhabdosome axis proximally reducing to 30–35° distally. The nema widens distally to a maximum width of 0.15 mm.

Remarks. – *Pa. kunkojensis* has been described previously only from Lithuania. *Parapetalolithus hispanicus*

Figure 17. A – *Parapetalolithus aknisos* sp. nov.: holotype, MGM6538-O, S1.29. • B, I – *Streptograptus storchi* Loydell: B – MGM6539-O, S1.49; I – MGM6546-O, S5.5. • C – *Streptograptus richardsonensis* (Lenz): MGM6540-O, S5.17. • D – *Parapetalolithus clavatus* (Bouček & Přibyl): MGM6541-O, S5.11. • E – *Parapetalolithus kunkojensis* (Paškevičius): MGM6542-O, S1.14. • F – *Parapetalolithus regius* (Hundt): MGM6543-O, S5.12. • G – *Streptograptus pericoi* Štorch: MGM6544-O, S5.1. • H – *Streptograptus dalecarlicus* Loydell & Maletz: MGM6545-O, S5.10. • J, O, V – *Streptograptus picarrai* sp. nov.: J – MGM6547-O, S5.14; O – MGM6552-O, S1.46; V – holotype, MGM6559-O, S1.21. • K – *Parapetalolithus curvithecatus* (Ge): MGM6548-O, S1.29. • L, R – *Parapetalolithus sierranortensis* sp. nov.: L – holotype, MGM6549-O, S1.47; R – MGM6555-O, S1.46. • M – *Spirograptus guerichi* Loydell, Štorch & Melchin: MGM6550-O, S1.48. • N – *Stimulograptus sedgwickii* (Portlock): MGM6551-O, S1.4. • P, W – *Pristiograptus bjerringus* (Bjerreskov, 1975): P – MGM6553-O, S5.27; W – MGM6560-O, S5.29. • Q, S – *Parapetalolithus hispanicus* (Haberfelner): Q – MGM6554-O, S1.50; S – MGM6556-O, S1.54. • T – *Spirograptus turriculatus* (Barrande): MGM6557-O, S1.33. • U – *Streptograptus pseudoruncinatus* (Bjerreskov): MGM6558-O, S5.28. • X – *Pristiograptus pristinus* Přibyl: MGM6561-O, S1.20a. Scale bar represents 1 mm.
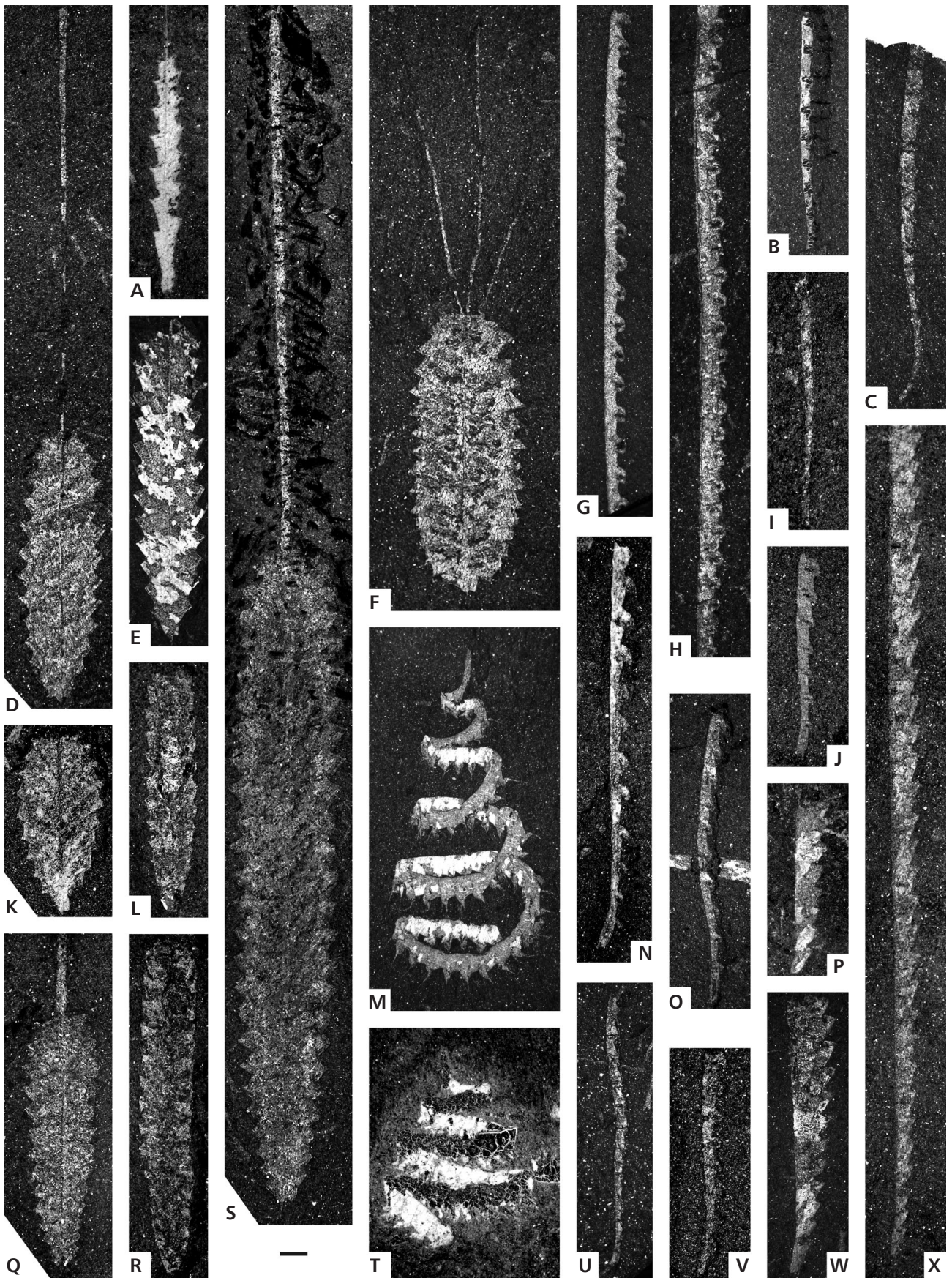
(Figs 16AG, 17Q, S, 18Y) exhibits a similar rhabdosome width (and range of variability in rhabdosome width) to *Pa. kunkojensis*, but has a less protracted proximal end of its markedly widening rhabdosome and more closely spaced thecae.

Parapetalolithus mui sp. nov.
Figures 16F, I, P, 18Z, AI, AK

partim 1982 *Petalograptus intermedius* (Bouček & Přibyl, 1941). – Lenz, pp. 16, 17, figs 2e, f, 13k (?figs 13i, j, *non* figs 2g, i, j, n, 13f, l).

partim 1984 *Petalolithus globosus* Ge. – Chen, p. 43, pl. 4, fig. 1 (*non* figs 2, 4, 16).

      1984 *Petalolithus latus* (Barrande). – Chen, p. 47, pl. 6, figs 1, 2 (*non* pl. 5, figs 11, 13).

Holotype. – MGM7806-O (Figs 16F, 18Z), from S1.16, upper *Stimulograptus halli* Biozone.

Derivation of name. – After the late Mu En-zhi, who devoted much of his life to the study of Chinese graptolites.

Material. – 28 diagenetically flattened specimens, from the upper *Stimulograptus halli* Biozone through to the middle *Spirograptus guerichi* Biozone.

Diagnosis. – Robust *Parapetalolithus* attaining a maximum width exceeding 3.5 mm. Thecae are inclined at 50–60° to the rhabdosome axis proximally, decreasing to 25–40° distally.

Description. – The thecate portion of the rhabdosome is up to 12 mm long. The sicula is 1.3–1.75 mm long with an apertural width of 0.25–0.4 mm; the virgella is up to 0.85 mm long. The ventral thecal walls of the first thecal pair are concave. Rhabdosome width is highly variable: at $th1^1$ it is 1.25–1.8 mm, at $th2^1$ 1.8–2.5 mm, at $th3^1$ 2.3–2.9 mm, at $th5^1$ 2.7–3.75 mm and at $th10^1$ 3.5–4.1 mm. 2TRD is 1.05–1.65 mm at $th2^1$, 1.0–1.55 at $th3^1$, 1.25–1.75 mm at $th5^1$ and 1.5–1.95 mm at $th10^1$. Thecae are inclined at 50–60° to the rhabdosome axis proximally, decreasing to 25–40° distally. Thecal apertures are mostly normal to the thecal axis. The nema is up to 0.15 mm wide. One specimen, the thecate portion of which is 8 mm long, has a nema extending a further 21 mm from its distal end.

Remarks. – *Pa. mui* is characterized by the high angle of its proximal thecae to the rhabdosome axis proximally. This and its greater rhabdosome width distinguish it from *Pa. hispanicus* (Figs 16AG, 17Q, S, 18Y). It has a less protracted proximal end than *Pa. kunkojensis* (Fig. 20A). Chen's (1984) specimens from the Qiaotin section, Nanjiang, Sichuan are from the middle of the *Spirograptus guerichi* Biozone. One (Chen 1984, pl. 6, fig. 1) is significantly longer than any rhabdosome from El Pintado and shows a decrease in rhabdosome width distal to the twelfth thecal pair.

Parapetalolithus sierranortensis sp. nov.
Figures 17L, R, 18AQ

Holotype. – MGM6549-O (Figs 17L, 18AQ), from S1.47, middle *Spirograptus guerichi* Biozone.

Derivation of name. – After the Sierra Norte Andalusian Geopark, which belongs to the European and Global Geoparks Network (IUGS-UNESCO), within which the El Pintado sections are situated.

Figure 18. A – *Glyptograptus auritus* Bjerreskov: MGM7813-O, S5.11. • B–D – *Glyptograptus fastigatus* Haberfelner: B – MGM6531-O, S1.48; C – MGM6562-O, S5.14; D – MGM6526-O, S1.49. • E, S – *Glyptograptus supernus* Fu: E – MGM7803-O, S1.51; S – MGM6569-O, S5.4. • F – *Glyptograptus skolops* sp. nov.: holotype, MGM6529-O, S5.21. • G–I – *Glyptograptus plautus* sp. nov.: G – holotype, MGM6563-O, S1.33; H – MGM6525-O, S1.33; I – MGM6564-O, S1.33. • J, Q, U – *Glyptograptus nanjiangensis* Chen: J – MGM6565-O, S5.14; Q – MGM6568-O, S1.22; U – MGM6570-O, S1.35. • K – *Glyptograptus elegans* Packham: MGM6566-O, S5.33. • L–N – *Glyptograptus exasperatus* sp. nov.: L – holotype, MGM6567-O, S5.12; M – MGM7812-O, S1.53; N – MGM7801-O, S1.52. • O – *Glyptograptus lucyae* sp. nov.: holotype, MGM7802-O, S1.33. • P – *Glyptograptus tamariscus* (Nicholson): MGM6527-O, S1.37. • R – *Glyptograptus latus* Packham: MGM7808-O, S1.4. • T – *Glyptograptus incertus* Elles & Wood: MGM6530-O, S1.4. • V – *Glyptograptus* sp.: MGM6571-O, S1.47. • W – *Parapetalolithus conveniens* (Koren'): MGM6572-O, S1.55. • X – *Parapetalolithus aknisos* sp. nov.: holotype, MGM6538-O, S1.29. • Y – *Parapetalolithus hispanicus* (Haberfelner): MGM6537-O, S1.28. • Z, AI, AK – *Parapetalolithus mui* sp. nov.: Z – holotype, MGM7806-O, S1.16; AI – MGM7816-O, S1.53; AK – MGM6579-O, S1.54. • AA – *Parapetalolithus praecedens* (Bouček & Přibyl): MGM6573-O, S1.4. • AB – *Parapetalolithus curvithecatus* (Ge): MGM6548-O, S1.29. • AC – *Parapetalolithus* sp.: MGM6574-O, S1.38. • AD – *Parapetalolithus elizabethae* sp. nov.: holotype, MGM7805-O, S1.2. • AE – *Parapetalolithus altissimus* (Elles & Wood): MGM6575-O, S5.1. • AF – *Parapetalolithus palmeus* (Barrande): MGM6576-O, S5.10. • AG – *Parapetalolithus clavatus* (Barrande): MGM6577-O, S5.12. • AH – *Parapetalolithus fusiformis* (Chen): MGM7811-O, S1.29. • AJ – *Parapetalolithus tenuis* (Barrande): MGM6578-O, S5.33. • AL–AN – *Parapetalolithus kunkojensis* (Paškevičius): AL – MGM6542-O, S1.14; AM – MGM7818-O, S1.16; AN – MGM6536-O, S1.16. • AO – *Parapetalolithus linearis* (Bouček & Přibyl): MGM7819-O, S5.5. • AP – *Parapetalolithus elongatus* (Bouček & Přibyl): MGM6534-O, S1.59. • AQ – *Parapetalolithus sierranortensis* sp. nov.: holotype, MGM6549-O, S1.47. • AR – *Parapetalolithus kurcki* (Rickards): MGM6580-O, S1.16. Scale bar represents 1 mm.
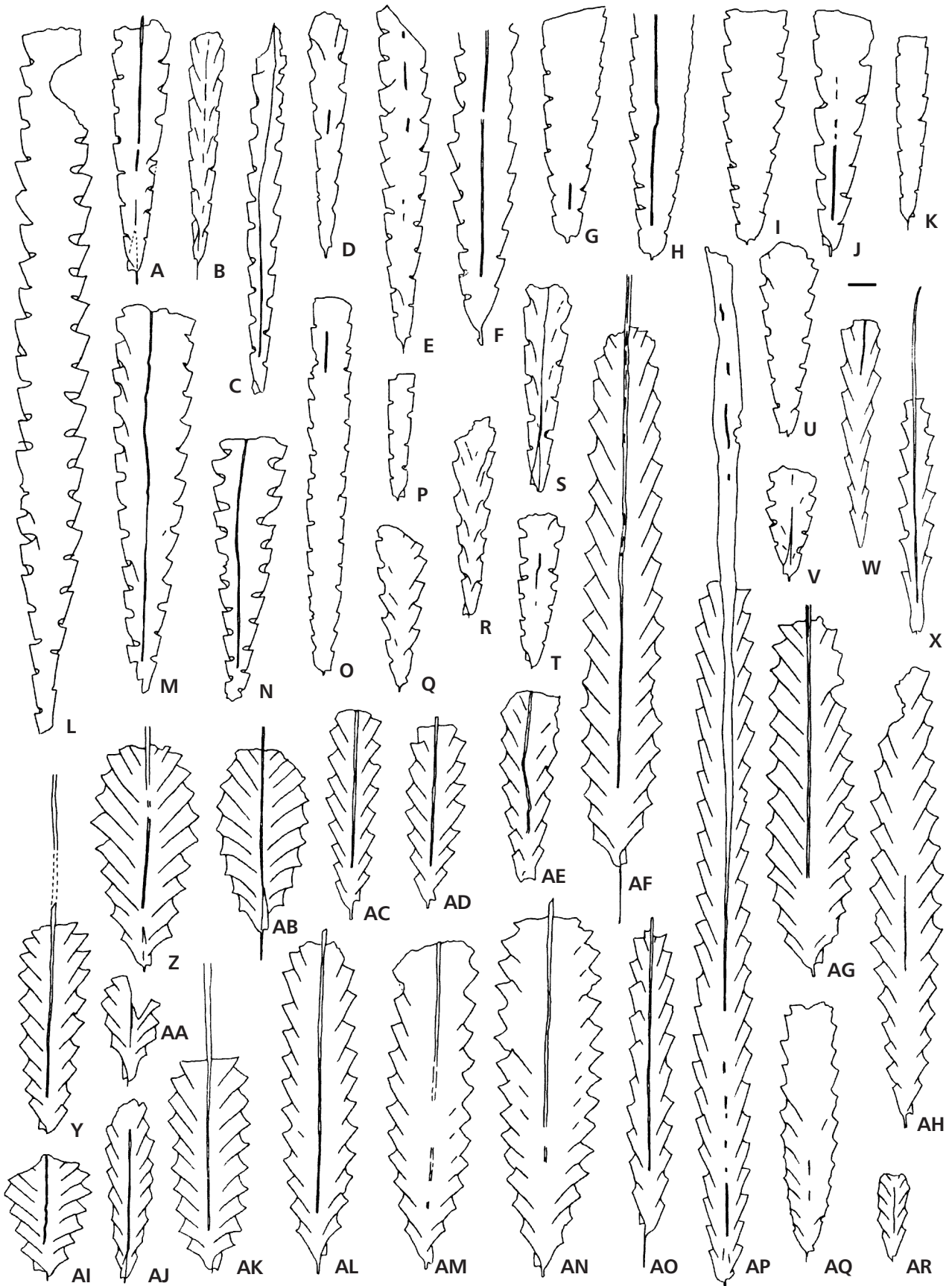
Material. – Four specimens from the lower to middle *Spirograptus guerichi* Biozone: three are diagenetically flattened; the fourth is preserved in very low relief.

Diagnosis. – *Parapetalolithus* attaining a maximum width of 1.9 mm, with strongly everted thecal apertures proximally. Thecae are inclined to the rhabdosome axis at 30–35° proximally declining to 15° distally.

Description. – The longest rhabdosome is 11.5 mm long. Sicular details are not visible. Rhabdosome width is 0.9 mm at $th1^1$, 1.2–1.3 mm at $th2^1$, 1.4–1.5 mm at $th3^1$, 1.65–1.8 mm at $th5^1$ and 1.9 mm at $th10^1$ after which there is no further increase. Thecae are closely spaced proximally: 2TRD at $th2^1$ is 1.15–1.25 mm, at $th3^1$ 1.25 mm, at $th5^1$ 1.25–1.5 mm and at $th10^1$ 1.7–1.75 mm. Thecae overlap for almost the entirety of their length. In proximal thecae, particularly the second to sixth thecal pairs, the ventral thecal walls curve outwards immediately beneath the thecal apertures which are concave and strongly everted. This eversion is reduced distally. Thecae are inclined to the rhabdosome axis at 30–35° proximally declining to 15° distally.

Remarks. – *Pa. sierranortensis* differs from *Pa. palmeus* in being significantly narrower (compare Fig. 18AQ and 18AF), tapering more noticeably proximally and in exhibiting greater eversion of the proximal thecal apertures.

Parapetalolithus sp.
Figure 18AC

Material. – One diagenetically flattened specimen, from S1.38, lower *Spirograptus guerichi* Biozone.

Description. – The thecate portion of the rhabdosome is 7 mm long and bears eight thecal pairs. Details of the sicula are not visible; what is preserved of the virgella extends 0.6 mm from the sicular aperture. $Th1^1$ commences its upward growth 0.3 mm below the sicular aperture. The proximal end is asymmetrical. Ventral thecal walls are straight or nearly so sub-aperturally. Rhabdosome width

increases gradually: it is 1.05 mm at $th1^1$, 1.15 mm at $th2^1$, 1.3 mm at $th3^1$, 1.65 mm at $th5^1$ and 1.6 mm at $th8^1$. 2TRD is 1.3 mm at $th2^1$, 1.4 mm at $th3^1$ and 1.55 mm at $th5^1$. Thecal inclination is around 25° throughout the rhabdosome.

Remarks. – *Pa.* sp. has more closely spaced thecae than *Pa. elongatus* (Figs 16AD, 18AP) and is also broader at its proximal end (rhabdosome width in El Pintado *Pa. elongatus* at $th1^1$ is 0.7–0.75 mm).

Genus *Lituigraptus* Ni, 1978

Lituigraptus bostrychodes sp. nov.
Figures 19I, 20G, M, 21P

> 1993b '*Monograptus*' pulcherrimus (Manck, 1928). – Loydell, pp. 129, 131, pl. 5, figs 9, 11, text-fig. 22, figs 13–15, 23, 25 (see for further synonymy entries).
> 2001 "*Monograptus*" pulcherrimus (Manck, 1928)?. – Štorch, p. 70, pl. 4, fig. 3, text-fig. 10, fig. 11.
> 2012 *Torquigraptus pulcherrimus* (Manck). – Štorch & Frýda, fig. 5c.

Holotype. – MGM6589-O (Figs 19I, 20M), from S1.14, uppermost *Lituigraptus rastrum* Subzone, middle *Stimulograptus halli* Biozone.

Derivation of name. – From the Greek, curly, referring to the shape of the rhabdosome.

Material. – 94 specimens, ranging in preservation from diagenetically flattened to medium relief, from the lower part of the *Stimulograptus halli* Biozone through to the middle of the *Spirograptus guerichi* Biozone.

Diagnosis. – Three dimensionally spiral rhabdosome, often forming an S- or Z-shape. Proximal thecae are almost rastritiform proximally, becoming more triangular distally. Dorso-ventral width increases from 0.6–0.7 mm at th1 and 1.1–1.15 mm at th5 to a distal maximum of 2.3 mm.

Figure 19. A – *Rastrites obuncus* sp. nov.: holotype, MGM6581-O, S1.29. • B – *Stimulograptus* sp.: MGM6582-O, S1.47. • C – *Stimulograptus eximius* sp. nov.: holotype, MGM6583-O, S1.19b. • D – *Oktavites contortus* (Perner): MGM6584-O, S1.44. • E – *Oktavites zanclus* sp. nov.: MGM6585-O, S1.15. • F – *Lituigraptus rastrum* (Richter): MGM6586-O, S1.14; see Fig. 20H for close-up of theca. • G – *Oktavites*? sp.: MGM6587-O, S1.6. • H – *Glyptograptus auritus* Bjerreskov: MGM6588-O, S1.44. • I – *Lituigraptus bostrychodes* sp. nov.: holotype, MGM6589-O, S1.14. • J – *Comograptus barbatus* (Elles & Wood): MGM6590-O, S1.5. • K – *Torquigraptus obtusus* (Schauer): specimen showing regeneration after damage, MGM6591-O, S1.56. • L – *Torquigraptus involutus* (Lapworth): MGM6592-O, S1.31. • M – *Streptograptus johnsonae* Loydell: MGM6593-O, S5.35. • N – *Streptograptus ansulosus* (Törnquist): MGM6594-O, S1.37. • O – *Rastrites* cf. *orlovi* Obut & Sobolevskaya: MGM6595-O, S1.16. • P, S – *Torquigraptus linterni* Williams *et al.*: P – MGM6596-O, S1.30; S – MGM6599-O, S1.21. • Q – *Paradiversograptus capillaris* (Carruthers): MGM6597-O, S1.24. • R – *Pristiograptus renaudi* (Philippot): MGM6598-O, S5.5. Scale bar represents 1 mm (A–I, K–S), 0.5 mm (J) or 0.25 mm (Q).
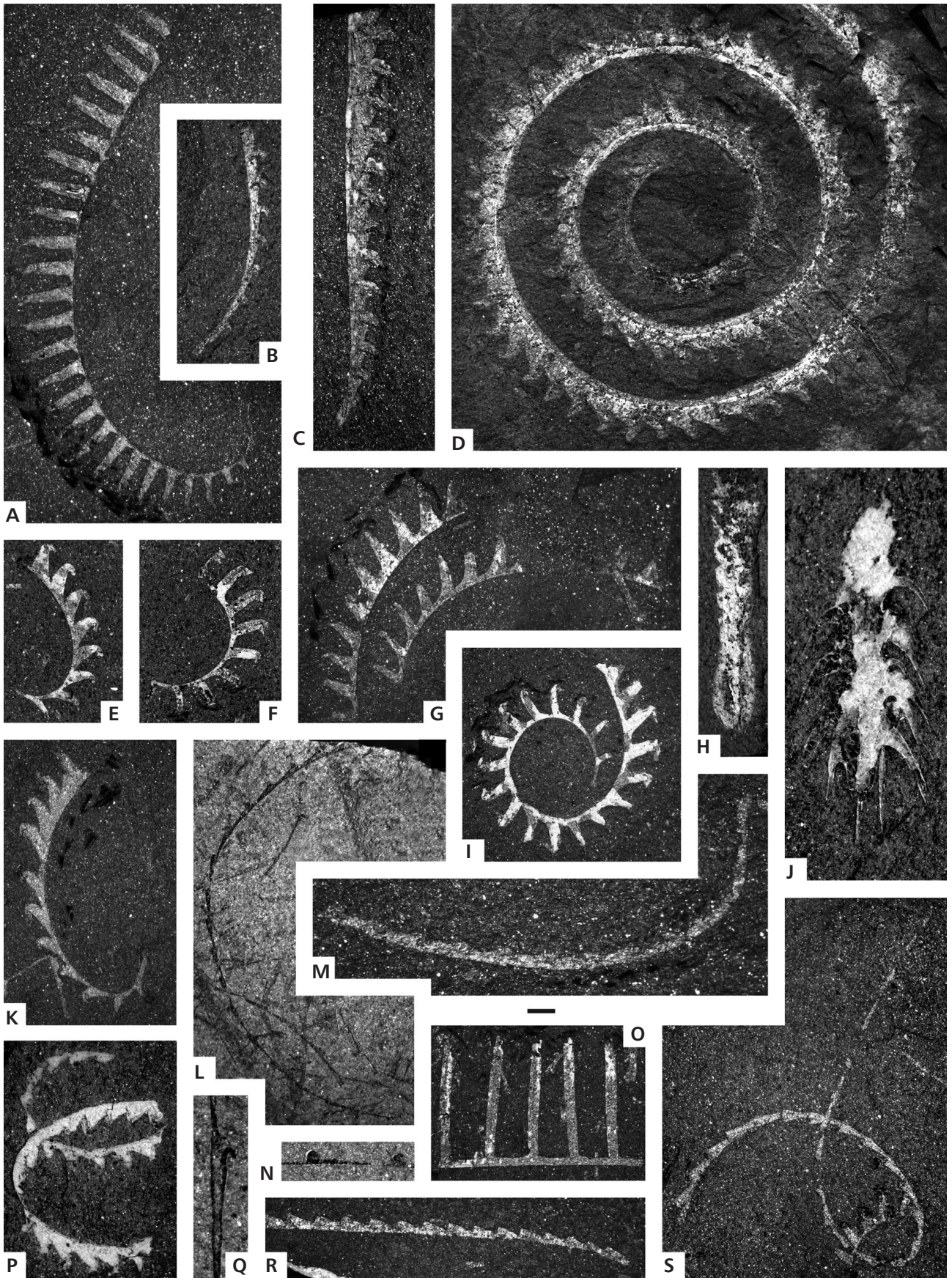
Description. – The rhabdosome is spirally curved either dorsally throughout (Fig. 19I) or more commonly forming an S- or Z-shape (Fig. 21P). The proximal end is also dorsally curved. The sicula is 0.8–0.85 mm long, with an apertural width of 0.1 mm. The position of its apex ranges from below the base of the metatheca of th1 to just above the top of th1. Ventral prothecal walls are gently inclined to the rhabdosome axis proximally, where the metathecae are almost rastritiform. Distally thecae become more triangular and appear to have laterally expanded complex thecal apertures (Fig. 20M). Dorso-ventral width is 0.6–0.7 mm at th1, 0.65–0.8 mm at th2, 0.65–0.9 mm at th3 and 1.1–1.15 mm at th5. 2TRD is 1.4–1.7 mm at th2, 1.5–1.7 mm at th3, 1.4–1.65 mm at th5. Distally, dorso-ventral width increases to 2.3 mm and 2TRD is 1.4–1.7 mm.

Remarks. – Owing to the unavailability of Manck's (1928) publication at the time of writing, Loydell (1993b) used Přibyl & Münch's (1942) description of *Demirastrites pulcherrimus* to identify specimens from Wales. Maletz (2006, pl. 1.1, fig. S) refigured Manck's holotype of this species (as had Müller 1963), demonstrating that it is a junior synonym of *Lituigraptus convolutus*. A new name is thus required for the species described as *pulcherrimus* by Přibyl & Münch (1942), Loydell (1993b) and others. Štorch & Frýda (2012) assigned material of this species to *Torquigraptus*. The thecal morphology appears more complex (Fig. 20M) than is typical of this genus, however, and for this reason *bostrychodes* is assigned to *Lituigraptus* herein. *Lituigraptus* is characterized by its almost rastriform thecae proximally and the complex, laterally expanded thecal apertures throughout the rhabdosome (see images of isolated *L. convolutus* in Loydell & Maletz (2009).

Lituigraptus rastrum (Richter, 1853)
Figures 11, 19F, 20H, L, 21A, B, D, H, K, L

  1853 *Monograpsus peregrinus* Barr. – Var. (*rastrum* R.); Richter, pp. 461, 462, pl. 12, fig. 31.
  1907 *Rastrites rastrum* Richter. – Törnquist, pp. 10, 11, pl. 2, figs 1–6.
  1967 *Rastrites rastrum* (Richter 1853). – Schauer, pp. 179, 180, pl. 4, figs 3, 4.

  2012 *Lituigraptus rastrum* (Richter). – Štorch & Frýda, fig. 5d.

Material. – 150 diagenetically flattened specimens, the vast majority of which are proximal fragments, from the middle part of the *Stimulograptus halli* Biozone.

Description. – All of the specimens are strongly dorsally curved. The sicula is preserved in only a few specimens. It is 0.95–1.1 mm long, with an apertural width of 0.15–0.2 mm. The sicular apex reaches to the base of the metatheca of th1. Prothecae are narrow proximally, with ventral walls parallel to the rhabdosome axis; distally they remain parallel or are very gently inclined so that the protheca widens very gradually towards the metatheca. Metathecae are narrow and rastritiform proximally, becoming broader distally, in many specimens this being accompanied by a gentle tapering of the metatheca towards the aperture. Proximal metathecae are normal to the rhabdosome axis; distally they are inclined at 75–90°. Thecal apertures appear hooked in many specimens, probably with lateral expansion of the aperture. Dorso-ventral width increases from 0.6–0.75 mm at th1 to 1.15–1.45 mm at th5 and 1.5–2.5 mm at th10. The widest distal fragment is 3 mm wide. 2TRD is 1.9–2.0 mm at th2 decreasing to 1.75 mm at th10. Distally it reaches a maximum of 2.25 mm.

Remarks. – *Lituigraptus rastrum* appears to be a highly variable species in terms of rate of rhabdosome widening. The appearance of the metathecae is undoubtedly influenced by the orientation of the rhabdosome with respect to the bedding surface. It is clear from Törnquist's (1907) and Štorch & Frýda's (2012) illustrations that complete rhabdosomes of *L. rastrum* exhibited three-dimensional coiling.

Törnquist (1907) quoted a maximum metathecal length of 4 mm in *L. rastrum*, but none of his figured specimens (which are more fully developed than those from El Pintado) is shown to exceed a dorso-ventral width of 3 mm.

Lituigraptus rastrum is a very important species biostratigraphically, occurring only in the middle part of the *Stimulograptus halli* Biozone, the *Lituigraptus rastrum* Subzone.

Figure 20. A – *Parapetalolithus kunkojensis* (Paškevičius): MGM6542-O, S1.14. • B – MGM6600-O, *Rastrites* rhabdosome fragments, mostly of single thecae: S5.16. • C – *Torquigraptus planus* (Barrande): MGM6601-O, S5.29. • D, I – *Stimulograptus eximius* sp. nov.: MGM6602-O, S1.16; I – MGM7822-O, distal fragment, S1.50. • E – *Oktavites contortus* (Perner): MGM6603-O, S1.4. • F – biserial graptolite in thin section in XPL, showing clay mineral growth around rhabdosome with the thickest growth extending laterally, MGM6604-O, S1.18b. • G, M – *Lituigraptus bostrychodes* sp. nov.: G – MGM6605-O, S1.14; M – holotype, MGM6589-O, close-up of thecae, S1.14. • H, L – *Lituigraptus rastrum* (Richter): H – MGM6586-O, close-up of theca, S1.14; L – MGM6606-O, S1.11. • J – *Rastrites hacari* sp. nov.: MGM7821-O, proximal end, S5.11. • K – *Glyptograptus fastigatus* Haberfelner: MGM6531-O, S1.48. • N – *Glyptograptus plautus* sp. nov.: MGM6525-O, S1.33. Scale bar represents 0.5 mm (A, G, J–L, N), 1 mm (B–E, I, L), 0.16 mm (F), 0.17 mm (H) and 0.18 mm (M).
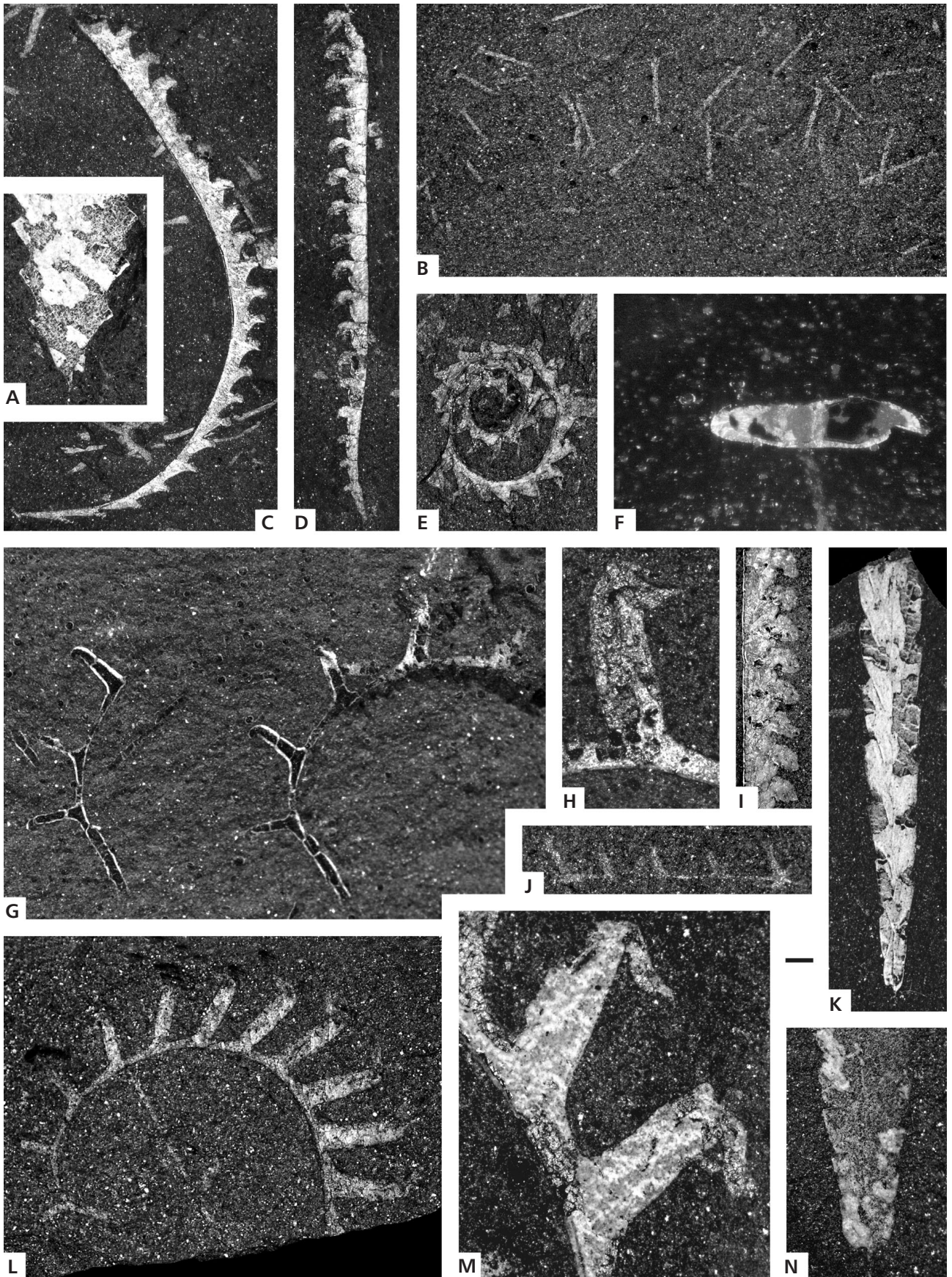
Genus *Oktavites* Levina, 1928

***Oktavites zanclus* sp. nov.**
Figures 19E, 21C, I, J

Holotype. – MGM6608-O (Fig. 21C), from S1.16, upper *Stimulograptus halli* Biozone.

Derivation of name. – From the Greek, sickle, referring to the shape of the rhabdosome.

Material. – 93 mostly diagenetically flattened specimens from the upper part of the *Stimulograptus halli* Biozone.

Diagnosis. – *Oktavites* with dorsally curved rhabdosome bearing triangular thecae with narrow prothecal bases. Dorso-ventral width is 0.6–0.7 mm at th1 increasing to a maximum of 1.35–1.4 mm by th10.

Description. – The rhabdosome is dorsally curved throughout with curvature most pronounced proximally. The sicula is 1.0–1.2 mm long with an apertural width of 0.15 mm. Its apex reaches to just below the top of th1. Thecae have narrow bases to their prothecae throughout the rhabdosome. The thecae become conspicuously broad and triangular from th4. Thecal apertures are hooked and appear somewhat laterally expanded. Dorso-ventral width is 0.6–0.7 mm at th1, 0.7–0.8 mm at th2, 0.8–0.9 mm at th3, 1.0–1.15 mm at th5 and 1.35–1.4 mm at th10, a width, which is not exceeded more distally. 2TRD is 1.35–1.7 mm at th2, 1.35–1.55 mm at th3, 1.25–1.5 mm at th5 and 1.5–1.6 mm at th10. Maximum 2TRD more distally is 1.9 mm.

Remarks. – This short-ranging species is broader and has a much less tightly curved rhabdosome than *O. contortus* (Figs 19D, 20E, 21W). It is very abundant through a short

interval immediately above the highest sample to yield *Lituigraptus rastrum*.

Genus *Pristiograptus* Jaekel, 1889

***Pristiograptus acuminatus* NIGP, 1974**
Figure 22R

> 1974 *Pristiograptus acuminatus* (sp. nov.); NIGP, p. 219, pl. 100, fig. 7.
> 1990 *Pribylograptus acuminatus* (Ge). – Ge, pp. 85, 86, pl. 11, figs 2, 3.
> 2002 *Pribylograptus acuminatus* (Ge). – Mu *et al.*, pp. 838, 839, pl. 222, figs 1, 2.

Holotype. – NIGP 21162, from the lower Telychian of Chengkou, Sichuan.

Material. – One partially damaged specimen, from the upper part of the *Stimulograptus halli* Biozone.

Description. – The specimen is 26 mm long, but is broken distally so must originally have had a greater length. The rhabdosome is damaged at the proximal end and also longitudinally in its distal part. Dorso-ventral width increases rapidly, from 0.5 mm at th1 to 1.15 mm at th10, attaining a distal maximum of 1.65 mm. Interthecal septa are at least partially obscured by clay mineral overgrowth making the amount of thecal overlap difficult to establish. 2TRD is 1.75 mm at th2, 1.8 mm at th3 and th5, 1.9 mm at th10 and 2.0 mm distally. Thecal apertures are horizontal.

Remarks. – The holotype is preserved obliquely (shown by the position of its nema) which has increased its width significantly. The species is characterized by its rapidly increasing dorso-ventral width and the horizontal orientation

---

Figure 21. A, B, D, H, K, L – *Lituigraptus rastrum* (Richter): A – MGM6606-O, S1.11; B – MGM6607-O, S1.12; D – MGM6609-O, S1.12; H – MGM6612-O, S1.11; K – MGM6615-O, S1.9; L – MGM6616-O, S1.9. • C, I, J – *Oktavites zanclus* sp. nov.: C – holotype, MGM6608-O, S1.16; I – MGM6613-O, S1.15; J – MGM6614-O, S1.18a. • E – *Stimulograptus* sp.: MGM6582-O, S1.47. • F, N, S – *Torquigraptus denticulatus* (Törnquist): F – MGM6610-O, S1.7; N – MGM6618-O, S1.6; S – MGM6623-O, S1.3. • G – *Stimulograptus distans* (Portlock): MGM6611-O, S1.3. • M, AD, AE, AP – *Torquigraptus muenchi* (Přibyl): M – MGM6617-O, S1.21; AD – MGM6634-O, S1.21; AE – MGM6635-O, S1.19a; AP – MGM6645-O, S1.18a. • O – *Streptograptus strachani* Loydell: MGM6619-O, S5.23. • P – *Lituigraptus bostrychodes* sp. nov.: MGM6620-O, S1.3. • Q – *Pseudostreptograptus williamsi* Loydell: MGM6621-O, S1.38. • R – *Streptograptus filiformis* Chen: MGM6622-O, S5.25. • T – "*Monograptus*" *admirabilis* (Přibyl & Münch): MGM6624-O, S1.30. • U – *Streptograptus tenuis* Loydell: MGM6625-O, S5.16. • V – *Stimulograptus becki* (Barrande): MGM6626-O, S5.24. • W – *Oktavites contortus* (Perner): MGM6627-O, S1.6. • X, AS – *Stimulograptus halli* (Barrande): X – MGM6628-O, S5.2; AS – MGM6647-O, S1.16. • Y – *Streptograptus picarrai* sp. nov.: holotype, MGM6559-O, S1.21. • Z, AA, AC – *Streptograptus dalecarlicus* Loydell & Maletz: Z – MGM6630-O, S5.4; AA – MGM6631-O, S1.46; AC – MGM6633-O, S1.47. • AB, AL, AM – *Streptograptus pericoi* Štorch: AB – MGM6632-O, S5.24; AL – MGM6641-O, S1.47; AM – MGM6642-O, S5.1. • AF – "*Monograptus*" *gemmatus* (Barrande): MGM6636-O, S1.54. • AG – *Streptograptus ansulosus* (Törnquist): MGM6637-O, S1.39. • AH – *Paradiversograptus capillaris* (Carruthers): MGM6597-O, S1.24. • AI – *Monograptus bjerreskovae* Loydell: MGM6638-O, S5.29. • AJ – *Monograptus marri* Perner: MGM6639-O, S5.28. • AK – *Monograptus priodon* (Bronn): MGM6640-O, S5.37. • AN, AO – *Streptograptus barrandei* (Suess): AN – MGM6643-O, S5.26; AO – MGM6644-O, S5.28. • AQ – *Streptograptus plumosus* (Baily): MGM6646-O, S5.15. • AR – *Stimulograptus sedgwickii* (Portlock): MGM6551-O, S1.4. • AT – *Stimulograptus eximius* sp. nov.: holotype, MGM6583-O, S1.19b. Scale bar represents 1 mm.
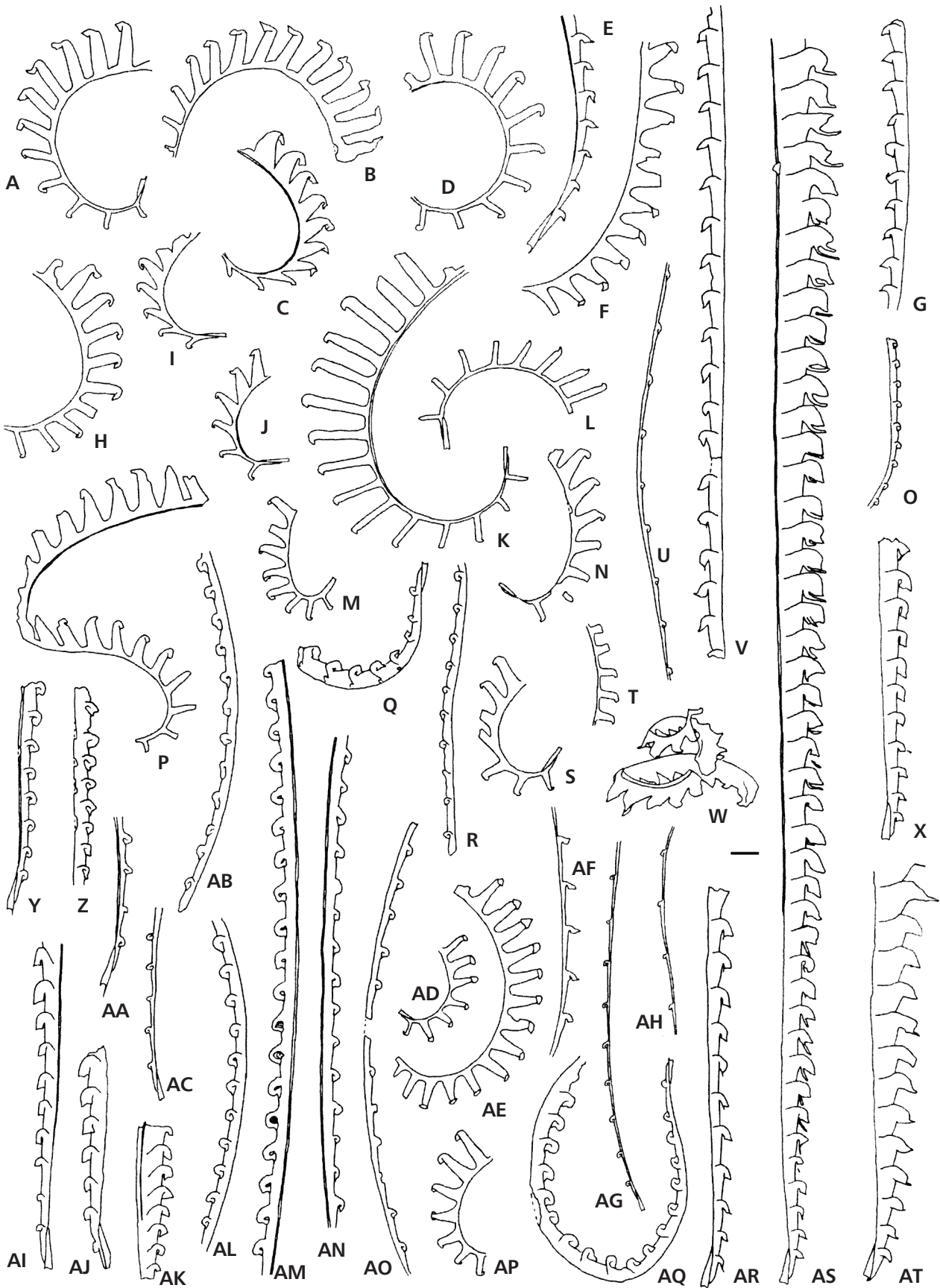
of the thecal apertures. Ge (1990) assigned the species to *Pribylograptus*. However, the thecae are simple tubes and thus the species is returned to *Pristiograptus* herein.

Pristiograptus xiushanensis NIGP, 1974
Figure 22G

> 1974 *Pristiograptus xiushanensis* (sp. nov.); NIGP, p. 219, pl. 100, fig. 7.
> 2002 *Pristiograptus xiushanensis* Mu *et al.* – Mu *et al.*, pp. 835, 836, pl. 221, figs 3–5.
> 2014 *Pristiograptus xiushanensis* Mu. – Chen *et al.*, fig. 3j.

Holotype. – NIGP 21446, from the Llandovery of Southwest China.

Material. – Four diagenetically flattened specimens: one from the lower part of the *Stimulograptus halli* Biozone and three from the middle part of the *Spirograptus guerichi* Biozone.

Description. – The rhabdosome is dorsally curved, most strongly at the proximal end. The sicula (preserved in two specimens) is 0.8–1.0 mm long, with an apertural width of 0.2 mm. Its apex reaches to just below the top of th1. Dorso-ventral width is 0.3–0.4 mm at th1, 0.4–0.5 mm at th2, 0.45–0.55 mm at th3 and 0.55–0.7 mm at th5. It is 0.6 mm at th10 and by th20 is 0.75 mm a figure that is not exceeded distally. 2TRD is 1.4–1.6 mm at th2, 1.5–1.6 mm at th3, 1.5–1.75 mm at th5, 1.5 mm at th10, 1.7 mm at th15 and 1.8–1.9 mm distally. Thecae are inclined at 25–30° to the rhabdosome axis. Thecal apertures range from normal to the thecal axis to horizontal. Thecal overlap is *ca.* one-quarter the thecal length proximally increasing to *ca.* one-third distally.

Remarks. – As noted by Loydell (1993b), *P. xiushanensis* differs from *P. renaudi* (Fig. 19R) in its more rapidly increasing dorso-ventral width proximally. Both are dorsally curved. The stratigraphical range of *P. xiushanensis* appears to be uncertain in China as it occurs in monospecific

assemblages (Chen *et al.* 2014). Because of its similarity to *P. renaudi*, Chen *et al.* (2014) suggested that it may be from the *Spirograptus guerichi* Biozone; one of the El Pintado specimens, however, is from the upper Aeronian, so the species' overall stratigraphical range straddles the Aeronian/Telychian stage boundary.

Genus *Rastrites* Barrande, 1850

Remarks. – Many *Rastrites* species were described by Schauer (1967) and by Štorch & Loydell (1992). Re-examination of the holotype of *Rastrites hybridus* has shown that Loydell's (2000) illustration is in error in indicating the presence of a sicula; the holotype lacks a proximal end. Measurements of thecal length and distance used herein follow Štorch & Loydell (1992). Intraspecific variation within *Rastrites* species is considerable, especially around the proximal end where the length and spacing of early thecae is similar in several species. Short proximal fragments are often therefore impossible to assign to a species; more complete specimens or distal fragments of several thecae are needed to make confident identifications. In the descriptions below, particularly of the new species *R. maletzi* and *R. robardeti* it is the distal thecal length (Fig. 25) that is the key diagnostic character for differentiation from related taxa such as *R. linnaei* and *R. schaueri*.

Rastrites hacari sp. nov.
Figures 20J, 22AF, AG

Holotype. – MGM6677-O (Fig. 22AF), from S1.56, middle *Spirograptus guerichi* Biozone.

Derivation of name. – After Manuel P. Hacar Rodríguez, Spanish geologist and great friend of the third author, who sadly died in December 2014.

Material. – 70 diagenetically flattened specimens, from the middle *Stimulograptus halli* Biozone through to the upper

---

Figure 22. A, J – *Torquigraptus magnificus* (Přibyl & Münch): A – MGM6648-O, S1.3; J – MGM6656-O, S1.1. • B, D, K, Z, AC, AD – *Torquigraptus minutus* (Chen): B – MGM6649-O, S1.62; D – MGM6651-O, S1.5; K – MGM6657-O, S1.4; Z – MGM6672-O, 5.11; AC – MGM6674-O, S5.13; AD – MGM6675-O, S1.62. • C – *Torquigraptus linterni* Williams *et al.*: MGM6650-O, S1.31. • E – *Pristiograptus bjerringus* (Bjerreskov): MGM6560-O, S5.29. • F, P – *Paradiversograptus rectus* (Manck): F – MGM6652-O, S1.18a; P – MGM6662-O, S1.14. • G – *Pristiograptus xiushanensis* NIGP: MGM6653-O, S1.46. • H – *Torquigraptus* sp.: MGM6654-O, S1.1. • I, L, M, T, W–Y, AE – *Torquigraptus obtusus* (Schauer): I – MGM6655-O, S5.3; L – MGM6658-O, S1.54; M – MGM6659-O, S1.54; T – MGM6666-O, S1.54; W – MGM6669-O, S5.8; X – MGM6670-O, S1.18a; Y – MGM6671-O, S1.48; AE – MGM6676-O, S1.51. • N – *Torquigraptus dextrorsus* (Linnarsson): MGM6660-O, S5.35. • O – *Paradiversograptus runcinatus* (Lapworth): MGM6661-O, S1.46. • Q – *Rastrites spina* (Richter): MGM6663-O, S1.16. • R – *Pristiograptus acuminatus* NIGP: MGM6664-O, S1.16. • S – *Rastrites* cf. *hybridus* Lapworth: MGM6665-O, S1.1. • U – *Rastrites hybridus* Lapworth: MGM6667-O, S1.16. • V – *Rastrites abbreviatus* Lapworth: MGM6668-O, S1.39. • AA – *Pristiograptus variabilis* (Perner): MGM6673-O, S1.4. • AB – *Pristiograptus pristinus* Přibyl: MGM6561-O, S1.20a. • AF, AG – *Rastrites hacari* sp. nov.: AF – holotype, MGM6677-O, S1.56; AG – MGM6678-O, S5.10. Scale bar represents 1 mm.
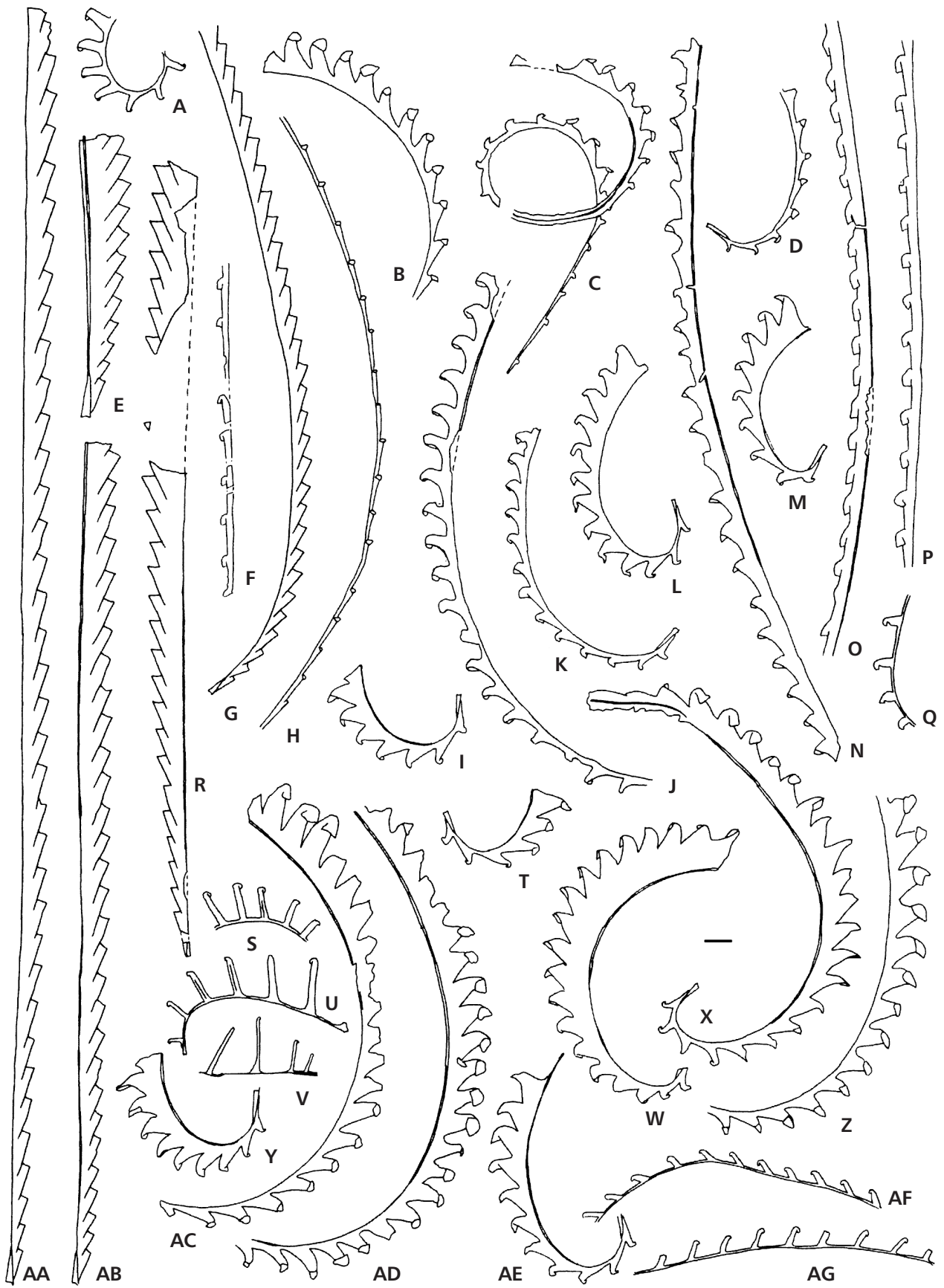
Spirograptus guerichi Biozone with most specimens coming from the middle of the *Spirograptus guerichi* Biozone.

Diagnosis. – Diminutive *Rastrites* with metathecal lengths less than 1 mm. Metathecae are inclined at 110–140° to the rhabdosome axis. Thecal distances are 0.8–1.35 mm.

Description. – The rhabdosome is either straight or gently curved, usually dorsally, but in a few specimens ventrally. The sicula is 0.85 mm long with an apertural width of 0.15 mm. Its apex reaches the metatheca of th2. Metathecae are very short, 0.6–0.9 mm long throughout the length of the rhabdosome. Thecal distances are 0.8–1.35 mm. Metathecae are inclined at 110–140° to the rhabdosome axis. Thecal apertures are hooked.

Remarks. – *Rastrites hacari* is similar in terms of thecal length to specimens described as *Rastrites spina* by Rickards (1970), Hutt (1975) and Štorch (1998b) from the middle Aeronian *Lituigraptus convolutus* Biozone and by Přibyl (1942) from the upper Aeronian *Stimulograptus sedgwickii* Biozone. *Rastrites hacari* differs in having more parallel-sided, narrower, less triangular metathecae which are inclined at 110–140° to the rhabdosome axis rather than at 90° or less as in *R. spina sensu* Přibyl (1942). Richter's type material of *Rastrites spina* has been examined by Jörg Maletz who described it (pers. comm.) as "very poor and strongly tectonized". Given the consistent use of the name *spina* by several authors and the equivocal nature of the type material it makes sense to erect a new species for these distinctive El Pintado specimens. *Rastrites spina* (Fig. 22Q) also occurs in El Pintado section 1, making its last appearance in the lowermost Telychian (Fig. 9).

    Rastrites fugax Barrande (Fig. 23R) differs from *R. hacari* in having longer thecae (1.3–1.7 mm long distally) that are more widely spaced (thecal distances are 1.8–3.0 m distally). It is described fully by Štorch & Loydell (1992).

Rastrites lenzi sp. nov.
Figure 23S

Holotype. – MGM6697-O (Fig. 23S), from S1.16, upper *Stimulograptus halli* Biozone.

Derivation of name. – After Alfred C. Lenz, Canadian graptolithologist.

Material. – 13 specimens, variably preserved from diagenetically flattened to full relief external moulds, from the upper part of the *Stimulograptus halli* Biozone. The longest (the holotype) bears th1–9.

Diagnosis. – *Rastrites* with strongly dorsally curved rhab-

dosome proximally. Thecal length increases from 0.7 mm at th1 to 2.2 mm at th8. Thecal distances increase markedly distally, from 0.6–0.75 mm between th1 and th2 to 2.65 mm between th8 and th9.

Description. – Rhabdosomes are dorsally curved throughout with the strongest curvature proximally. The sicula is 0.95–1.0 mm long with an apertural width of 0.1–0.15 mm. Its apex reaches from just under half way up th2 to just below the metatheca of th2. Prothecae are narrow, with ventral walls parallel to the rhabdosome axis. Proximal metathecae are inclined at 90–100° to the rhabdosome axis; more distal thecae at 120–125°. Thecal apertures are hooked. Thecal lengths are 0.7 mm at th1, 0.7–0.8 mm at th2, 0.95–1.0 mm at th3, 1.05–1.2 mm at th4, 1.5–1.55 mm at th5, 1.6–1.8 mm at th7 and 2.2 mm at th8. Thecal distances are 0.6–0.75 mm (th1–th2), 0.85–1.0 mm (th2–th3), 0.95–1.2 mm (th3–th4), 1.15–1.5 mm (th4–th5), 1.25–1.9 mm (th5–th6), 1.35–2.05 mm (th6–th7), 2.4 mm (th7–th8), and 2.65 mm (th8–th9).

Remarks. – *Rastrites lenzi* resembles *R. hybridus* (Fig. 22U) in rhabdosome shape and maximum thecal length, but differs in having shorter metathecae proximally and much more widely spaced metathecae distally. In the holotype of *R. hybridus* and in the specimens illustrated by Schauer (1967) distal thecal distances are 1.0–1.25 mm.

Rastrites maletzi sp. nov.
Figure 24H–J

    1942 *Rastrites distans* (Lapworth). – Přibyl, p. 9, pl. 1, figs 1–3.
    1967 *Rastrites distans* Lapworth, 1876. – Schauer, pp. 183, 184, pl. 6, figs 4–8.
    1982 *Rastrites* cf. *distans* Lapworth, 1876. – Lenz, pp. 124, 127, figs 10e, 35a.
partim 1984 *Rastrites distans* Lapworth. – Chen, p. 67, pl. 13, fig. 7, ?fig. 13 (*non* fig. 9).
    1992 *Rastrites* sp. cf. *schaueri* n. sp. – Štorch & Loydell, p. 70, figs 7a, 8a, f, g.

Holotype. – MGM6714-O (Fig. 24J), from S1.11, *Lituigraptus rastrum* Subzone, middle *Stimulograptus halli* Biozone.

Derivation of name. – After Jörg Maletz, German graptolithologist.

Material. – 140 specimens variably preserved from diagenetically flattened to full relief external moulds, from the middle *Stimulograptus halli* Biozone through to the upper *Spirograptus guerichi* Biozone.

Diagnosis. – Rastrites with distal metathecae 2.5–2.75 mm long and distal thecal distances of 1.75–2.3 mm.

Description. – Rhabdosomes are generally dorsally curved proximally (a few rhabdosomes are almost straight) becoming less strongly curved or almost straight distally. The sicula is 1.0–1.3 mm long with an apertural width of 0.15 mm. The sicular apex reaches to the metatheca of th2. Prothecae are narrow, with ventral walls parallel to the rhabdosome axis. Proximal metathecae are inclined at 90–115° to the rhabdosome axis; more distal thecae at 95–135°. Thecal apertures appear to be hooked. Thecal lengths are 0.95–1.15 mm at th1, 1.2–1.65 mm at th2, 1.65–2.4 mm at th3, 1.8–2.45 mm at th4 and 2.1–2.55 mm at th5. More distal thecae are typically 2.5–2.75 mm long. Thecal distances are 0.75–1.3 mm (th1–th2), 1.2–1.5 mm (th2–th3), 1.3–2.0 mm (th3–th4) and 1.5–2.0 mm (th4–th5). More distally thecal distance is 1.75–2.3 mm.

Remarks. – This species resembles *Rastrites schaueri* (Fig. 24G), but has shorter metathecae (Fig. 25). It was recognised as a new species (but not named) by Štorch & Loydell (1992). Some authors have referred material of *R. maletzi* to *Rastrites distans* Lapworth. The latter species was described, with a new lectotype selected, by Štorch & Loydell (1992). It is very different from *R. maletzi*: distal thecae are often perpendicular to the rhabdosome axis, are widely spaced (thecal distance is 4.2–4.8 mm) and have a length of 4.5–6.8 mm.

Rastrites cf. *maletzi* sp. nov.
Figure 23E, O

Material. – Two diagenetically flattened specimens, both with proximal end preserved, from the upper part of the *Spirograptus guerichi* Biozone.

Description. – The rhabdosome is dorsally curved proximally through approximately 90° after which the curvature decreases. Sicular details are unclear. Prothecae are narrow, with ventral walls parallel to the rhabdosome axis. The metatheca of th1 is inclined at 100–110° to the rhabdosome axis, subsequent metathecae at 90–100°. Thecal apertures are hooked. Thecal lengths are 1.05 mm at th1, 1.55–1.6 mm at th2, 1.9–2.2 mm at th3, 2.0–2.5 mm at th4 and 2.3–2.6 mm at th5. Thecal distances are 0.6 mm (th1–th2), 0.75–0.85 mm (th2–th3), 0.85 mm (th3–th4), 0.95–1.0 mm (th4–th5) and 1.2 mm (th5–th6).

Remarks. – This species resembles *Rastrites maletzi* sp. nov. (Fig. 24H–J) in terms of metathecal length but differs in its significantly more closely spaced metathecae. It also exhibits stronger rhabdosome curvature in both available

specimens. Most probably this represents another new species.

Rastrites obuncus sp. nov.
Figures 19A, 23T, Y

Holotype. – MGM6581-O (Figs 19A, 23T), from S1.29, lower *Spirograptus guerichi* Biozone. Its counterpart (Fig. 23Y) is MGM6702-O.

Derivation of name. – From the Latin, hooked, referring to the shape of the rhabdosome.

Material. – Sixteen diagenetically flattened specimens, from two samples (representing a stratigraphical thickness of 40 cm) in the lower part of the *Spirograptus guerichi* Biozone.

Diagnosis. – Rastrites with fishhook shaped rhabdosome. Thecal length increases from 0.75 mm at th1 to 2.5 mm distally. Thecal distances are 0.8–1.0 mm. Thecae are inclined at 90–95° to the rhabdosome axis.

Description. – The rhabdosome is dorsally curved, with a fishhook shape overall. The sicula is preserved in one specimen (the holotype and its counterpart). It is 1.0 mm long with an apertural width of 0.15 mm. The apex reaches approximately half way up th2. A thin virgella extends 0.25 mm from the sicular aperture. Th1 is 0.75 mm long; the metathecae of th2 and th3 are damaged; th4 is 1.25 mm long and th5 is 1.35 mm long. Measurements of more distal thecae can be taken from the holotype. Thecal lengths are 1.9 mm (th10), 2.1 mm (th15) and 2.25 mm (th20). Maximum distal thecal length (measured in other specimens assigned to this species) is 2.5 mm. Thecal distances are 0.8 mm (th1–th2 and th2–th3), 0.65 mm (th3–th4), 0.7 mm (th4–th5), 0.75 mm (th10–th11), 0.85 mm (th15–th16) and 0.9 mm (th20–th21). In distal thecae thecal distance is 0.8–1.0 mm. Metathecae are typically narrow rastritiform proximally becoming broader distally. They are inclined at 90–95° to the rhabdosome axis. Thecal apertures are hooked.

Remarks. – The shape of the rhabdosome, thecal spacing and broad distal metathecae serve to distinguish *R. obuncus* from most other lower Telychian *Rastrites* species. *Rastrites hybridus* can have a similar overall rhabdosome shape (see illustrations in Schauer 1967), but distally has narrower and shorter metathecae. *Rastrites obuncus* differs from *R. perfectus* (Fig. 24A) in having broader metathecae that are more closely spaced, especially proximally. Also, although the type material of *R. perfectus* from eastern Germany (see Přibyl 1942) is tectonically deformed, it is

evident that the rhabdsome is not as tightly dorsally curved proximally as in *R. obuncus*.

Rastrites cf. *obuncus* sp. nov.
Figure 23I

2006 *Rastrites rastrum* (Richter). – Maletz, pl. 1.1, fig. k.

Material. – Nine diagenetically flattened specimens, from the middle part of the *Stimulograptus halli* Biozone.

Description. – The rhabdosome is dorsally curved, with a fishhook shape overall. None of the specimens possesses a proximal end. Metathecae are narrow proximally, but broaden conspicuously distally. They are inclined at 80–85° to the rhabdosome axis proximally and 65–75° distally. Thecal apertures are hooked. Metathecal length increases from 1.1 mm in the most proximally preserved undamaged theca to a distal maximum of 3.5 mm. Thecal distances are 0.55–0.7 mm proximally and 0.6–0.95 mm distally.

Remarks. – The specimens resemble *R. obuncus* sp. nov. (Figs 19A, 23T, Y) in terms of overall rhabdosome shape and in thecal spacing, but differ in having longer thecae that are inclined at a lower angle to the rhabdosome axis.

Rastrites cf. *orlovi* Obut & Sobolevskaya (*in* Obut *et al.* 1965)
Figures 19O, 23Z

cf. 1965 *Rastrites orlovi* Obut & Sobolevskaya, sp. nov. – Obut *et al.*, pp. 91, 92, pl. 17, figs 10–14.
? 1982 *Rastrites* cf. *perfectus* Přibyl, 1942. – Lenz, p. 132, figs 11f, h, 36a, b.

Material. – Four diagenetically flattened, incomplete specimens, from a single sample in the upper part of the *Stimulograptus halli* Biozone.

Description. – The longest rhabdosome fragment is 27 mm long; its proximal end and parts of most metathecae are obscured by other graptolites. The proximal part is gently dorsally curved; distally the rhabdosome is straight. Thecae are mostly normal to the rhabdosome axis, but are inclined at 105–110° in one specimen. Maximum thecal length distally is 4.8 mm; thecal distances are 1.2–1.6 mm. Metathecae terminate in small apertural hooks.

Remarks. – The El Pintado specimens are very similar to *Rastrites orlovi* in terms of thecal length, but differ in thecal inclination and slightly wider thecal spacing.

Rastrites patulus sp. nov.
Figure 23H, P, Q, W

Holotype. – MGM6695-O (Fig. 23Q), from S5.29, upper *Spirograptus guerichi* Biozone.

Derivation of name. – From the Latin, broad, referring to the metathecae.

*Material.* – 18 diagenetically flattened specimens from a stratigraphical thickness of 0.4 m in the upper part of the *Spirograptus guerichi* Biozone.

Diagnosis. – *Rastrites* with a dorsally curved rhabdosome proximally bearing broad metathecae increasing in length from 1.0–1.5 mm at th1 to a maximum of 3.9 mm distally. Thecal distance distally is 1.8–2.7 mm.

Description. – Rhabdosomes are dorsally curved (through up to 90°) proximally becoming less strongly curved or almost straight distally. The sicula is 1.2–1.45 mm long with an apertural width of 0.1–0.2 mm. The sicular apex reaches either to the top of th2, most commonly just above the top of the metatheca of th2 and in one specimen half way up the protheca of th3. Prothecae are narrow, parallel-sided or gradually widening towards the metathecae. The metathecae are broad, 0.4–0.6 mm wide distally. The metatheca of th1 is inclined at 110–135° to the rhabdosome axis; from th2 onwards they are inclined at 100–110°. Thecal apertures appear hooked and significantly laterally expanded.

Figure 23. A, F, J – *Torquigraptus obtusus* (Schauer): A – MGM6679-O, S5.1; F – MGM6684-O, S1.23; J – MGM6688-O, S1.51. • B – *Rastrites* cf. *abbreviatus* Lapworth: MGM6680-O, S1.15. • C, N – *Rastrites* sp.: C – MGM6681-O, S5.7; N – MGM6692-O, S1.34. • D – *Rastrites gracilis* Přibyl: MGM6682-O, S1.31. • E, O – *Rastrites* cf. *maletzi* sp. nov.: E – MGM6683-O, S5.15; O – MGM6693-O, S5.15. • G, K – *Rastrites carnicus* Seelmeier: G – MGM6685-O, S1.18a; K – MGM6689-O, S1.21. • H, P, Q, W – *Rastrites patulus* sp. nov.: H – MGM6686-O, S5.29; P – MGM6694-O, S5.30; Q – holotype, MGM6695-O, S5.29; W – MGM6700-O, S5.29. • I – *Rastrites* cf. *obuncus* sp. nov.: MGM6687-O, S1.6. • L – *Rastrites distans* Lapworth: MGM6690-O, S5.36. • M – *Rastrites robardeti* sp. nov.: MGM6691-O, S1.20b. • R – *Rastrites fugax* Barrande: MGM6696-O, S5.13. • S – *Rastrites lenzi* sp. nov.: holotype, MGM6697-O, S1.16. • T, Y – *Rastrites obuncus* sp. nov.: T – holotype, MGM6581-O, S1.29; Y – MGM6702-O, S1.29. • U – *Rastrites* cf. *distans* Lapworth: MGM6698-O, S5.35. • V – *Rastrites spengillensis* Rickards: MGM6699-O, S5.26. • X – *Rastrites* sp. aff. *maximus* Lapworth: MGM6701-O, S5.10. • Z – *Rastrites* cf. *orlovi* Obut & Sobolevskaya: MGM6703-O, S1.16. • AA, AB – *Rastrites maximus* Lapworth: AA – MGM6704-O, S5.11; AB – MGM6705-O, S5.7. Scale bar represents 1 mm.
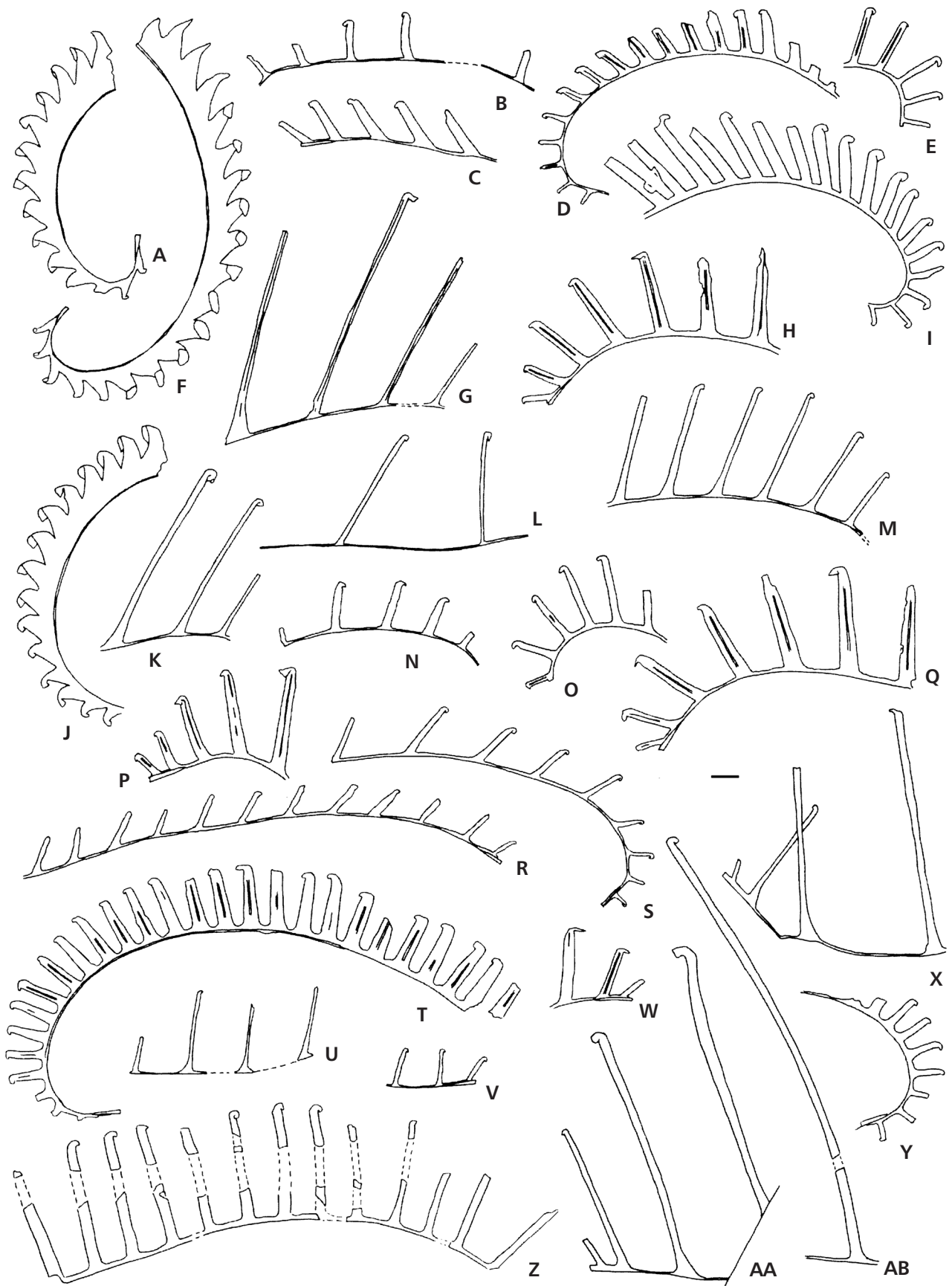
Thecal lengths are 1.0–1.5 mm at th1, 1.4–2.1 mm at th2, 2.25–3.2 mm at th3, 2.85–3.7 mm at th4 and 3.0–3.8 mm at th5. Maximum distal thecal length is 3.9 mm. Thecal distances are 0.5–0.9 mm (th1–th2), 0.95–1.4 mm (th2–th3), 1.25–1.8 mm (th3–th4) and 1.35–2.0 mm (th4–th5). More distally thecal distance is 1.8–2.7 mm.

Remarks. – *R. patulus* has a similar maximum thecal length to *Rastrites schaueri* (Fig. 24G), but has longer metathecae proximally and broader metathecae throughout the rhabdosome.

Rastrites robardeti sp. nov.
Figures 23M, 24D–F

partim 1967 *Rastrites linnaei* Barrande 1850. – Schauer, pp. 180–182, pl. 5, figs 2, 7 (*non* figs 1, 3–5, 8).

Holotype. – MGM6710-O (Fig. 24F), from S1.13, *Lituigraptus rastrum* Subzone, middle *Stimulograptus halli* Biozone.

Derivation of name. – After the French geologist Michel Robardet, the last author's mentor, who has made numerous important contributions to the understanding of the Palaeozoic of south-west Europe, including discovery of the Ordovician–Devonian successions in the northern part of Seville Province.

Material. – 250 specimens, from the middle *Stimulograptus halli* Biozone through to the upper *Spirograptus guerichi* Biozone.

Diagnosis. – *Rastrites* with distal thecal lengths of 4.2–4.6 mm and distances of 2.0–2.6 mm. Proximal metathecae are inclined at 85–125° to the rhabdosome axis; more distal thecae at 105–130°.

Description. – Rhabdosomes are generally dorsally curved proximally (a few rhabdosomes are almost straight) becoming less strongly curved or almost straight distally; the degree of curvature is very variable (compare Figs 24E and 24F). The sicula is 1.1–1.5 mm long with an apertural width of 0.15–0.2 mm. The sicular apex reaches to the metatheca of th2 or just above. Prothecae are narrow, with ventral walls parallel to the rhabdosome axis. Proximal metathecae are inclined at 85–125° to the rhabdosome axis; more distal thecae at 105–130°. Thecal apertures appear hooked in many specimens. Thecal lengths are 1.0–1.8 mm at th1, 1.6–3.5 mm at th2, 2.4–4.5 mm at th3, 3.4–4.6 mm at th4 and 3.9–4.5 mm at th5. More distal thecae are 4.2–4.6 mm long. Thecal distances are 0.6–1.0 mm (th1–th2), 0.9–1.8 mm (th2–th3), 1.0–2.3 mm (th3–th4) and 1.1 mm (th4–th5). More distally thecal distance is 2.0–2.6 mm.

Remarks. – *Rastrites robardeti* sp. nov. is intermediate in dimensions (thecal length and distance; Fig. 25) between *R. schaueri* and *R. linnaei* both of which appear in El Pintado section 1 at the same stratigraphical level.

Rastrites sp.
Figure 23C, N

Material. – Two diagenetically flattened specimens: one from the lower part and one (a proximal end) from the middle of the *Spirograptus guerichi* Biozone.

Description. – The rhabdosome is only very gently dorsally curved proximally, becoming straight distally. The sicula is 1.25 mm long with an apertural width of 0.1 mm. The sicular apex reaches to the metatheca of th2. Prothecae are narrow, with ventral walls parallel to the rhabdosome axis. The broad metathecae are inclined at 100–130° to the rhabdosome axis. Thecal apertures appear hooked. Thecal lengths are 1.4 mm at th1, 1.7 mm at th2, 1.8 mm at th3 and 1.95 mm at th4. Thecal distances are 1.0 mm (th1–th2), 1.5 mm (th2–th3), 1.7 mm (th3–th4) and 1.75 mm (th4–th5).

Remarks. – In terms of thecal length and spacing these specimens are similar to *Rastrites maletzi* sp. nov., but they possess much broader metathecae similar to those of *Rastrites patulus* sp. nov. (which has longer metathecae).

Genus *Stimulograptus* Přibyl & Štorch, 1983

Stimulograptus eximius sp. nov.
Figures 19C, 20D, I, 21AT

Holotype. – MGM6583-O (Figs 19C, 21AT), from S1.19b, upper *Stimulograptus halli* Biozone.

Derivation of name. – From the Latin, exceptional, referring to the remarkably rapid increase in rhabdosome width proximally.

Material. – 71 specimens, variably preserved from diagenetically flattened to full relief external moulds, from the lower *Stimulograptus halli* Biozone through to the upper *Spirograptus guerichi* Biozone. The species is most common in the upper *halli* Biozone through to the middle *guerichi* Biozone.

Diagnosis. – Broad *Stimulograptus* increasing in dorsoventral width from 0.6–0.7 mm at th1 to 1.35–1.55 mm at th10 to a distal maximum of 2.4 mm. Ventral prothecal walls inclined at 25° to the rhabdosome axis except in thecae at the proximal end.
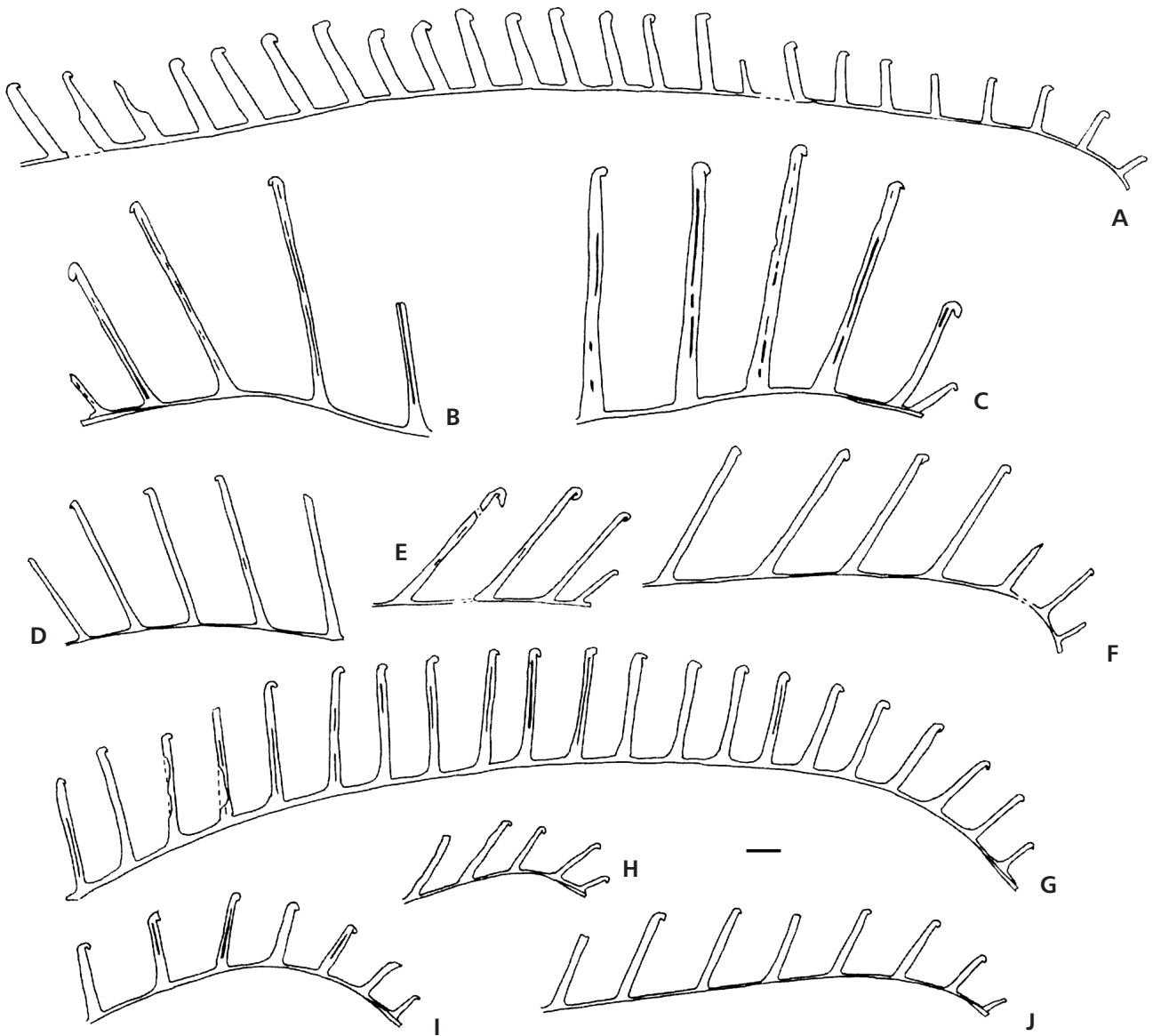
Figure 24. A – *Rastrites perfectus* Přibyl: MGM6706-O, S1.23. • B, C – *Rastrites linnaei* Barrande: B – MGM7823-O, S1.50; C – MGM6707-O, S5.35. • D–F – *Rastrites robardeti* sp. nov.: D – MGM6708-O, S1.19b; E – MGM6709-O, S5.1; F – holotype, MGM6710-O, S1.13. • G – *Rastrites schaueri* Štorch & Loydell: MGM6711-O, S1.22. • H–J – *Rastrites maletzi* sp. nov.: H – MGM6712-O, S5.11; I – MGM6713-O, S1.53; J – holotype, MGM6714-O, S1.11. Scale bar represents 1 mm.
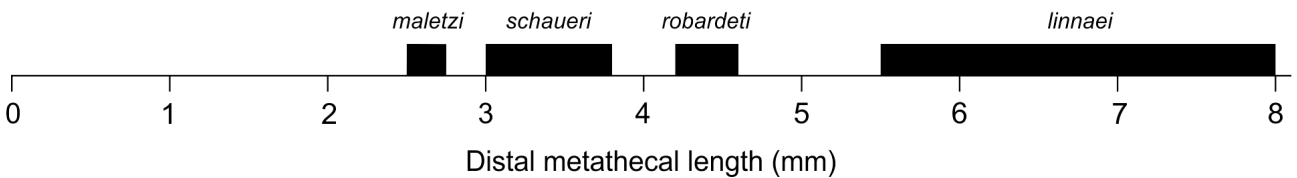
Figure 25. Comparison of the maximum thecal length in the upper Aeronian–lower Telychian *Rastrites* species *R. maletzi* sp. nov., *R. schaueri* Štorch & Loydell, *R. robardeti* sp. nov. and *R. linnaei* Barrande. Data from El Pintado specimens and from Štorch & Loydell (1992).

Description. – Rhabdosomes are either straight throughout or gently dorsally or dorso-ventrally curved proximally and then straight. The longest rhabdosome is 100 mm long. The sicula is 1.3–1.9 mm long, with an apertural width of 0.3–0.35 mm. The level of the sicular apex ranges from the aperture of th1 to just above the top of th1. Thecae are of

typical stimulograptid form, with interthecal septa almost normal to the rhabdosome axis. Except in the most proximal thecae the ventral prothecal wall is inclined at 25° to the rhabdosome axis. The methecal hook comprises approximately half of the rhabdosome width. Thecal apertures are furnished with paired ventro-laterally directed spines up to 0.5 mm long. Dorso-ventral width is 0.6–0.7 mm at th1, 0.65–0.85 mm at th2, 0.7–0.95 mm at th3, 1.0–1.3 mm at th5, 1.35–1.55 mm at th10, 1.55–1.8 mm at th15 and 1.75–2.0 mm at th20. The maximum dorso-ventral width distally is 2.4 mm. 2TRDs are 1.75–2.15 mm at th2, 1.75–2.2 mm at th3, 1.9–2.25 mm at th5, 1.95–2.4 mm at th10 and 2.3–2.7 mm at th15, with a distal maximum of 3.0 mm.

Remarks. – St. eximius differs from *St. halli* (Fig. 21X, AS) in its more rapidly increasing dorso-ventral width proximally and in the greater inclination of its ventral prothecal walls.

Stimulograptus sp.
Figures 19B, 21E

Material. – Two diagenetically flattened specimens, comprising one proximal end bearing th1–7 and one rhabdosome fragment of twelve thecae (probably commencing at th3), from the middle part of the *Spirograptus guerichi* Biozone.

Description. – The rhabdosome is dorsally curved over the first five thecae and then becomes almost straight. The sicula is 1.6 mm long with an apertural width of 0.25 mm. Its apex reaches to just below the top of th1. Ventral prothecal walls are at a low angle to the rhabdosome axis. Metathecal hooks proximally are small in relation to the overall thecal length, but comprise approximately half of the rhabdosome width. Thecal apertures are furnished with paired spines. Dorso-ventral width is 0.5 mm at th1, 0.45 mm at th2, 0.55 mm at th3, 0.75 mm at th5 and 0.8 mm at th7. 2TRDs are 2.3 mm at th2, 2.2 mm at th3 and 2.05 mm at th5. At the distal end of the specimen lacking a proximal end dorso-ventral width is 0.8 mm and 2TRD is 2.2 mm.

Remarks. – The dorsal curvature proximally is reminiscent of that in *St. utilis* Loydell, 1991a. The latter species is, however, narrower (*e.g.* at th5 maximum dorso-ventral width is 0.6 mm), has more closely spaced thecae distally and exhibits ventral rhabdosome curvature distally rather than being straight. Gutiérrez-Marco & Štorch (1998) recognised another dorso-ventrally curved *Stimulograptus* species, which they referred to *St.* cf. *utilis*, from the upper part of the *Spirograptus guerichi* Biozone of the Western Iberian Cordillera of Spain. Their illustrated specimen is much less strongly curved dorsally than the El Pintado *Stimulograptus* sp. It appears therefore that a number of rare and/or geographically restricted proximally dorsally curved *Stimulograptus*

species characterize the lower Telychian, in addition to the more widespread *St. becki* (see Loydell 1993b and Štorch 1998a for full descriptions of the latter species).

Genus *Streptograptus* Yin, 1937, emend. Loydell, 1990b

Remarks. – Descriptions of chemically isolated material of several *Streptograptus* and *Pseudostreptograptus* species were provided by Loydell & Maletz (2004). Other taxa are described in Lenz (1982; *S. richardsonensis*) and Štorch (1998a; *S. pericoi*).

Streptograptus picarrai sp. nov.
Figures 17J, O, V, 21Y

> 1993b *Streptograptus* sp. – Loydell, p. 101, pl. 3, fig. 8, text-fig. 18, fig. 6.

Holotype. – MGM6559-O (Figs 17V, 21Y), from S1.21, lower *Spirograptus guerichi* Biozone.

Derivation of name. – After José Manuel Piçarra d'Almeida, Portuguese graptolithologist.

Material. – Sixteen specimens, most of which are diagenetically flattened, from the lowermost to upper part of the *Spirograptus guerichi* Biozone.

Diagnosis. – Broad *Streptograptus* increasing in dorso-ventral width from 0.4–0.5 mm at th1 to 1.15 mm at th15. Rhabdosome is gently dorsally curved proximally (over the first three to five thecae), straight or gently ventrally curved thereafter.

Description. – The rhabdosome is up to 16 mm long. It exhibits very gentle dorsal curvature, over the first three to five thecae and is straight or more usually very gently ventrally curved thereafter. The sicula is 1.05–1.3 mm long with an apertural width of 0.2–0.35 mm. Its apex reaches to just below the top of th1. Dorso-ventral width (higher values are in obliquely preserved specimens where rhabdosome width has been accentuated) is 0.4–0.5 mm at th1, 0.45–0.6 mm at th2, 0.5–0.65 mm at th3, 0.55–0.8 mm at th5 and 0.65–0.9 mm at th10 and 1.15 mm at th15. The prothecae of proximal thecae are parallel-sided or widen slightly towards the metatheca; those of distal thecae are broad-based and narrow towards the metatheca. The coiled metathecae comprise just under half the rhabdosome width. 2TRDs are 1.6–2.0 mm at th2, 1.65–2.05 mm at th3, 1.6–2.0 mm at th5 increasing to 1.8–2.25 mm distally.

Remarks. – Loydell (1993b) described a single specimen of this species (comprising only th1–th6), from the *Spiro-*

graptus guerichi Biozone of Wales. Its greater breadth serves to distinguish it from other species with similar rhabdosome curvature (*e.g. S. pseudoruncinatus*, Fig. 17U).

Genus *Torquigraptus* Loydell, 1993b

Remarks. – For most *Torquigraptus* species the El Pintado material adds no new morphological information. Descriptions of *Torquigraptus* species are spread across a number of publications. Loydell's (1993b) monograph contains descriptions of *T. involutus* (Fig. 19L) and *T. planus* (Fig. 20C), Linnarsson (1881) describes *T. dextrorsus* (Fig. 22N), Štorch (1998b) and Loydell & Maletz (2009) describe *T. denticulatus* (Fig. 21F, N, S), Štorch (2001) describes *T. magnificus* (Fig. 22A, J) and Williams *et al.* (2003) erected *T. linterni* (Figs 19P, S, 22C). *T. muenchi* (Fig. 21M, AD, AE, AP) was originally described by Přibyl (1942) as a species of *Demirastrites*, but it has the twisted thecal apertures typical of *Torquigrapus*.

Fragmentary specimens of *Torquigraptus* are very difficult to identify. This is a result in part of the considerable intraspecific variation in some species (*e.g.* see description of *T. obtusus* below), which is a characteristic feature also of some stratigraphically younger *Torquigraptus* species (see Štorch 1998a on *T. tullbergi*). Further difficulties are presented by the great similarity of the narrow proximal portions of some species, *e.g. T. involutus*, *T. linterni* and *T. planus*, and the varying appearances of rhabdosomes and/or thecae as a result of their orientation to bedding. These factors in combination necessitate collection of specimens bearing many thecae in order to enable confident identifications.

Torquigraptus minutus (Chen, 1984)
Figure 22B, D, K, Z, AC, AD

partim 1982 *Monograptus decipiens valens* (Přibyl & Münch, 1942). – Lenz, pp. 75, 76, fig. 23g (*non* figs 6g, j, l, 23b, d, e).
partim 1982 *Monograptus planus planus* (Barrande, 1850). – Lenz, p. 94, figs 7h, l, 26e, f (*non* fig. 26k).
partim 1984 *Oktavites planus* (Barrande). – Chen, p. 68, pl. 13, fig. 14, pl. 18, fig. 7 (*non* pl. 14, figs 1, 4).
    1984 *Streptograptus nanshanensis minutus* subsp. nov.; Chen, p. 76, pl. 19, figs 5, 6, 9, 10.
    1989 *Monograptus decipiens valens* (Přibyl & Münch). – Melchin, fig. 11n.
    1989 *Monograptus decipiens* n. ssp. – Melchin, fig. 11o.
    1990 *Oktavites planus* (Barrande). – Ge, pp. 101, 102, pl. 11, fig. 7, pl. 12, fig. 6, pl. 16, figs 3, 10 (?fig. 11).
    1990 *Oktavites toernquisti* (Sudbury). – Ge, p. 104, pl. 17, figs 7, 8.

    1990 *Demirastrites decipiens valens* Přibyl & Münch. – Ge, p. 105, pl. 15, figs 5, 6, 18.
    1990 *Demirastrites magnificus* Přibyl & Münch. – Ge, p. 106, pl. 14, fig. 5, pl. 15, figs 9–11, 13, 14 (?fig. 12).
    1993a *Monograptus minutus* (Chen, 1984). – Loydell, p. 335, fig. 4a–c.

Holotype. – NIGP 59903, figured Chen (1984, pl. 19, fig. 6) from the *Spirograptus guerichi* Biozone of the Qiaotin section, Nanjiang, Sichuan, China.

Material. – 160 specimens, most of which are diagenetically flattened, from the *Stimulograptus halli* Biozone through to the upper part of the *Spirograptus guerichi* Biozone.

Description. – The rhabdosome is dorsally curved in its proximal and mesial parts; distal fragments are also dorsally curved or exhibit twisting of the rhabdosome axis. The sicula is 0.9–1.25 mm long with an apertural width of 0.15 mm. Its apex reaches to a level from below the aperture of th1 to just below its top. Thecae throughout the rhabdosome characteristically have narrow prothecal bases. Proximal thecae are axially elongated; mesially and distally they have a more triangular appearance. Twisting of the thecal apertural region is visible on all thecae. Dorso-ventral width increases slowly initially, from 0.35–0.4 mm at th1 to 0.5–0.7 mm at th5 and 0.7–0.8 mm at th10. Some mesial fragments (*e.g.* Fig. 22B) show a more rapid increase in width (a doubling over ten thecae) after which the rate of increase slows. The distal maximum width is 2.1 mm. In the few specimens with a sicula (so that 2TRD can be measured at a specific theca) 2TRD is 1.8–2.4 mm at th2, 1.8–2.25 mm at th3, 1.9–2.1 mm at th5 and 1.8 mm at th10. Other proximal–mesial fragments (lacking a sicula) exhibit a wider range of 2TRDs, 1.55–2.85 mm. In distal fragments 2TRD is 1.6–2.5 mm.

Remarks. – *T. minutus* is a geographically widespread species characterized by having a greater number of axially elongated proximal thecae than *T. obtusus*. From *T. planus* (Fig. 20C) it differs in having more prominent metathecae proximally, and narrower prothecal bases and ventral prothecal walls at a higher angle to the rhabdosome axis distally.

Torquigraptus obtusus (Schauer, 1971)
Figures 19K, 22I, L, M, T, W–Y, AE, 23A, F, J

    1971 *Monograptus* (*Spirogr.*) *planus obtusus* n. subsp.; Schauer, p. 74, pl. 27, fig. 5, pl. 33, figs 8, 9.
    1979 *Monograptus planus* (Barrande). – Jaeger & Robardet, pl. 2, fig. 22.

partim 1982   *Monograptus decipiens valens* (Přibyl & Münch, 1942). – Lenz, pp. 75, 76, figs 6g, j, l, 23b, d, e (*non* fig. 23g).

       1982   *Monograptus planus obtusus* Schauer, 1971. – Lenz, p. 97, figs 8m, 27a, g.

       1990   *Oktavites planus obtusus* (Schauer). – Ge, p. 102, pl. 16, figs 5–8, pl. 22, fig. 12.

       1991a   *M. clingani* (Carruthers, 1867). – Loydell, fig. 5.

       1992   *Monograptus obtusus* Schauer, 1971. – Štorch, p. 199, pl. 1, fig. 2, fig. 2, text-fig. 2e, i, j.

       1993b   "*Monograptus*" *obtusus* Schauer, 1971. – Loydell, pp. 128, 129, pl. 5, fig. 10, text-figs 3, 13.

Holotype. – The specimen illustrated by Schauer (1971, pl. 25, fig. 5) from the *Spirograptus guerichi* Biozone of Weinberg bei Hohenleuben, Thüringia, Germany.

Material. – 254 mostly diagenetically flattened specimens, from the upper *Stimulograptus halli* Biozone through to the middle *Spirograptus guerichi* Biozone.

Description. – The rhabdosome is dorsally curved throughout, most tightly at the proximal end. The sicula is 0.8–1.1 mm long, with an apertural width of 0.15 mm. Its apex reaches to a level from below the aperture of th1 to below its top. Thecae are triangular throughout with twisted apertures. The width of the base of the protheca in relation to total rhabdosome width increases significantly from proximal thecae, where the base of the protheca is narrow, to distal thecae where it can comprise greater than half of the rhabdosome width. The increase in overall rhabdosome dorso-ventral width and the increase in relative breadth of prothecal bases distally vary significantly between specimens. Stratigraphically older collections consist exclusively of more slowly widening specimens bearing more proximal thecae with narrow prothecal bases. Stratigraphically younger collections, from the lower to middle *guerichi* Biozone contain a wider variation, including specimens identical to those from the *halli* Biozone (*e.g.* Fig. 22AE), but also much more rapidly widening rhabdosomes with broader prothecal bases developed earlier in the rhabdosome (*e.g.* Figs 22W, 23A). As a result of this considerable intraspecific variation and the effect of apparent widening or narrowing resulting from the orientation of the rhabdosome in relation to bedding, dorso-ventral width shows considerable variation: at th1 it is 0.45–0.7 mm, at th5 0.95–1.45 mm and at th10 1.3–1.85 mm. Maximum dorso-ventral width distally is 2.25 mm. 2TRDs are 1.5–2.05 mm at th2, 1.35–2.05 mm at th5 and 1.7–2.2 mm at th10. One specimen (Fig. 19K) shows evidence for regeneration after damage: th8 possesses an unusually elongated protheca and its width and morphology are characteristic of more distal thecae.

Remarks. – *T. obtusus* differs from *T. minutus* in having axially elongated thecae only at its extreme proximal end and in the bases of prothecae being broader, especially distally. In both the Czech Republic (Štorch 1992) and in the El Pintado sections *T. obtusus* disappears significantly below the top of the *Spirograptus guerichi* Biozone. Loydell (1993b) incorrectly stated that this species lacks twisted thecal apertures, probably a result of the few Welsh specimens available being preserved in obverse view in which the thecal apertures are largely hidden. *T. obtusus* is similar to '*Monograptus*' *pseudocommunis* Zalasiewicz, 1994 in rhabdosome shape and thecal outline. The latter species has a much narrower proximal end with thecae that more axially elongated and reaches a lesser maximum width of 1 mm.

Torquigraptus sp.
Figure 22H

Material. – 72 diagenetically flattened specimens, mostly from the lower part of the *Stimulograptus halli* Biozone where the species is very common.

Description. – All of the rhabdosome fragments are very narrow and are gently dorsally curved. The longest is more than 20 mm long. None possesses a sicula. Ventral prothecal walls are inclined at up to 5° to the rhabdosome axis. Thecal apertures appear to be twisted. Dorso-ventral width is 0.2–0.3 mm. 2TRDs are 2.3–2.9 mm.

Remarks. – The appearance of these specimens is similar to that of the proximal portions of several *Torquigraptus* species, *e.g. T. planus* (Fig. 20C) and *T. linterni* (Figs 19P, S, 22C). There is, however, no appreciable increase in dorso-ventral width. The material most probably represents a new species.

Conclusions

1. The El Pintado sections provide the most complete, largely undeformed, graptolitic section through the upper Aeronian and lower Telychian thus far documented.

2. A high diversity of graptolites (118 species) is present: the composition of the assemblages (few retiolitids, rare *Metaclimacograptus asejradi*, generally uncommon *Parapetalolithus*) is typical of an outer shelf setting.

3. Palaeobiogeographical differentiation of graptolite faunas in the early Telychian appears to have been very limited.

4. Several taxa (Fig. 12) show consistent biostratigraphical ranges across several terranes/palaeocontinents and are particularly valuable in biostratigraphical subdivision of the upper Aeronian and lower Telychian.

5. Of the various biozonations proposed for the upper Aeronian and lower Telychian, use of the *Stimulograptus halli* Biozone (with a *Lituigraptus rastrum* Subzone forming its middle part) for the upper Aeronian, and retention of the *Spirograptus guerichi* and *Sp. turriculatus* biozones for the lower Telychian is recommended. It is recognised that distinguishing between the upper *St. sedgwickii* Biozone and lower *halli* Biozone is dependent upon identification of the biozonal index species.

6. In future, biostratigraphers need to be aware of the stratigraphically early occurrence of *Sp. turriculatus* low in the *guerichi* Biozone in El Pintado section 1. Fortunately, the *guerichi* Biozone contains a wide range of distinctive taxa and remains easily recognizable as a result.

7. The $\delta^{13}C_{org}$ record through the upper Aeronian and lower Telychian at El Pintado reveals no major excursions. A protracted interval of higher values occurs in the upper *guerichi* and lower *turriculatus* biozones. This coincides with a significant reduction in graptolite diversity, the "*utilis* event".

8. The $\delta^{13}C_{org}$ records through the *guerichi* Biozone of El Pintado and Arctic Canada are remarkably similar (Fig. 15) and have the potential (if integrated with graptolite biostratigraphy) to be used as an additional tool for correlation between these two widely geographically separated areas.

Acknowledgements

References

BARRANDE, J. 1850. *Graptolites de Bohême*. vi +74 pp. Published by the author, Prague.

BASSETT, M.G. 1985. Towards a 'common language' in stratigraphy. *Episodes 8*, 87–92.

BERGSTRÖM, S.M., ERIKSSON, M.E., YOUNG, S.E. & WIDMARK, E.-M. 2012. Conodont biostratigraphy, and $\delta^{13}C$ and $\delta^{34}S$ isotope chemostratigraphy, of the uppermost Ordovician and Lower Silurian at Osmundsberget, Dalarna, Sweden. *GFF 134*, 251–272. DOI 10.1080/11035897.2012.758169

BERGSTRÖM, S.M., TOPRAK, F.Ö., HUFF, W.D. & MUNDIL, R. 2008. Implications of a new, biostratigraphically well-controlled, radio-isotopic age for the lower Telychian Stage of the Llandovery Series (Lower Silurian, Sweden). *Episodes 31*, 309–314.

BJERRESKOV, M. 1971. The stratigraphy of the Llandovery Series on Bornholm. *Bulletin of the Geological Society of Denmark 21*, 34–50.

BJERRESKOV, M. 1975. Llandoverian and Wenlockian graptolites from Bornholm. *Fossils and Strata 8*, 1–94.

BOUČEK, B. 1953. Biostratigraphy, development and correlation of the Želkovice and Motol Beds of the Silurian of Bohemia. *Sborník Ústředního ústavu geologického 20*, 421–484.

BOUČEK, B. & PŘIBYL, A. 1941. Ueber die Gattung *Petalolithus* Suess aus dem böhmischen Silur. *Mitteilungen der Tschechischen Akademie der Wissenschaften 51*, 1–17.

CARVAJAL Y ACUÑA, E. 1944. Criaderos de hierro de España. Tomo VI. Hierros de Sevilla. *Memoria del Instituto Geológico y Minero de España 46*, 265–454.

CAVE, R. & HAINS, B.A. 1986. *Geology of the country between Aberystwyth and Machynlleth. Memoir for 1:50 000 geological sheet 163 (England & Wales).* 148 pp. HMSO, London.

CHEN, X. 1984. Silurian graptolites from southern Shaanxi and northern Sichuan with special reference to classification of Monograptidae. *Palaeontologia Sinica, New Series B 166(20)*, 1–102.

CHEN, X., FAN, J.X., CHEN, Q., TANG, L. & HOU, X.D. 2014. Toward a stepwise Kwangsian orogeny. *Science China, Earth Sciences 57*, 379–387.

COOPER, R.A., SADLER, P.M., MUNNECKE, A. & CRAMPTON, J.S. 2014. Graptoloid evolutionary rates track Ordovician–Silurian global climate change. *Geological Magazine 151*, 349–364. DOI 10.1017/S0016756813000198

CRAMER, B.D., BRETT, C.E., MELCHIN, M.J., MÄNNIK, P., KLEFFNER, M.A., MCLAUGHLIN, P.I., LOYDELL, D.K., MUNNECKE, A., JEPPSSON, L., CORRADINI, C., BRUNTON, F.R. & SALTZMAN, M.R. 2011. Revised correlation of Silurian Provincial Series of North America with global and regional chronostratigraphic units and $\delta^{13}C_{carb}$ chemostratigraphy. *Lethaia 44*, 185–202. DOI 10.1111/j.1502-3931.2010.00234.x

DAVIES, J.R., FLETCHER, C.J.N., WATERS, R.A., WILSON, D., WOODHALL, D.G. & ZALASIEWICZ, J.A. 1997. *Geology of the country around Llanilar and Rhayader. Memoir for 1:50 000 geological sheets 178 and 179 (England and Wales).* 267 pp. The Stationery Office, London.

DAVIES, J.R., MOLYNEUX, S.G., VANDENBROUCKE, T.R.A., VERNIERS, J., WATERS, R.A., WILLIAMS, M. & ZALASIEWICZ, J.A. 2011. Pre-conference trip to the Type Llandovery area, 29–71. *In* RAY, D.C. (ed.) *Siluria revisited: a field guide.* 166 pp. International Subcommission on Silurian Stratigraphy.

DAVIES, J.R., WATERS, R.A., MOLYNEUX, S.G., WILLIAMS, M., ZALASIEWICZ, J.A., VANDENBROUCKE, T.R.A. & VERNIERS, J. 2013. A revised sedimentary and biostratigraphical architecture for the Type Llandovery area, Central Wales. *Geological Magazine 150*, 300–332. DOI 10.1017/S0016756812000337

FLOYD, J. 2001. The Southern Uplands terrane: a stratigraphical review. *Transactions of the Royal Society of Edinburgh, Earth Sciences 91*, 349–362. DOI 10.1017/S0263593300008233

FU, L. & SONG, L. 1986. Stratigraphy and paleontology of Silurian in Ziyang Region (transitional belt). *Bulletin of the Xi'an Insti-*

tute of Geology and Mineral Resources, Chinese Academy of Geological Sciences 14, 1–198.

GE, M. 1990. Silurian graptolites from Chengkou, Sichuan. *Palaeontologia Sinica, New Series B 179(26)*, 1–157.

GUTIÉRREZ-MARCO, J.C., LENZ, A.C., ROBARDET, M. & PIÇARRA, J.M. 1996. Wenlock–Ludlow graptolite biostratigraphy and extinction: a reassessment from the southwestern Iberian Peninsula (Spain and Portugal). *Canadian Journal of Earth Sciences 33*, 656–663. DOI 10.1139/e96-049

GUTIÉRREZ-MARCO, J.C., ROBARDET, M. & PIÇARRA, J.M. 1998. Silurian stratigraphy and paleogeography of the Iberian Peninsula (Spain and Portugal), 13–44. *In* GUTIÉRREZ-MARCO, J.C. & RÁBANO, I. (eds) *Proceedings 6th International Graptolite Conference (GWG-IPA) & 1998 Field Meeting, IUGS Subcommission on Silurian Stratigraphy. Temas Geológico-Mineros ITGE 23*.

GUTIÉRREZ-MARCO, J.C. & ŠTORCH, P. 1998. Graptolite biostratigraphy of the Lower Silurian (Llandovery) shelf deposits of the Western Iberian Cordillera, Spain. *Geological Magazine 135*, 71–92. DOI 10.1017/S0016756897007802

HOWE, M.P.A. 1983. Measurement of thecal spacing in graptolites. *Geological Magazine 120*, 635–638. DOI 10.1017/S0016756800027795

HUTT, J.E. 1974. The Llandovery graptolites of the English Lake District. Part 1. *Palaeontographical Society Monograph 128(540)*, 1–56.

HUTT, J.E. 1975. The Llandovery graptolites of the English Lake District. Part 2. *Palaeontographical Society Monograph 129(542)*, 57–137.

INANLI, F.Ö., HUFF, W.D. & BERGSTRÖM, S. M. 2009. The lower Silurian (Llandovery) Osmundsberg K-bentonite in Baltoscandia and the British Isles: chemical fingerprinting and regional correlation. *GFF 131*, 269–279. DOI 10.1080/11035890903243251

JAEGER, H. & ROBARDET, M. 1979. Le Silurien et le Dévonien basal dans le nord de la Province de Seville (Espagne). *Géobios 12(5)*, 687–714. DOI 10.1016/S0016-6995(79)80097-2

JAEKEL, O. 1889. Über das Alter des sogen. Graptolithengesteins mit besonderer Berücksichtigung der in demselben enhalten Graptolithen. *Zeitschrift der Deutschen Geologischen Gesellschaft 41*, 653–690.

JONES, O.T. 1909. The Hartfell-Valentian succession in the district around Plynlimon and Pont Erwyd (North Cardiganshire). *Quarterly Journal of the Geological Society of London 65*, 463–537. DOI 10.1144/GSL.JGS.1909.065.01-04.32

JONES, O.T. & PUGH, W.J. 1916. The geology of the district around Machynlleth and the Llyfnant valley. *Quarterly Journal of the Geological Society of London 71*, 343–385. DOI 10.1144/GSL.JGS.1915.071.01-04.16

KOREN', T.N. & RICKARDS, R.B. 1996. Taxonomy and evolution of Llandovery biserial graptoloids from the southern Urals, western Kazakhstan. *Special Papers in Palaeontology 54*, 1–103.

LAPWORTH, C. 1873. Notes on the British graptolites and their allies. 1. On an improved classification of the Rhabdophora. *Geological Magazine 1(10)*, 500–504, 555–560. DOI 10.1017/S0016756800469256

LAPWORTH, C. 1878. The Moffat Series. *Quarterly Journal of the Geological Society of London 34*, 240–346. DOI 10.1144/GSL.JGS.1878.034.01-04.23

LEGRAND, P. 2003. Silurian stratigraphy and palaeogeography of the northern African margin of Gondwana. *New York State Museum Bulletin 493*, 59–104.

LENZ, A.C. 1982. Llandoverian graptolites of the northern Canadian Cordillera: *Petalograptus*, *Cephalograptus*, *Rhaphidograptus*, *Dimorphograptus*, Retiolitidae, and Monograptidae. *Life Science Contributions, Royal Ontario Museum 130*, 1–154.

LENZ, A.C., ROBARDET, M., GUTIÉRREZ-MARCO, J.C. & PIÇARRA, J.M. 1996. Devonian graptolites from southwestern Europe: a review with new data. *Geological Journal 31*, 349–358. DOI 10.1002/(SICI)1099-1034(199612)31:4<349::AID-GJ714>3.0.CO;2-K

LEVINA, E.F. 1928. Graptoliti iz Aq-Tengi v Turkestanskom chrebte. *Trudy Srednie-aziatskogo gosudarstvennogo universiteta, Series 7a, Geologiya Fascicule 5*, 1–18.

LINNARSSON, G. 1881. Graptolitskiffrar med *Monograptus turriculatus* vid Klubbudden nära Motala. *Geologiska Föreningens i Stockholm Förhandlingar 5(12)*, 503–527. DOI 10.1080/11035898109443966

LOYDELL, D.K. 1990a. *Sinodiversograptus* – its occurrence in Australia and northern Canada. *Journal of Paleontology 64*, 847–849.

LOYDELL, D.K. 1990b. On the graptolites described by Baily (1871) from the Silurian of Northern Ireland and the genus *Streptograptus* Yin. *Palaeontology 33*, 937–943.

LOYDELL, D.K. 1991a. The biostratigraphy and formational relationships of the upper Aeronian and lower Telychian (Llandovery, Silurian) formations of western mid-Wales. *Geological Journal 26*, 209–244. DOI 10.1002/gj.3350260304

LOYDELL, D.K. 1991b. Dob's Linn – the type locality of the Telychian (Upper Llandovery) *Rastrites maximus* Biozone? *Newsletters on Stratigraphy 25*, 155–161.

LOYDELL, D.K. 1992. Upper Aeronian and lower Telychian (Llandovery) graptolites from western mid-Wales. Part 1. *Palaeontographical Society Monograph 146(589)*, 1–55.

LOYDELL, D.K. 1993a. Worldwide correlation of Telychian (Upper Llandovery) strata using graptolites, 323–340. *In* HAILWOOD, E.A. & KIDD, R.B. (eds) *High resolution stratigraphy. Geological Society of London, Special Publication 70*.

LOYDELL, D.K. 1993b. Upper Aeronian and lower Telychian (Llandovery) graptolites from western mid-Wales. Part 2. *Palaeontographical Society Monograph 147(592)*, 56–180.

LOYDELL, D.K. 1994. Early Telychian changes in graptoloid diversity and sea level. *Geological Journal 29*, 355–368. DOI 10.1002/gj.3350290404

LOYDELL, D.K. 2000. *Rastrites hybridus hybridus* Lapworth, 1876. *Atlas of graptolite type specimens*, Folio 1.85. The Palaeontographical Society, London.

LOYDELL, D.K. 2007a. Early Silurian positive $\delta^{13}C$ excursions and their relationship to glaciations, sea-level changes and extinction events. *Geological Journal 42*, 531–546. DOI 10.1002/gj.1090

LOYDELL, D.K. 2007b. Graptolites from the Upper Ordovician and lower Silurian of Jordan. *Special Papers in Palaeontology 78*, 1–66.

LOYDELL, D.K., BUTCHER, A. & FRÝDA, J. 2013. The middle Rhuddanian (lower Silurian) 'hot' shale of North Africa and Arabia: an atypical hydrocarbon source rock. *Palaeogeography, Palaeoclimatology, Palaeoecology 386*, 233–256. DOI 10.1016/j.palaeo.2013.05.027

LOYDELL, D.K. & FRÝDA, J. 2007. Carbon isotope stratigraphy of

the upper Telychian and lower Sheinwoodian (Llandovery–Wenlock, Silurian) of the Banwy River section, Wales. *Geological Magazine 144*, 1015–1019. DOI 10.1017/S0016756807003895

Loydell, D.K., Kaljo, D. & Männik, P. 1998. Integrated biostratigraphy of the lower Silurian of the Ohesaare core, Saaremaa, Estonia. *Geological Magazine 135*, 769–783. DOI 10.1017/S0016756898001423

Loydell, D.K. & Maletz, J. 2002. Isolated '*Monograptus*' *gemmatus* from the Silurian of Osmundsberget, Sweden. *GFF 124*, 193–196. DOI 10.1080/11035890201244193

Loydell, D.K. & Maletz, J. 2004. The Silurian graptolite genera *Streptograptus* and *Pseudostreptograptus*. *Journal of Systematic Palaeontology 2*, 65–93. DOI 10.1017/S1477201904001117

Loydell, D.K. & Maletz, J. 2009. Isolated graptolites from the *Lituigraptus convolutus* Biozone (Silurian, Llandovery) of Dalarna, Sweden. *Palaeontology 52*, 273–296. DOI 10.1111/j.1475-4983.2008.00843.x

Loydell, D.K., Männik, P. & Nestor, V. 2003. Integrated biostratigraphy of the lower Silurian of the Kolka-54 core, Latvia. *Geological Magazine 147*, 253–280. DOI 10.1017/S0016756809990574

Loydell, D.K., Nestor, V. & Männik, P. 2010. Integrated biostratigraphy of the lower Silurian of the Aizpute-41 core, Latvia. *Geological Magazine 140*, 205–229. DOI 10.1017/S0016756802007264

Loydell, D.K., Sarmiento, G.N., Štorch, P. & Gutiérrez-Marco, J.C. 2009. Graptolite and conodont biostratigraphy of the upper Telychian–lower Sheinwoodian (Llandovery–Wenlock) strata, Jabalón River section, Corral de Calatrava, central Spain. *Geological Magazine 146*, 187–198. DOI 10.1017/S0016756808005840

Loydell, D.K., Štorch, P. & Melchin, M.J. 1993. Taxonomy, evolution and biostratigraphical importance of the Llandovery graptolite *Spirograptus*. *Palaeontology 36*, 909–926.

Maletz, J. 2006. Graptolithen, 132–137. *In* Heuse, T. & Leonhardt, D. (eds) *Stratigraphie von Deutschland VII, Silur. Schriftenreihe der Deutschen Gesellschaft für Geowissenschaften 46.*

Maletz, J., Ahlberg, P., Suyarkova, A. & Loydell, D.K. 2014. Silurian graptolite biostratigraphy of the Röstånga-1 drill core, Scania – a standard for southern Scandinavia. *GFF 136*, 175–178. DOI 10.1080/11035897.2013.865665

Maletz, J. Bates, D.E.B., Brussa, E.D., Cooper, R.A., Lenz, A.C., Riva, J.F., Toro, B.A. & Zhang, Y.D. 2014. Part V, revised, Chapter 12: Glossary of the Hemichordata. *Treatise Online 62*, 1–23.

Manck, E. 1928. Das Vogtland, die klassische Fundstätte von Graptolithen. *Frisch auf 1*, 9.

Melchin, M.J. 1989. Llandovery graptolite biostratigraphy and palaeobiogeography, Cape Phillips Formation, Canadian Arctic Islands. *Canadian Journal of Earth Sciences 26*, 1726–1746. DOI 10.1139/e89-147

Melchin, M.J. & Holmden, C. 2006. Carbon isotope stratigraphy of the Llandovery in Arctic Canada: implications for global correlation and sea-level change. *GFF 128*, 173–180. DOI 10.1080/11035890601282173

Melchin, M.J., MacRae, K.-D. & Bullock, P. 2015. A multi-peak organic carbon isotope excursion in the late Aeronian (Llandovery, Silurian): evidence from Arisaig, Nova Scotia, Canada. *Palaeoworld 24*, 191–197. DOI 10.1016/j.palwor.2014.12.004

Melchin, M.J., Mitchell, C.E., Naczk-Cameron, A., Fan, J.X.

& Loxton, J. 2011. Phylogeny and adaptive radiation of the Neograptina (Graptoloida) during the Hirnantian mass extinction and Silurian recovery. *Proceedings of the Yorkshire Geological Society 5*, 281–309. DOI 10.1144/pygs.58.4.301

Melchin, M.J., Sadler, P.M. & Cramer, B.D. 2012. The Silurian Period, 525–558. *In* Gradstein, F.M., Ogg, J.G., Schmitz, M.D. & Ogg, G.M. (eds) *The geologic time scale 2012. Volume 2.* Elsevier, Amsterdam.

Mitchell, C.E., Melchin, M.J., Cameron, C.B. & Maletz, J. 2013. Phylogenetic analysis reveals that *Rhabdopleura* is an extant graptolite. *Lethaia 46*, 34–56. DOI 10.1111/j.1502-3931.2012.00319.x

Mu, E.Z., Li, J.J., Ge, M.Y., Lin, Y.K. & Ni, Y.N. 2002. *Graptolites of China.* 1205 pp. Science Press, Beijing. [in Chinese]

Müller, H. 1963. *Lehrbuch der Paläozoologie. Band II. Invertebraten. Teil 3. Arthropoda 2 Stomochorda.* 612 pp. Fischer, Jena.

Nanjing Institute of Geology and Palaeontology, Academia Sinica (NIGP) 1974. *Handbook of stratigraphy and palaeontology of Southwest China.* 454 pp. Science Press, Beijing.

Ni, Y.N. 1978. Lower Silurian graptolites from Yichang, western Hubei. *Acta Palaeontologica Sinica 17*, 387–416.

Ni, Y.N., Chen, T.E., Cai, C.Y., Li, G.H., Duan, Y.X. & Wang, J.D. 1982. The Silurian rocks in western Yunnan. *Acta Palaeontologica Sinica 21*, 119–132.

Packham, G.H. 1962. Some diplograptids from the British Lower Silurian. *Palaeontology 5*, 498–526.

Obut, A.M., Sobolevskaya, R.F. & Bondarev, V.I. 1965. *Silurian graptolites of Taimir.* 120 pp. Akademiya nauk SSR, Sibirskoe otdelenie, Institut geologii i geofiziki. Izdatelstvo Nauka, Moskva. [in Russian]

Page, A., Gabbott, S.E., Wilby, P.R. & Zalasiewicz, J.A. 2008. Ubiquitous Burgess Shale-style "clay templates" in low-grade metamorphic rocks. *Geology 36*, 855–858. DOI 10.1130/G24991A.1

Paškevičius, J. 1979. *Biostratigraphy and graptolites of the Lithuanian Silurian.* 268 pp. Mokslas, Vilnius.

Piçarra, J.M., Gutiérrez-Marco, J.C., Lenz, A.C. & Robardet, M. 1998. Přídolí graptolites from the Iberian Peninsula: a review of previous data and new records. *Canadian Journal of Earth Sciences 35*, 65–75. DOI 10.1139/cjes-35-1-65

Přibyl, A. 1942. Příspěvek k poznání německých zástupců rodu *Rastrites* Barr. *Rozpravy II. třídy České akademie věd a umění 52(4)*, 1–10.

Přibyl, A. & Münch, A. 1942. Revision der mitteleuropäischen Vertreter der Gattung *Demirastrites* Eisel. *Rozpravy II. třídy České akademie věd a umění 52(30)*, 1–26.

Přibyl, A. & Štorch, P. 1983. *Monograptus (Stimulograptus)* subgen. n. (Graptolites) from the Lower Silurian of Bohemia. *Věstník Ústředního ústavu geologického 58*, 221–226.

Raiswell, R. 1987. Non-steady state microbiological diagenesis and the origin of concretions and nodular limestones, 41–54. *In* Marshall, J.D. (ed.) *Diagenesis of sedimentary sequences. Geological Society of London, Special Publication 36.*

Richter, R. 1853. Thüringische Graptolithen. *Zeitschrift der Deutschen Geologischen Gesellschaft 5*, 439–464.

Rickards, R.B. 1970. The Llandovery (Silurian) graptolites of the Howgill Fells, northern England. *Palaeontographical Society Monograph 123(524)*, 1–108.

Rickards, R.B. & Chen, X. 2002. Graptolites, 73–83. *In* Holland, C.H. & Bassett, M.G. (eds) *Telychian rocks of the Brit-*

ish Isles and China (Silurian, Llandovery Series): an experiment to test precision in stratigraphy. 210 pp. National Museums & Galleries of Wales, Geological Series 21, Cardiff.

ROBARDET, M. & GUTIÉRREZ-MARCO, J.C. 2002. Silurian, 51–66. *In* GIBBONS, W. & MORENO, T. (eds) *The geology of Spain.* 649 pp. The Geological Society, London.

ROBARDET, M. & GUTIÉRREZ-MARCO, J.C. 2004. The Ordovician, Silurian and Devonian sedimentary rocks of the Ossa-Morena Zone (SW Iberian Peninsula, Spain). *Journal of Iberian Geology 30*, 73–92.

ROBARDET, M., PIÇARRA, J.M., ŠTORCH, P., GUTIÉRREZ-MARCO, J.C. & SARMIENTO, G.N. 1998. Ordovician and Silurian stratigraphy and faunas (graptolites and conodonts) in the Ossa Morena Zone of the SW Iberian Peninsula (Portugal and Spain), 289–318. *In* GUTIÉRREZ-MARCO, J.C. & RÁBANO, I. (eds) *Proceedings 6th International Graptolite Conference (GWG-IPA) & 1998 Field Meeting, IUGS Subcommission on Silurian Stratigraphy. Temas Geológico-Mineros ITGE 23.*

SCHAUER, M. 1967. Biostratigraphie und Taxionomie von *Rastrites* (Pterobranchiata, Graptolithina) aus dem anstehenden Silur Ostthüringens und des Vogtlandes. *Freiberger Forschungshefte C213*, 171–199.

SCHAUER, M. 1971. Biostratigraphie und Taxionomie der Graptolithen des tieferen Silurs unter besonderer Berücksichtigung der tektonischen Deformation. *Freiberger Forschungshefte C273*, 1–185.

SENNIKOV, N.V., YOLKIN, E.A., PETRUNINA, Z.E., GLADKIKH, L.A., OBUT, O.T., IZOKH, N.G. & KIPRIYANOVA, T.P. 2008. *Ordovician-Silurian biostratigraphy and paleogeography of the Gorny Altai.* 156 pp. Siberian Branch, Russian Academy of Sciences, Novosibirsk.

SHERWIN, L. 1974. Llandovery graptolites from the Forbes district, New South Wales. *Special Papers in Palaeontology 13*, 149–175.

SIMON, W. 1951. Untersuchungen im Paläozoikum von Sevilla (Sierra Morena, Spanien). *Abhandlungen der Senckenbergischen Naturforschenden Gesellschaft 485*, 31–62.

ŠTORCH, P. 1983. The genus *Diplograptus* (Graptolithina) from the lower Silurian of Bohemia. *Věstník Ústředního ústavu geologického 58*, 159–170.

ŠTORCH, P. 1992. Some new and little known graptolites from the Lower Silurian of Bohemia (Prague Basin, Barrandian Area). *Časopis pro mineralogii a geologii 37(3)*, 193–201.

ŠTORCH, P. 1994. Graptolite biostratigraphy of the Lower Silurian (Llandovery and Wenlock) of Bohemia. *Geological Journal 29*, 137–165. DOI 10.1002/gj.3350290204

ŠTORCH, P. 1995. Biotic crises and post-crisis recoveries recorded by Silurian planktonic graptolite faunas of the Barrandian area (Czech Republic). *Geolines 3*, 59–70.

ŠTORCH, P. 1998a. New data on Telychian (Upper Llandovery) graptolites from Spain. *Journal of the Czech Geological Society 43*, 113–141.

ŠTORCH, P. 1998b. Graptolites of the *Pribylograptus leptotheca* and *Lituigraptus convolutus* biozones of Tmaň (Silurian, Czech Republic). *Journal of the Czech Geological Society 43*, 209–272.

ŠTORCH, P. 2001. Graptolites, stratigraphy and depositional setting of the middle Llandovery (Silurian) volcanic-carbonate facies at Hýskov (Barrandian area, Czech Republic). *Věstník Ústředního ústavu geologického 76*, 55–76.

ŠTORCH, P. & FRÝDA, J. 2012. The late Aeronian graptolite *sedgwickii* Event, associated positive carbon isotope excursion and facies changes in the Prague Synform (Barrandian area, Bohemia). *Geological Magazine 149*, 1089–1106. DOI 10.1017/S001675681200026X

ŠTORCH, P., GUTIÉRREZ-MARCO, J.C., SARMIENTO, G.N. & RÁBANO, I. 1998. Upper Ordovician and Lower Silurian of Corral de Calatrava, southern part of the Central Iberian Zone, 319–325. *In* GUTIÉRREZ-MARCO, J.C. & RÁBANO, I. (eds) *Proceedings 6th International Graptolite Conference (GWG-IPA) & 1998 Field Meeting, IUGS Subcommission on Silurian Stratigraphy. Temas Geológico-Mineros ITGE 23.*

ŠTORCH, P. & LOYDELL, D. 1992. Graptolites of the *Rastrites linnaei* Group from the European Llandovery (Lower Silurian). *Neues Jahrbuch für Geologie und Paläontologie, Abhandlungen 184*, 63–86.

ŠTORCH, P., MITCHELL, C.E., FINNEY, S.C. & MELCHIN, M.J. 2011. Uppermost Ordovician (upper Katian–Hirnantian) graptolites of north-central Nevada, U.S.A. *Bulletin of Geosciences 86*, 301–386. DOI 10.3140/bull.geosci.1264

TEMPLE, J.T. 1988. Biostratigraphical correlation and the stages of the Llandovery. *Journal of the Geological Society, London 145*, 875–879. DOI 10.1144/gsjgs.145.5.0875

TOGHILL, P. 1968. The graptolite assemblages and zones of the Birkhill Shales (Lower Silurian) at Dobb's Linn. *Palaeontology 11*, 654–668.

TÖRNQUIST, S.L. 1907. Observations on the genus *Rastrites* and some allied species of *Monograptus. Lunds Universitets Årsskrift, N.F., Afd. 2, 3(5)*, 1–22.

UNDERWOOD, C.J. 1992. Graptolite preservation and deformation. *Palaios 7*, 178–186. DOI 10.2307/3514928

VAN GROOTEL, G., ZALASIEWICZ, J., VERNIERS, J. & SERVAIS, T. 1998. Chitinozoa and graptolite biozonation of the Aeronian and lower Telychian in the Brabant Massif (Belgium), 135–136. *In* GUTIÉRREZ-MARCO, J.C. & RÁBANO, I. (eds) *Proceedings 6th International Graptolite Conference (GWG-IPA) & 1998 Field Meeting, IUGS Subcommission on Silurian Stratigraphy. Temas Geológico-Mineros ITGE 23.*

WILLIAMS, M., ZALASIEWICZ, J., RUSHTON, A.W.A., LOYDELL, D.K. & BARNES, R.P. 2003. A new, stratigraphically significant *Torquigraptus* species (Silurian graptolite) from the Southern Uplands Terrane. *Scottish Journal of Geology 39*, 17–28. DOI 10.1144/sjg39010017

WORSLEY, D., AARHUS, N., BASSETT, M.G., HOWE, M.P.A., MØRK, A. & OLAUSSEN, S. 1983. The Silurian succession of the Oslo region. *Norges Geologiske Undersøkelse 384*, 1–57.

YIN, T.H. 1937. Brief description of the Ordovician and Silurian fossils from Shihtien. *Bulletin of the Geological Society of China 16*, 281–302. DOI 10.1111/j.1755-6724.1937.mp16001012.x

ZALASIEWICZ, J. 1994. Middle to late Telychian (Silurian: Llandovery) graptolite assemblages of central Wales. *Palaeontology 37*, 375–396.

ZALASIEWICZ, J., WILLIAMS, M., MILLER, M., PAGE, A. & BLACKETT, E. 2007. Early Silurian (Llandovery) graptolites from central Saudi Arabia: first documented record of Telychian faunas from the Arabian Peninsula. *GeoArabia 12*, 15–36.

ZHANG, Y.D., WANG, Y., ZHAN, R.B., FAN, J.X., ZHOU, Z.Q. & FANG, X. 2014. *Ordovician and Silurian stratigraphy and palaeontology of Yunnan, Southwest China.* 138 pp. Science Press, Beijing.